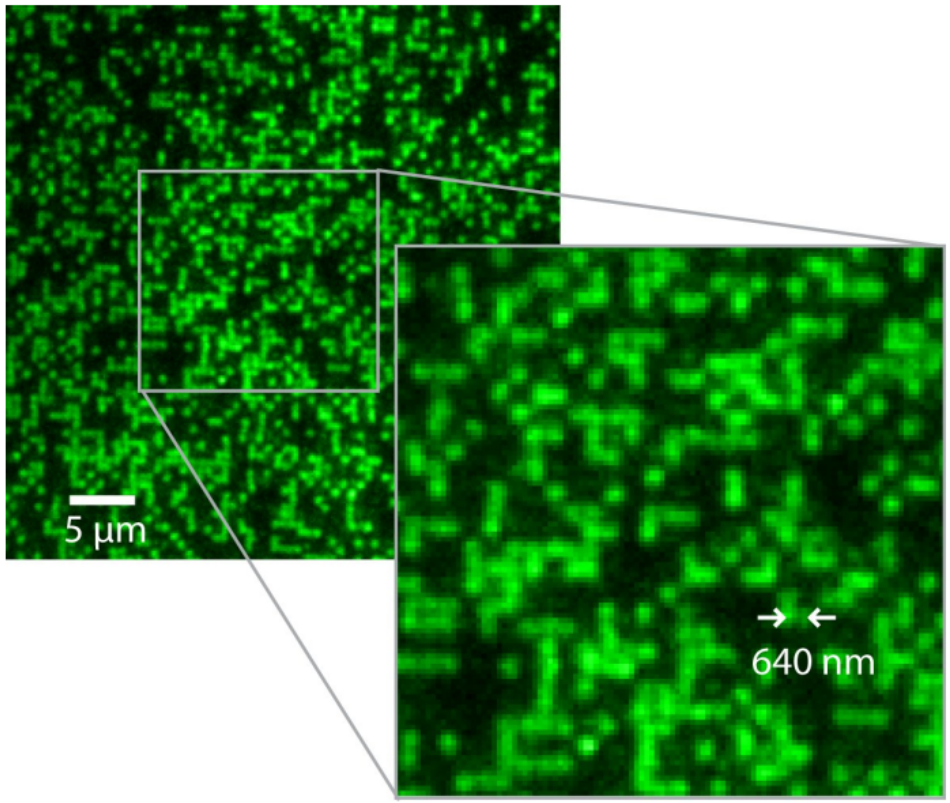
Course on optical lattices

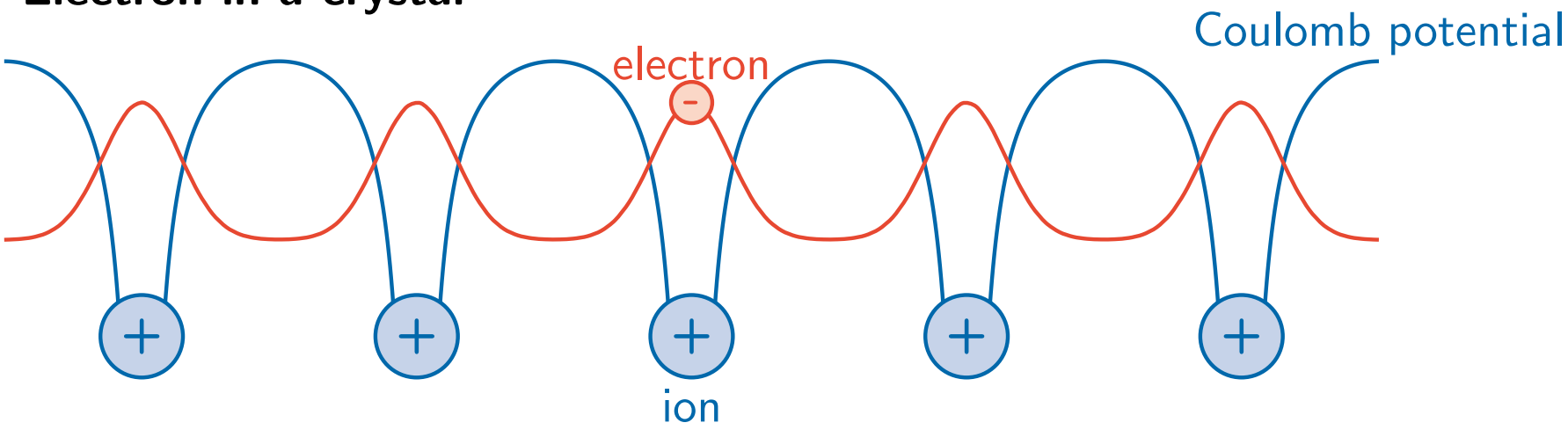
Fabrice Gerbier, Raphael Lopes, Sylvain Nascimbene, Aurélien Perrin

M2 ICFP 2021/2022

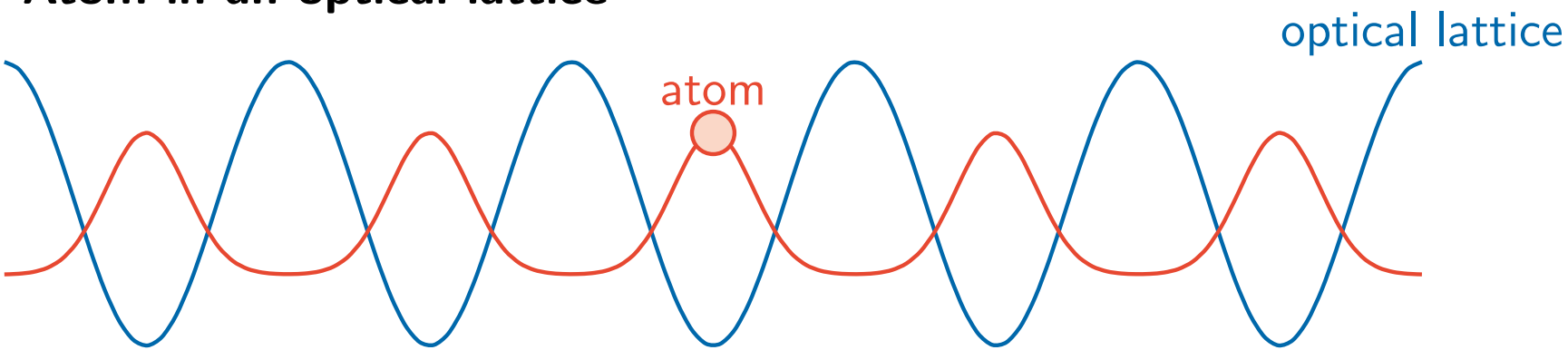


Simulating the electron gas in a crystal

Electron in a crystal

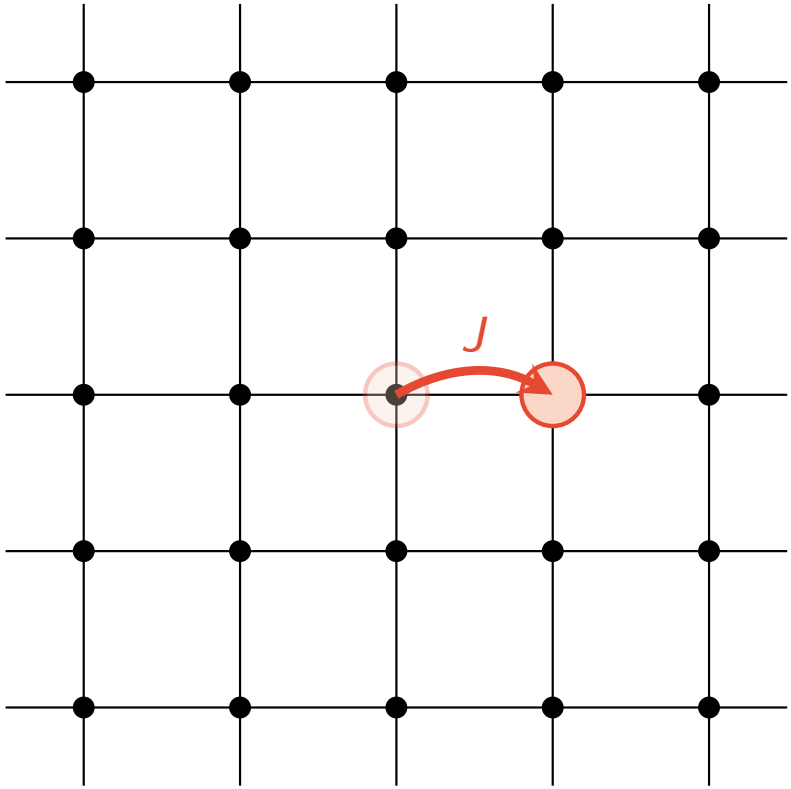


Atom in an optical lattice



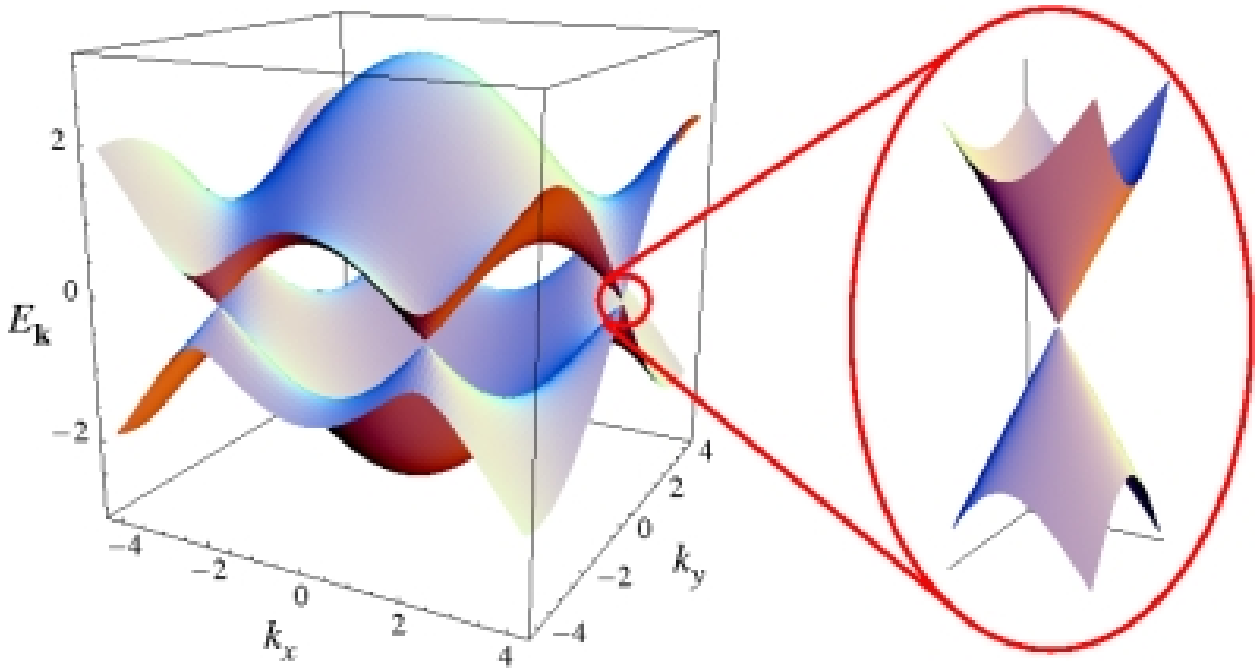
New physics in lattice structures

- Motion restricted to energy bands
  - Weak lattice regime: suppression of kinetic energy (effective mass $m^* > m$)
  - Strong lattice regime: discrete lattice models (dynamics via hopping)



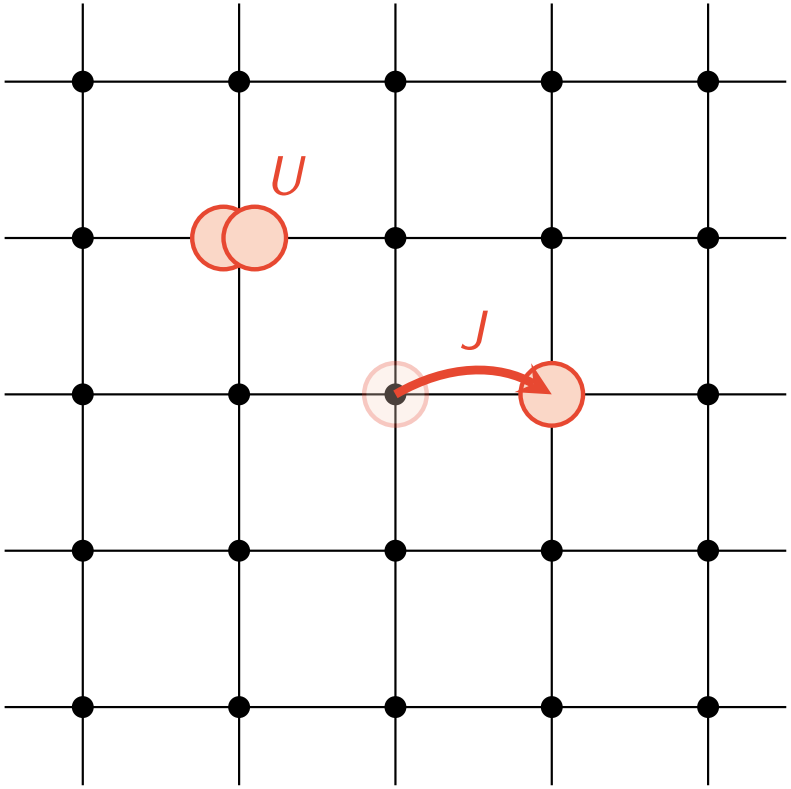
New physics in lattice structures

- Motion restricted to energy bands
- Exotic structures, e.g. graphene with relativistic dispersion



New physics in lattice structures

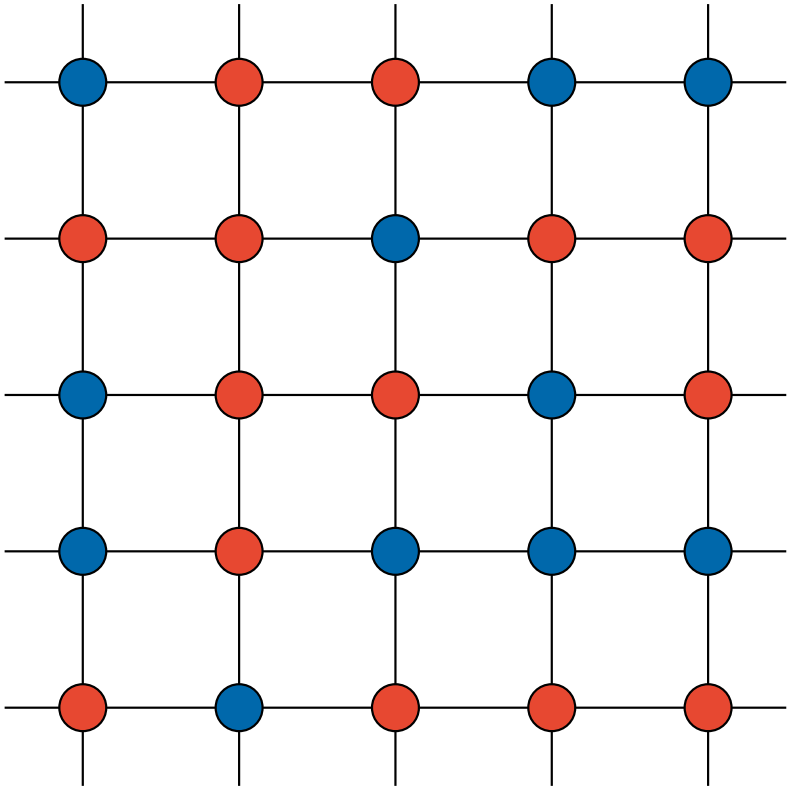
- Motion restricted to energy bands
- Exotic structures, e.g. graphene with relativistic dispersion
- Hubbard model: archetype of solid-state model



quantum phase transition to a Mott insulator

New physics in lattice structures

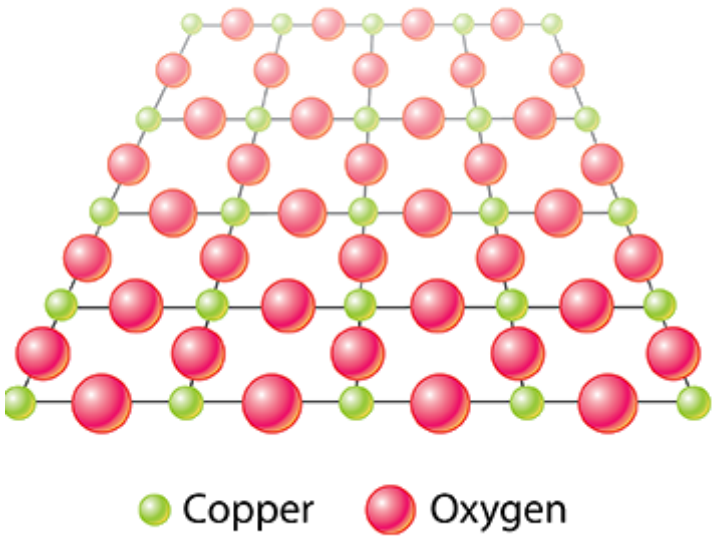
- Motion restricted to energy bands
- Exotic structures, e.g. graphene with relativistic dispersion
- Hubbard model: archetype of solid-state model
- Quantum magnetism in lattice spin models

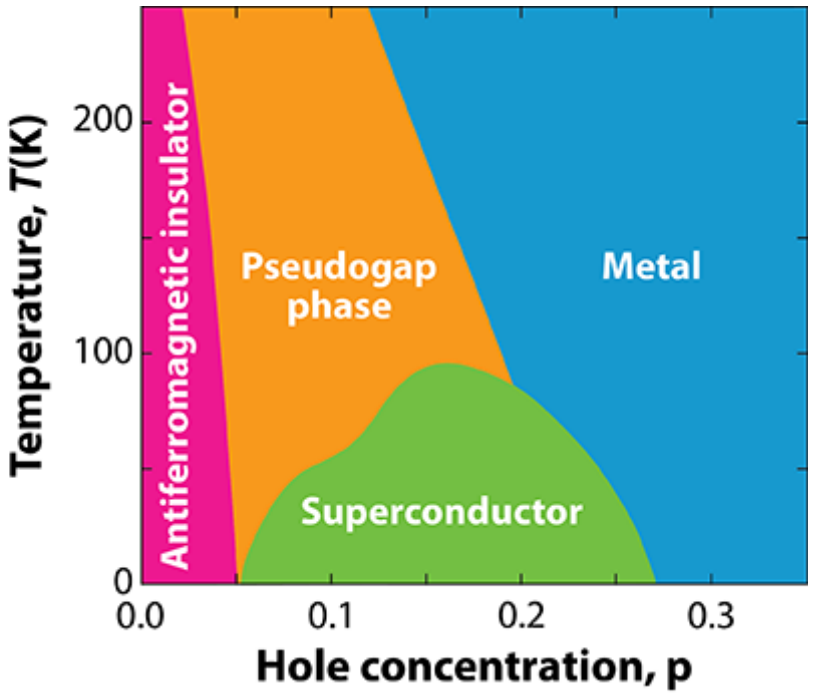


how do the spins order?

New physics in lattice structures

- Motion restricted to energy bands
- Exotic structures, e.g. graphene with relativistic dispersion
- Hubbard model: archetype of solid-state model
- Quantum magnetism in lattice spin models
- Possible connections with high-T_c superconductors





Outline of the course on optical lattices

1. Band structure and dynamics in optical lattices
   - Band structure in one dimension
   - Dynamics of a particle in an optical lattice
   - Wannier functions and tight-binding limit
   - Complex lattices in 1D: SSH model
   - Complex lattices in 2D: graphene and quantum Hall bands
2. Superfluid/Mott insulator transition
   - Hubbard Hamiltonian
   - Superfluid/Mott insulator: phase diagram
   - Gutzwiller variational approach
   - Interference experiments
   - Transport experiments
   - Mott shell structure
   - Low-energy excitations
3. Fermi-Hubbard model and quantum magnetism
   - Attractive Fermi-Hubbard model
   - Repulsive Fermi-Hubbard model and Mott insulator
   - Quantum magnetism

Outline

1. Band structure and dynamics in optical lattices
   - Band structure in one dimension
   - Dynamics of a particle in an optical lattice
   - Wannier functions and tight-binding limit
   - Complex lattices in 1D: SSH model
   - Complex lattices in 2D: graphene and quantum Hall bands
2. Superfluid/Mott insulator transition
   - Hubbard Hamiltonian
   - Superfluid/Mott insulator: phase diagram
   - Gutzwiller variational approach
   - Interference experiments
   - Transport experiments
   - Mott shell structure
   - Low-energy excitations
3. Fermi-Hubbard model and quantum magnetism
   - Attractive Fermi-Hubbard model
   - Repulsive Fermi-Hubbard model and Mott insulator
   - Quantum magnetism

Outline

1. Band structure and dynamics in optical lattices
   - Band structure in one dimension
   - Dynamics of a particle in an optical lattice
   - Wannier functions and tight-binding limit
   - Complex lattices in 1D: SSH model
   - Complex lattices in 2D: graphene and quantum Hall bands
2. Superfluid/Mott insulator transition
   - Hubbard Hamiltonian
   - Superfluid/Mott insulator: phase diagram
   - Gutzwiller variational approach
   - Interference experiments
   - Transport experiments
   - Mott shell structure
   - Low-energy excitations
3. Fermi-Hubbard model and quantum magnetism
   - Attractive Fermi-Hubbard model
   - Repulsive Fermi-Hubbard model and Mott insulator
   - Quantum magnetism

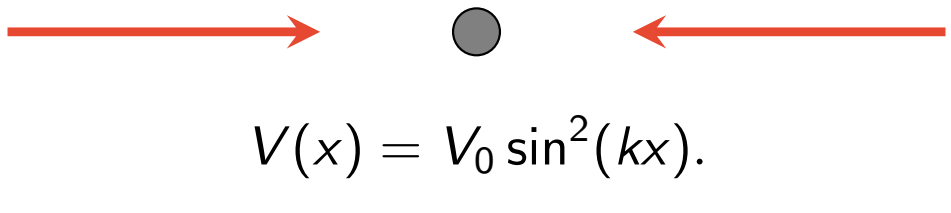
Optical lattice potential

Reminder: optical dipole potential

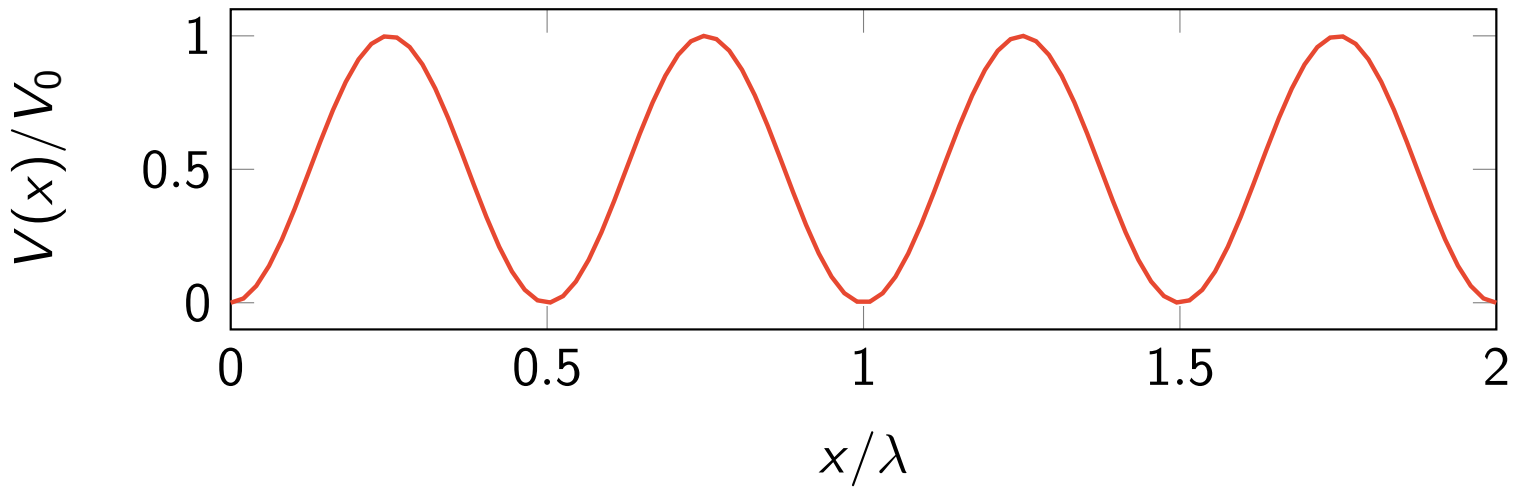
$$V(\mathbf{r}) = \frac{d^2 E(\mathbf{r})^2}{4\hbar\Delta},$$

where d is the electric dipole, $E(\mathbf{r})$ is the electric field amplitude and Δ is the laser detuning.

We consider a 1D optical lattice



$$V(x) = V_0 \sin^2(kx).$$



Quantum dynamics in an optical lattice

The movement of the atoms is governed by the Hamiltonian

$$H = \frac{p^2}{2m} + V_0 \sin^2(kx).$$

The wavenumber defines a naturale energy scale, the *recoil energy*

$$E_\mathrm{r} = \frac{\hbar^2 k^2}{2m}.$$

Typical value

$$m = 100\, m_u, \quad \lambda = 1\,\mu\mathrm{m} \quad \rightarrow \quad E_\mathrm{r} = k_\mathrm{B} \times 100\,\mathrm{nK} = h \times 2\,\mathrm{kHz}.$$

Quantum dynamics in an optical lattice

The movement of the atoms is governed by the Hamiltonian

$$H = \frac{p^2}{2m} + V_0 \sin^2(kx).$$

The wavenumber defines a naturale energy scale, the *recoil energy*

$$E_\mathrm{r} = \frac{\hbar^2 k^2}{2m}.$$

Typical value

$$m = 100\, m_u, \quad \lambda = 1\,\mu\mathrm{m} \quad \rightarrow \quad E_\mathrm{r} = k_\mathrm{B} \times 100\,\mathrm{nK} = h \times 2\,\mathrm{kHz}.$$

The Schrödinger equation then reads (Mathieu equation)

$$-\psi''(\tilde{x}) + \frac{\tilde{V}_0}{2}[1 - \cos(2\tilde{x})]\psi(\tilde{x}) = \tilde{E}\psi(\tilde{x}),$$

where $\tilde{x} = kx$, $\tilde{E} = E/E_\mathrm{r}$ and $\tilde{V}_0 = V_0/E_\mathrm{r}$.
In the following we will most of the time omit the $\tilde{\cdot}$.

Bloch theorem

Discrete translation symmetry $V(x+\pi) = V(x)$ implies that the translation operator T_π,

$$T_\pi \psi(x) = \psi(x-\pi),$$

commutes with the Hamiltonian.
T_π is unitary $\rightarrow$ eigenvalues $e^{-i\theta}$, such that

$$\psi_\theta(x-\pi) = e^{-i\theta}\psi_\theta(x).$$

For $V_0 = 0$ one should recover plane waves $e^{iqx} \rightarrow$ motivation to define $q = \theta/\pi$.,

$$\psi_q(x-\pi) = e^{-iq\pi}\psi_q(x).$$

In other words, one can write

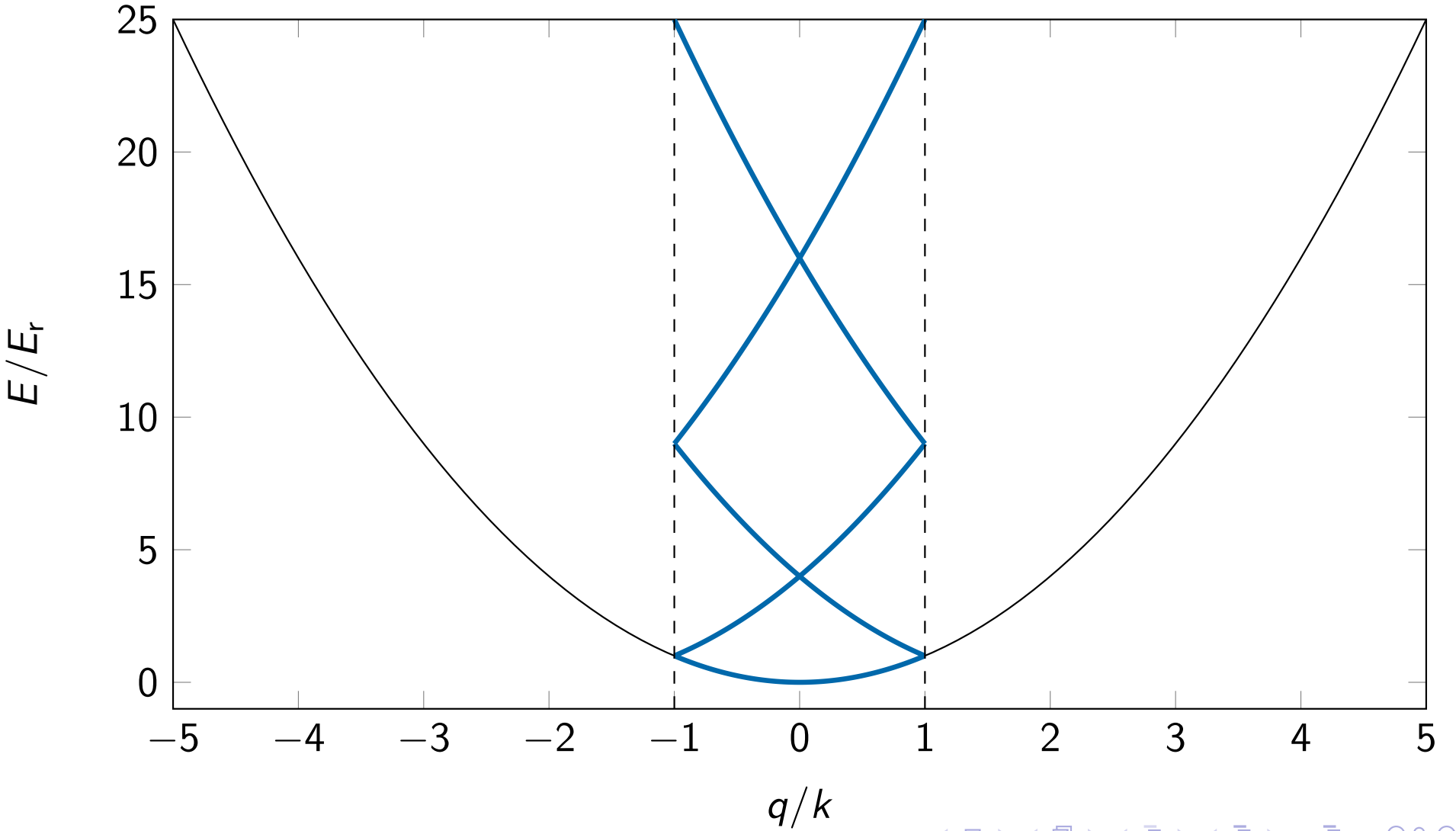
$$\psi_q(x) = e^{iqx}u_q(x),$$

where u_q is π-periodic.

Bloch theorem: one can look for eigenstates as Bloch waves $\psi_q(x)$, i.e. product of plane waves and π-periodic functions.

Free particle spectrum

One should restrict the quasi-momentum to the first Brillouin zone $-k < q < k$.



Solving the Schrödinger equation: the central equation

Bloch functions can be decomposed in a Fourier series, as

$$\psi_q(x) = \sum_{p\in\mathbb{Z}} c_p(q) \mathrm{e}^{\mathrm{i}(2p+q)x}, \quad -1 < q < 1.$$

The coefficients $c_p(q)$ are solutions of the system

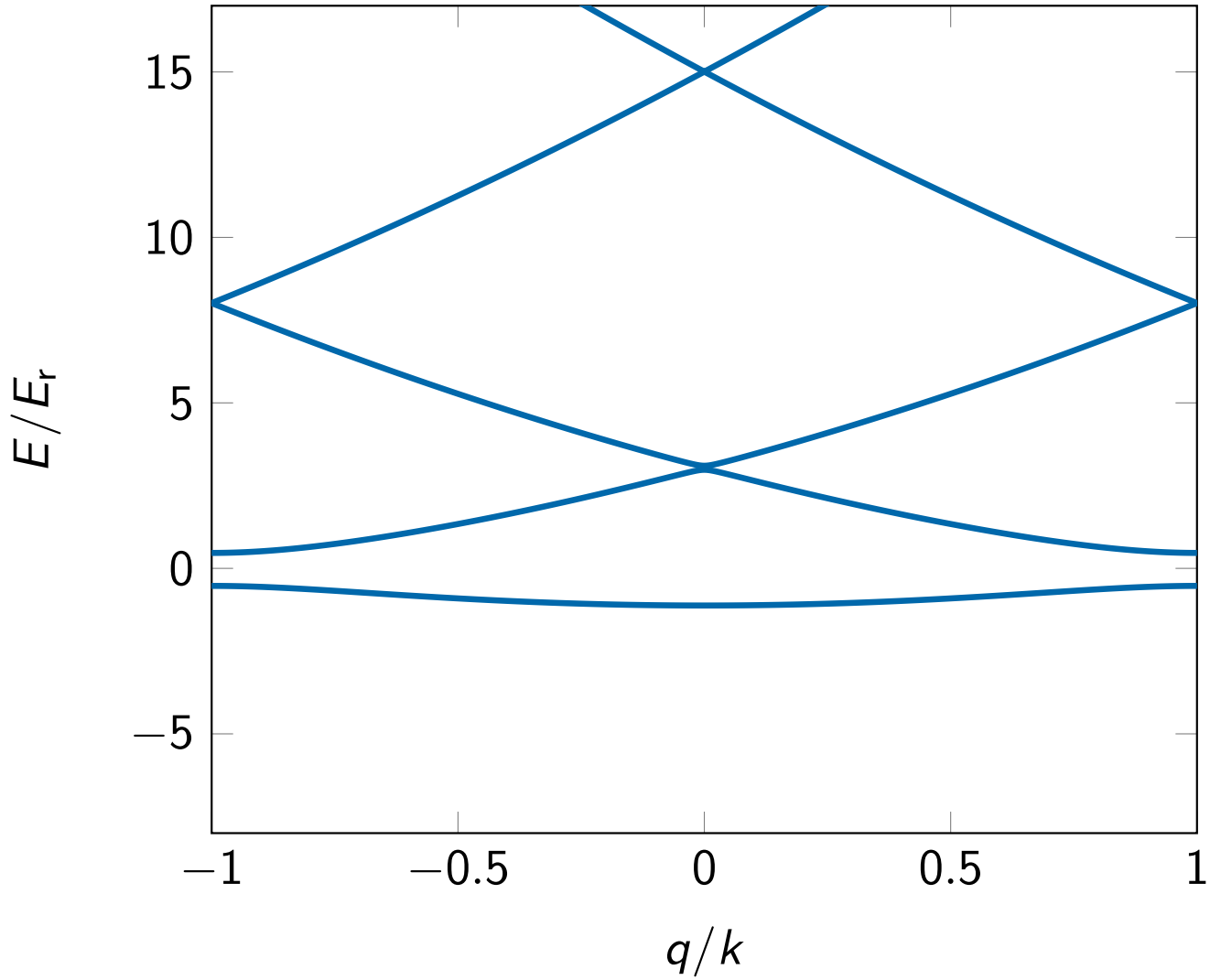
$$\left[(2p+q)^2 + \frac{V_0}{2}\right] c_p - \frac{V_0}{4}(c_{p-1} + c_{p+1}) = E c_p.$$

To calculate the energies of the first bands, one truncates this system to $|p| \leq p_{\mathrm{max}}$, with $p_{\mathrm{max}} \sim 10$. The discarded coefficients do not matter as they corresponds to off-resonant coupling to high-energy momentum states.

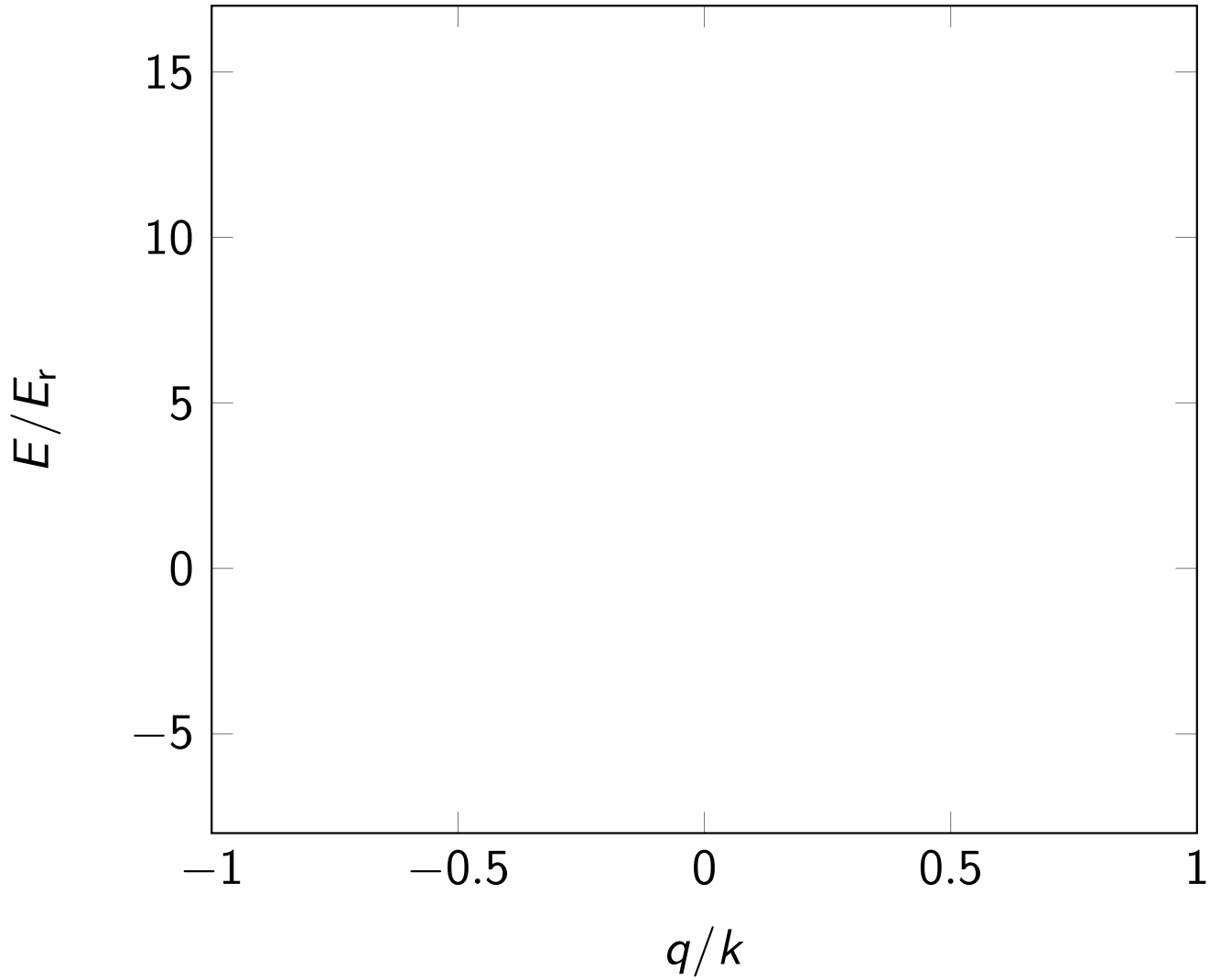
Matrix of the linear system for $p_{\max} = 3$

$$\begin{pmatrix}
(q-6)^2 + \frac{V_0}{2} & -\frac{V_0}{4} & 0 & 0 & 0 & 0 & 0 \\
-\frac{V_0}{4} & (q-4)^2 + \frac{V_0}{2} & -\frac{V_0}{4} & 0 & 0 & 0 & 0 \\
0 & -\frac{V_0}{4} & (q-2)^2 + \frac{V_0}{2} & -\frac{V_0}{4} & 0 & 0 & 0 \\
0 & 0 & -\frac{V_0}{4} & q^2 + \frac{V_0}{2} & -\frac{V_0}{4} & 0 & 0 \\
0 & 0 & 0 & -\frac{V_0}{4} & (q+2)^2 + \frac{V_0}{2} & -\frac{V_0}{4} & 0 \\
0 & 0 & 0 & 0 & -\frac{V_0}{4} & (q+4)^2 + \frac{V_0}{2} & -\frac{V_0}{4} \\
0 & 0 & 0 & 0 & 0 & -\frac{V_0}{4} & (q+6)^2 + \frac{V_0}{2}
\end{pmatrix}$$

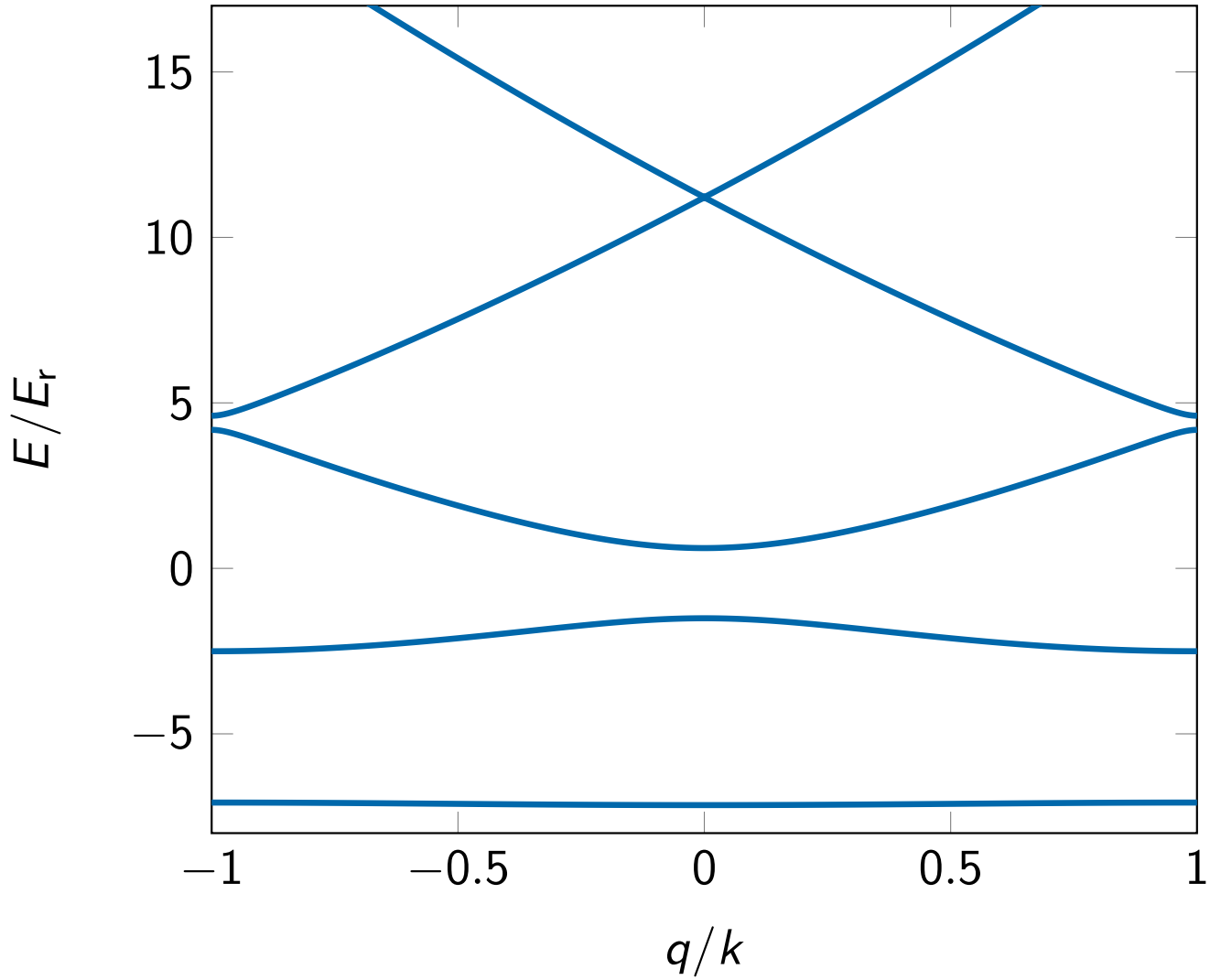
Band structure for $V_0 = 2\,E_\mathrm{r}$.



Band structure for $V_0 = 4\,E_r$.

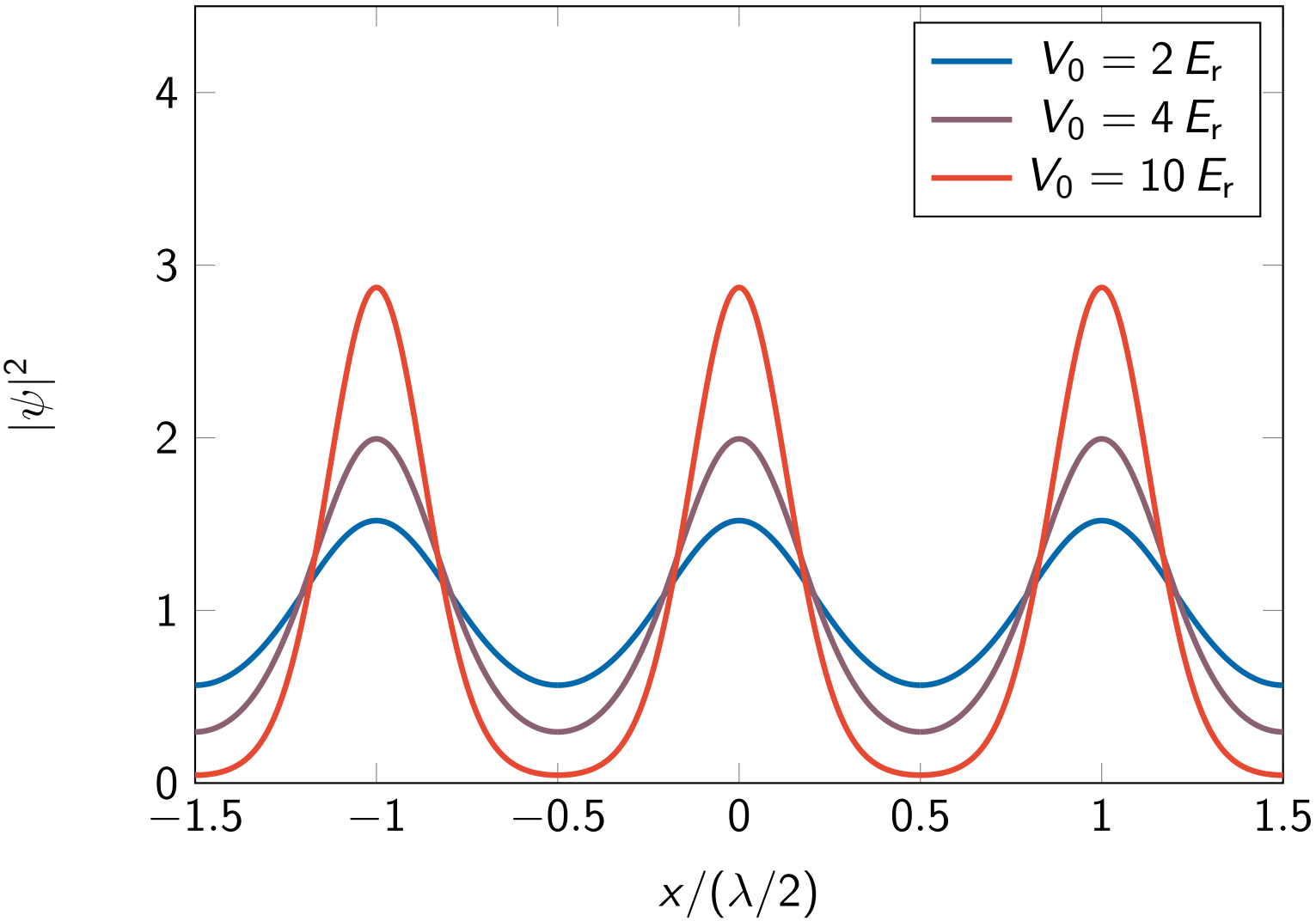


Band structure for $V_0 = 10\,E_r$.



Bloch states

We plot the density of Bloch states for $q = 0$ in the ground band.

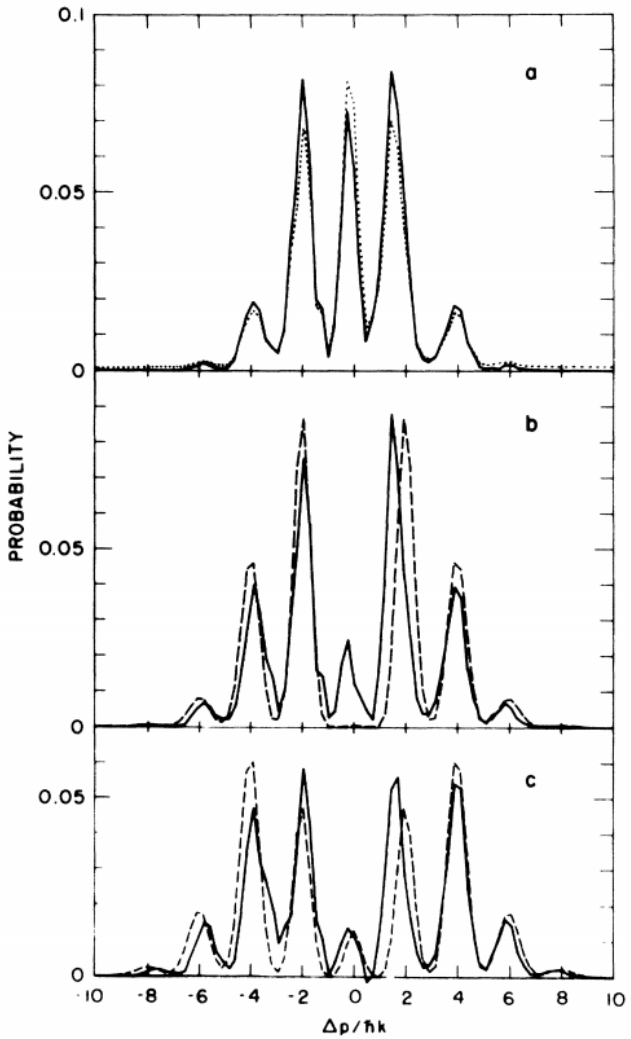


Outline

1. Band structure and dynamics in optical lattices
   - Band structure in one dimension
   - Dynamics of a particle in an optical lattice
   - Wannier functions and tight-binding limit
   - Complex lattices in 1D: SSH model
   - Complex lattices in 2D: graphene and quantum Hall bands
2. Superfluid/Mott insulator transition
   - Hubbard Hamiltonian
   - Superfluid/Mott insulator: phase diagram
   - Gutzwiller variational approach
   - Interference experiments
   - Transport experiments
   - Mott shell structure
   - Low-energy excitations
3. Fermi-Hubbard model and quantum magnetism
   - Attractive Fermi-Hubbard model
   - Repulsive Fermi-Hubbard model and Mott insulator
   - Quantum magnetism

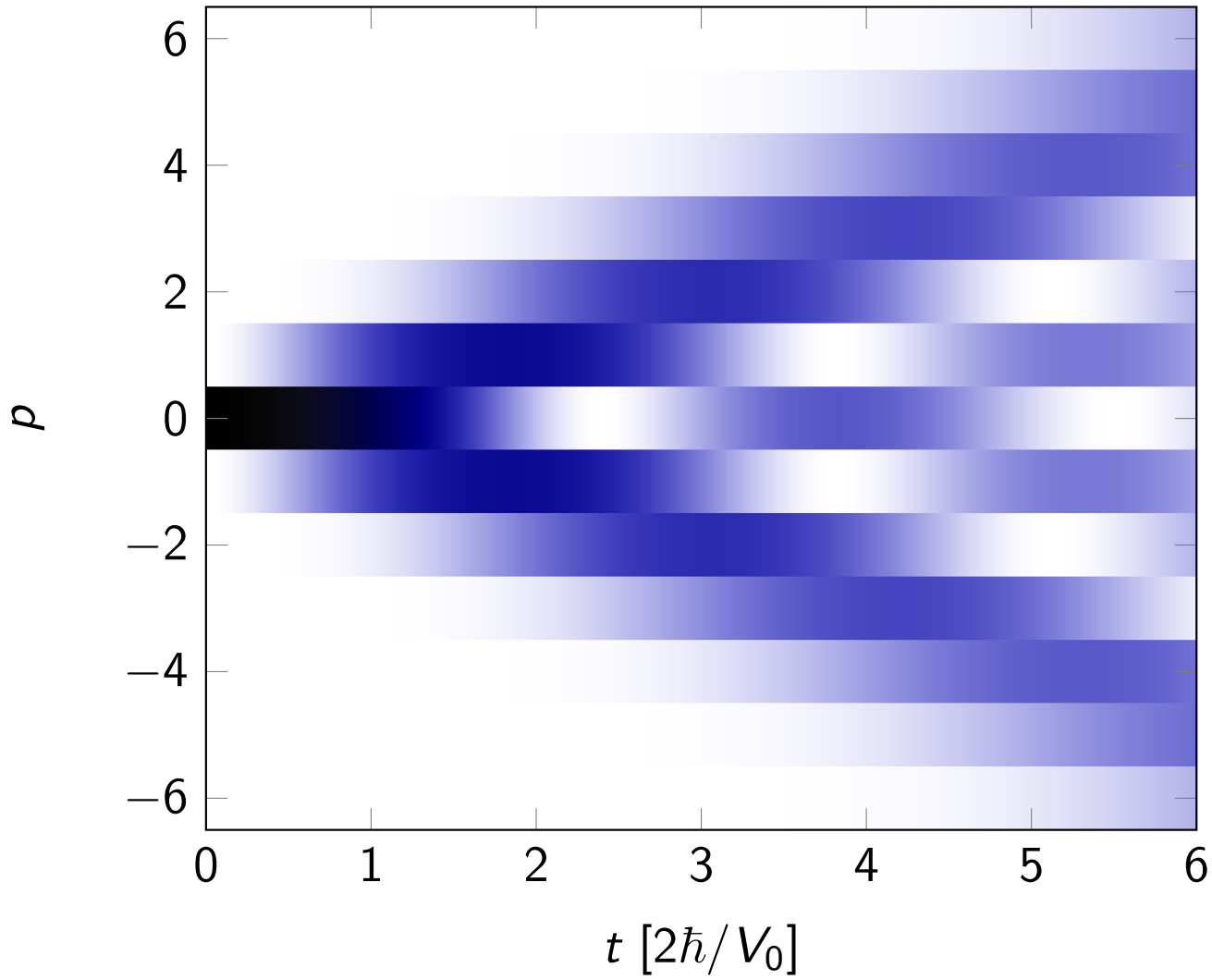
Kapitza-Dirac diffraction

We consider the sudden application of the lattice potential.



Gould et al, PRL 1986 (way before BEC times)

Momentum state dynamics during KD diffraction



Loading of the ground band: adiabaticity criterion

We consider the adiabatic loading of the state $q = 0$ in the ground band, using a linear increase of the lattice depth

$$V_0(t) = V_0^{\mathrm{f}} t/\tau.$$

For moderate lattice depths, the ground state for a depth V_0 reads

$$|\psi_0\rangle \simeq |p = 0\rangle + \frac{V_0}{16E_{\mathrm{r}}}(|p = 2\hbar k\rangle + |p = -2\hbar k\rangle),$$

while the coupled excited state (band $n = 2$; band $n = 1$ is odd) is

$$|\psi_2\rangle \simeq \frac{1}{\sqrt{2}}(|p = 2\hbar k\rangle + |p = -2\hbar k\rangle),$$

with an energy difference $\Delta E \simeq 4E_{\mathrm{r}}$.

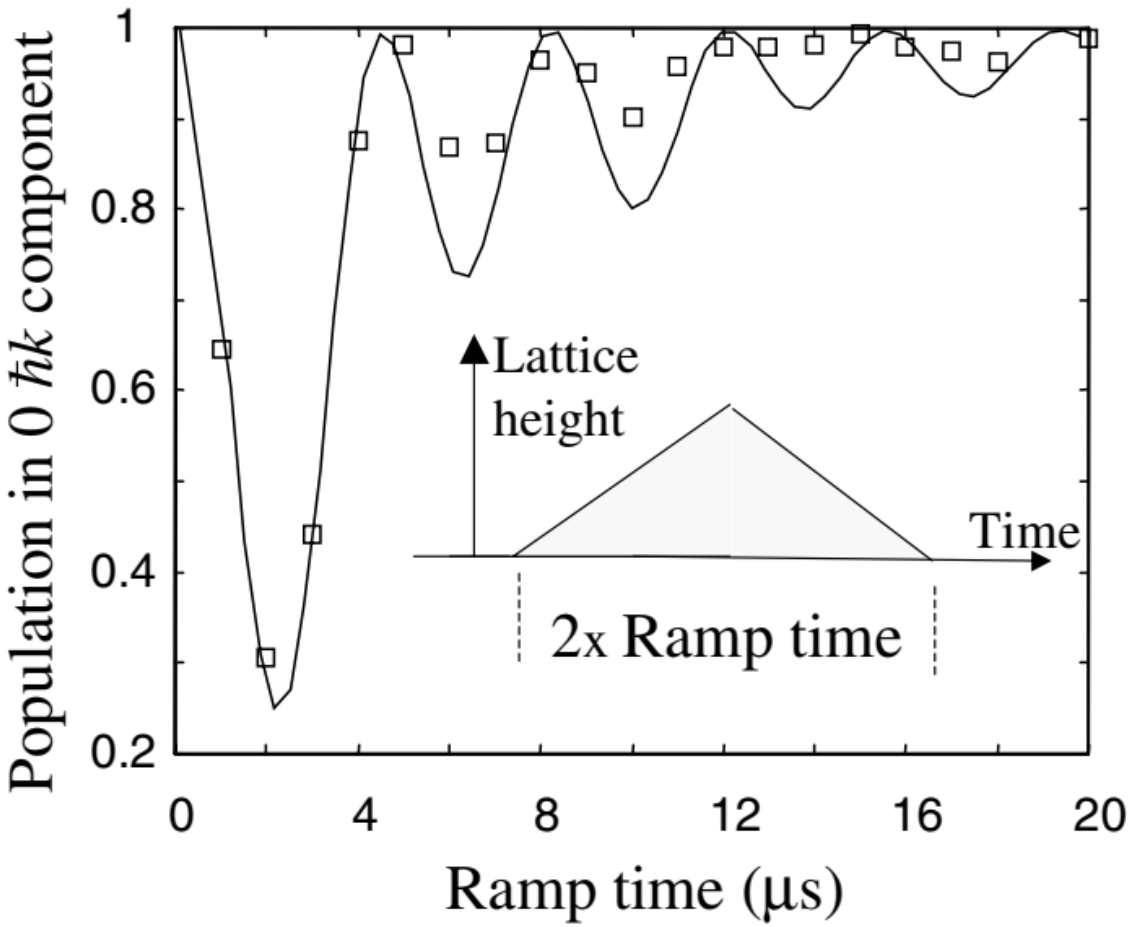
Adiabaticity criterion:

$$\hbar \left| \langle \psi_2 | \frac{\mathrm{d}}{\mathrm{d}t} |\psi_0\rangle \right| \ll \Delta E,$$

i.e.

$$\tau \gg \frac{1}{32\sqrt{2}} \frac{V_0^{\mathrm{f}}}{E_{\mathrm{r}}} \frac{\hbar}{E_{\mathrm{r}}}.$$

Loading of the ground band: adiabaticity criterion



Denschlag et al, J. Phys. B 2002

Time-of-flight vs band mapping

- Accessing the in situ density distribution is difficult (but feasable).

Time-of-flight vs band mapping

- Accessing the in situ density distribution is difficult (but feasable).
- Momentum distribution accessed after time-of-flight
  (free expansion after sudden release from the lattice potential)

$$\psi(\mathbf{r}, t) \simeq \left(\frac{m}{\mathrm{i}t}\right)^{3/2} \tilde{\psi}_0 \left(\mathbf{p} = \frac{m\mathbf{r}}{t}\right) \mathrm{e}^{\mathrm{i}mr^2/(2\hbar t)}.$$

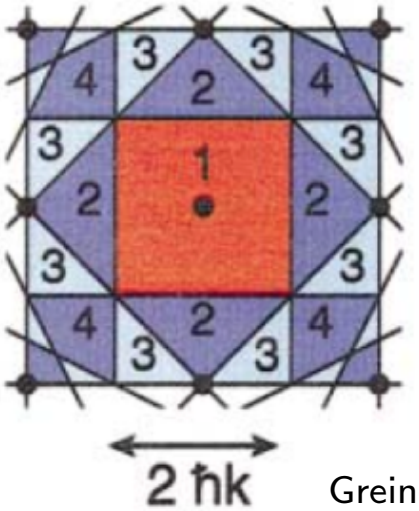
Time-of-flight vs band mapping

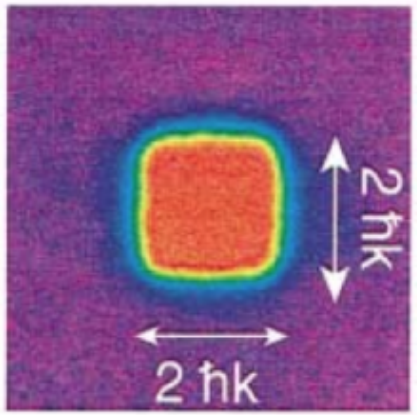
- Accessing the in situ density distribution is difficult (but feasable).
- Momentum distribution accessed after time-of-flight
  (free expansion after sudden release from the lattice potential)

$$\psi(\mathbf{r}, t) \simeq \left(\frac{m}{\mathrm{i}t}\right)^{3/2} \tilde{\psi}_0\left(\mathbf{p} = \frac{m\mathbf{r}}{t}\right) \mathrm{e}^{\mathrm{i}mr^2/(2\hbar t)}.$$

- Quasi-momentum accessed after band-mapping
  (lattice switched off adiabatically)
  quasi-momentum $q \to$ momentum $p = q + 2kn$, $n \in \mathbb{Z}$.

  Example: a thermal gas uniformly filling the lowest band of a cubic lattice





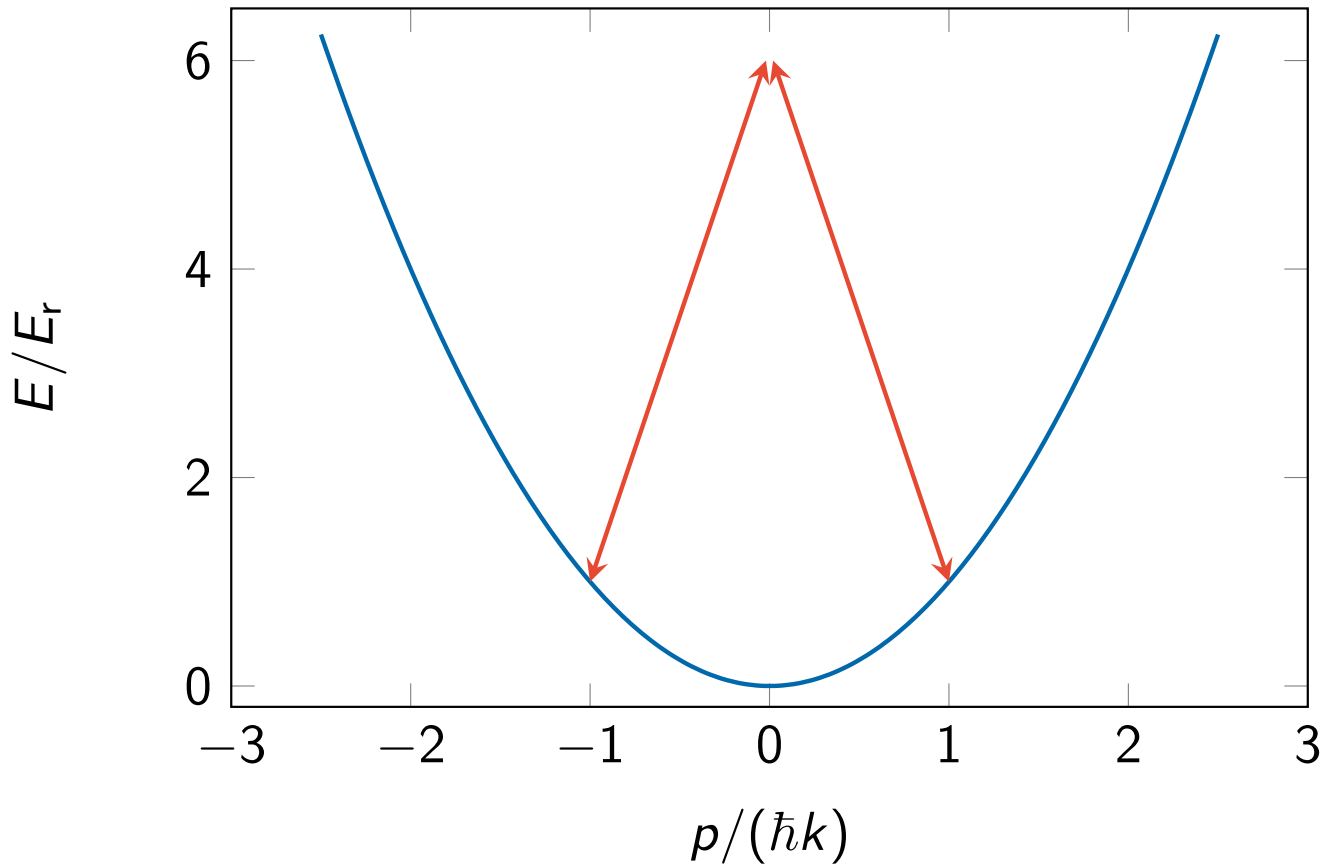
Greiner et al, PRL 2001

Bragg diffraction

The lattice can be used to couple two momenta

$$|p\rangle \leftrightarrow |p + 2\hbar k\rangle \,.$$

Resonance condition $p^2 = (p + 2\hbar k)^2$ fulfilled for $p = -\hbar k$ only.

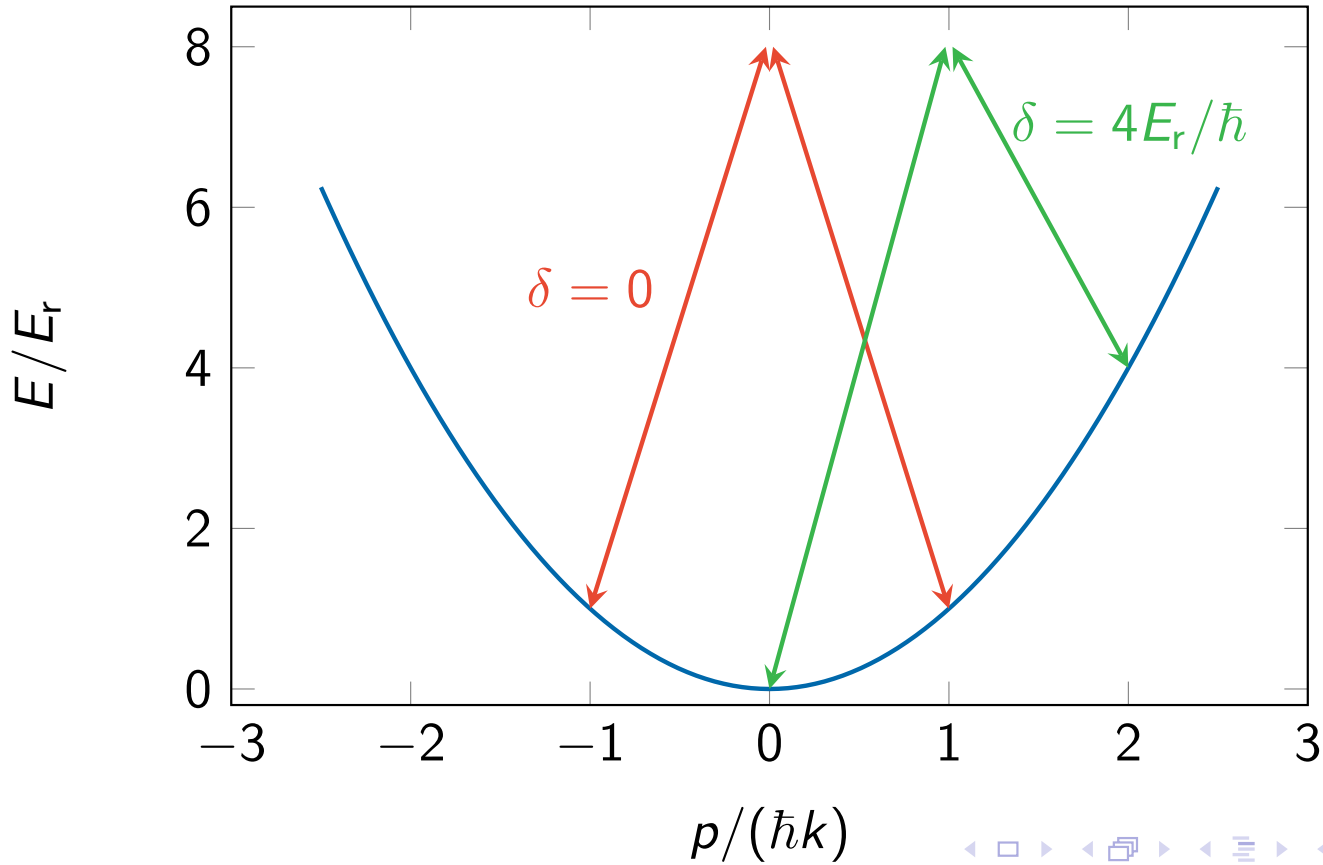


Resonant Bragg diffraction in a moving lattice

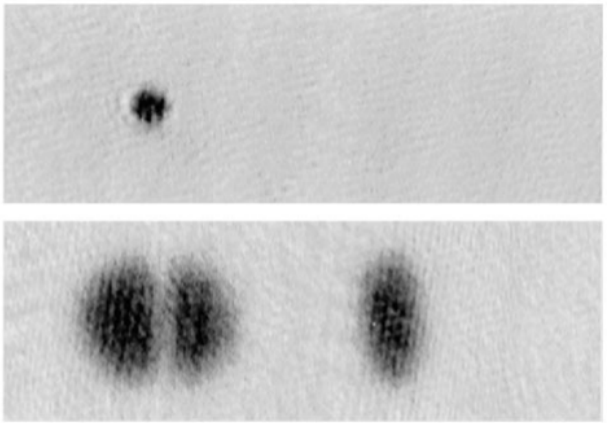
Frequency difference δ between the two laser beams
$\rightarrow$ lattice moving at a speed $\delta/(2k)$.
Resonance condition

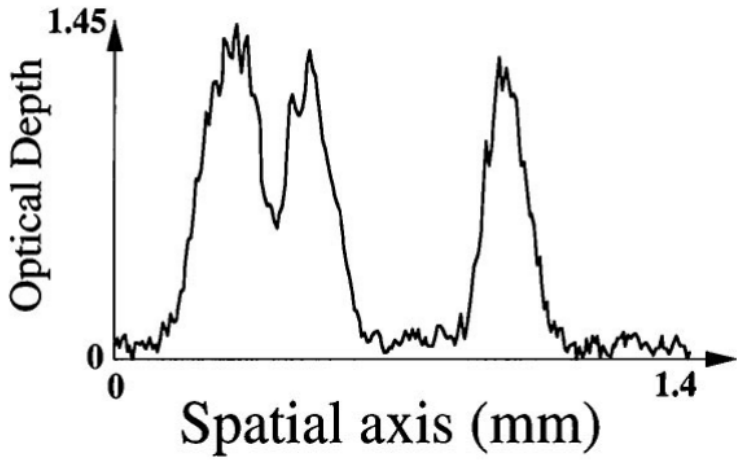
$$\frac{p^2}{2m} = \frac{(p + 2\hbar k)^2}{2m} - \hbar\delta.$$

fulfilled for $p = 0$ for $\hbar\delta = 4E_r$.



Momentum spectroscopy of a BEC



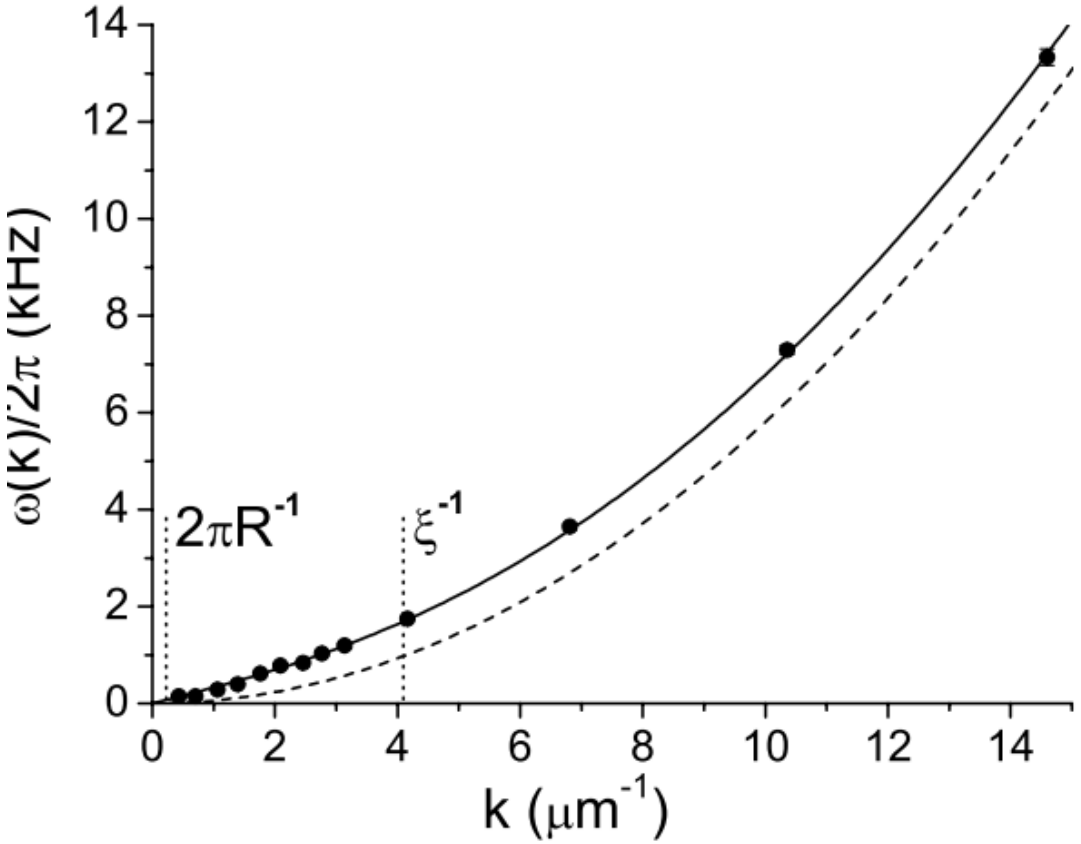


Kozuma et al, PRL 1999

Application 1: spectroscopy of Bogoliubov excitations

Dispersion relation of Bogoliubov excitations

$$\hbar\omega(k) = \sqrt{\hbar^2 c^2 k^2 + \left(\frac{\hbar^2 k^2}{2m}\right)^2}.$$

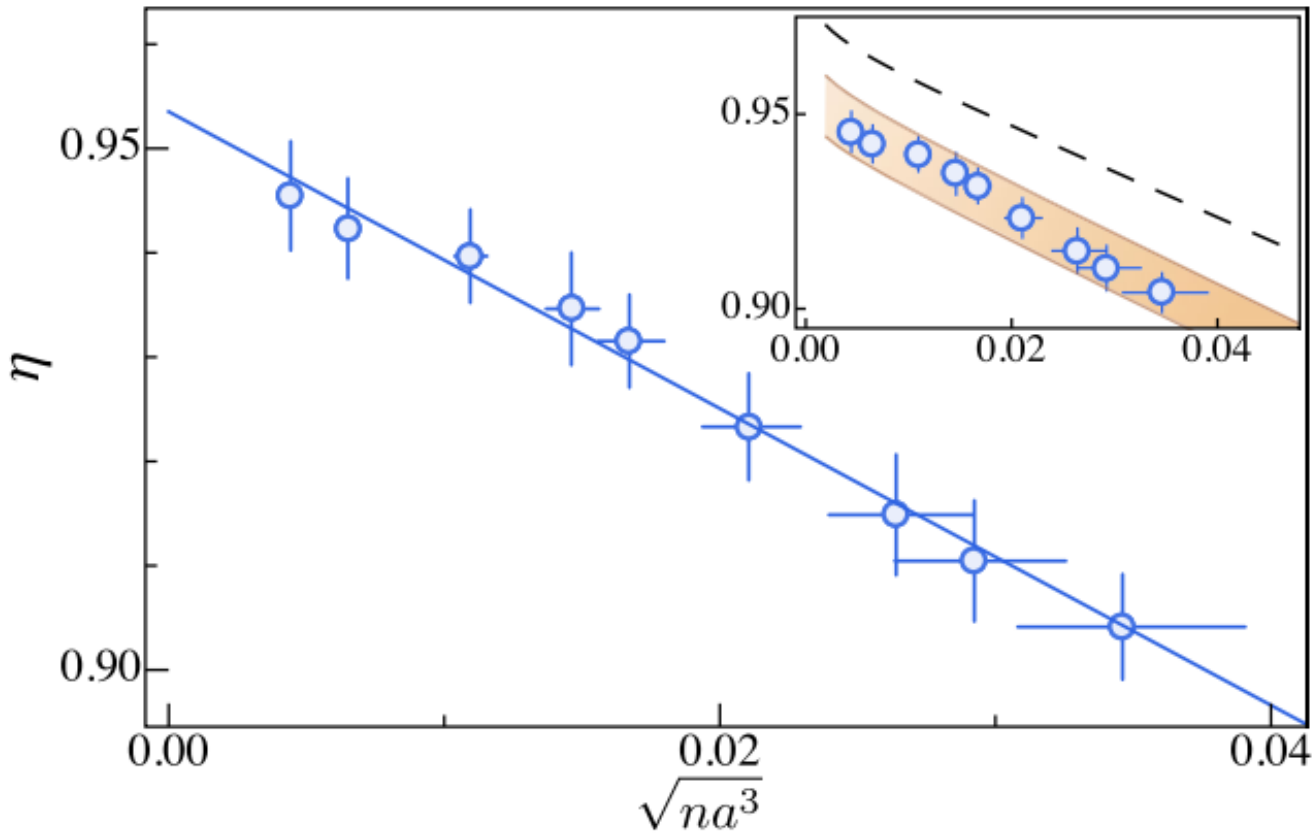


Steinhauer et al, PRL 2002

Application 2: quantum depletion of a BEC

Condensed fraction of a BEC

$$\frac{n_0}{n} = 1 - \frac{8}{3\sqrt{\pi}}\sqrt{na^3}$$



Lopes et al, PRL 2017

Propagation of a wavepacket: group velocity

We consider the evolution of a wavepacket within the ground band

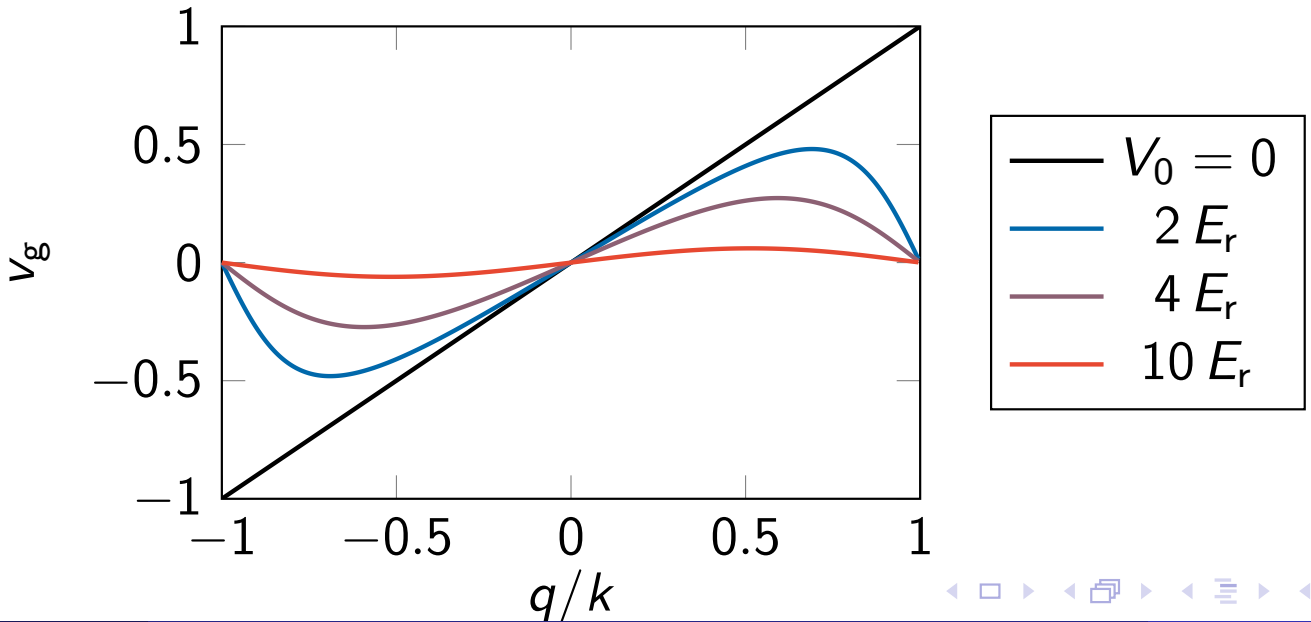
$$\psi(x,0) = \int c(q)\psi_{0,q}(x)\mathrm{d}q.$$

For a wavepacket centered around q_0, we find the evolution

$$\psi(x,t) \simeq \mathrm{e}^{-\mathrm{i}\omega_0 t}\psi(x - v_\mathrm{g} t, 0),$$

where

$$v_\mathrm{g} = \frac{1}{\hbar}\left.\frac{\mathrm{d}E_0(q)}{\mathrm{d}q}\right|_{q=q_0}, \quad \omega_0 = E_0(q_0)/\hbar - q_0 v_\mathrm{g}.$$

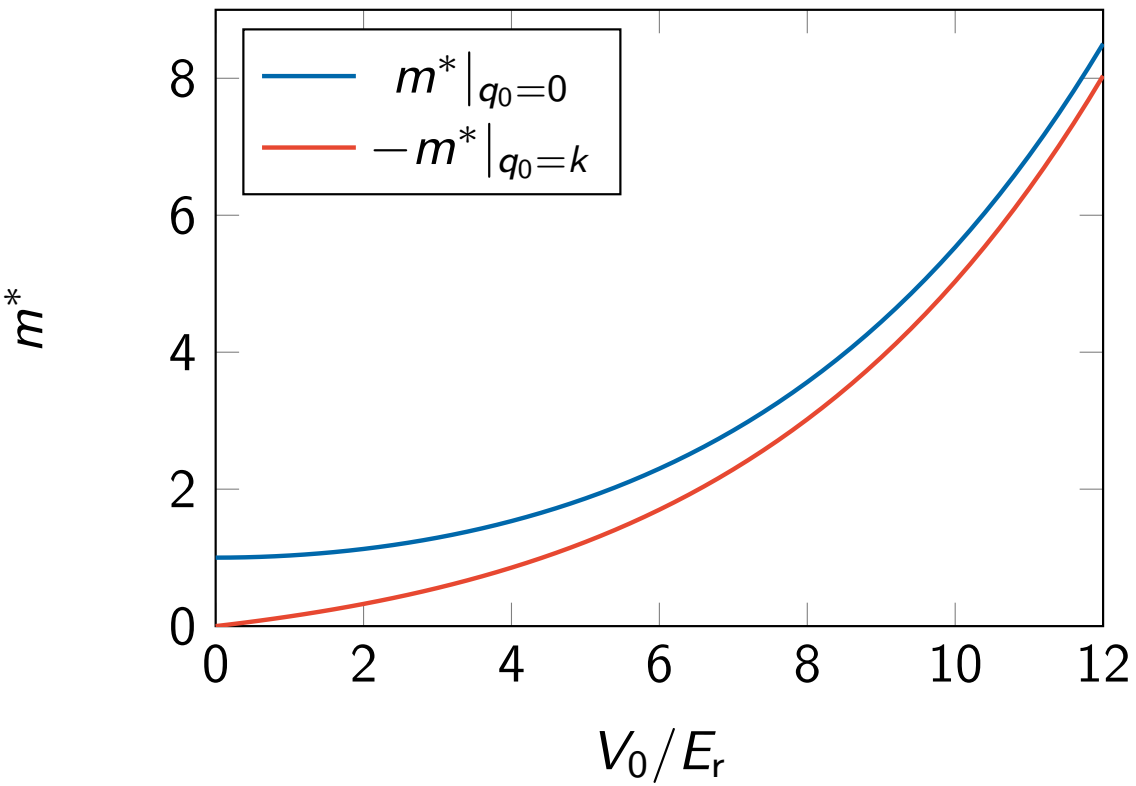


Propagation of a wavepacket: effective mass

The group velocity cancels for $q_0 = 0$ and $q_0 = k$ (band edge). The energy curvature can be interpreted with an effective mass as

$$E(q) = \frac{\hbar^2 (q - q_0)^2}{2m^*} + \text{cst.}$$

For $q_0 = k$ the effective mass is negative! $\rightarrow$ dynamical instability.



Action of an external force

We consider the action of a force on the atom dynamics, described by

$$H = \frac{p^2}{2m} + V_0 \sin^2(kx) - Fx.$$

- The linear potential breaks the discrete translation symmetry
  $\rightarrow$ Bloch theorem does not apply.
- For $V_0 = 0$, the momentum of a classical particle evolves as
  $p(t) = p(t = 0) + Ft$.
  $\rightarrow$ suggests gauge transform to a moving frame

$$H' = UHU^\dagger + \mathrm{i}\hbar(\partial_t U)U^\dagger, \quad U = \mathrm{e}^{-\mathrm{i}xFt/\hbar},$$
$$= \frac{(p + Ft)^2}{2m} + V_0 \sin^2(kx).$$

H' invariant under lattice translations $\rightarrow$ conserves the quasi-momentum.

Consequence in the laboratory frame: $q(t) = q_i + Ft/\hbar$

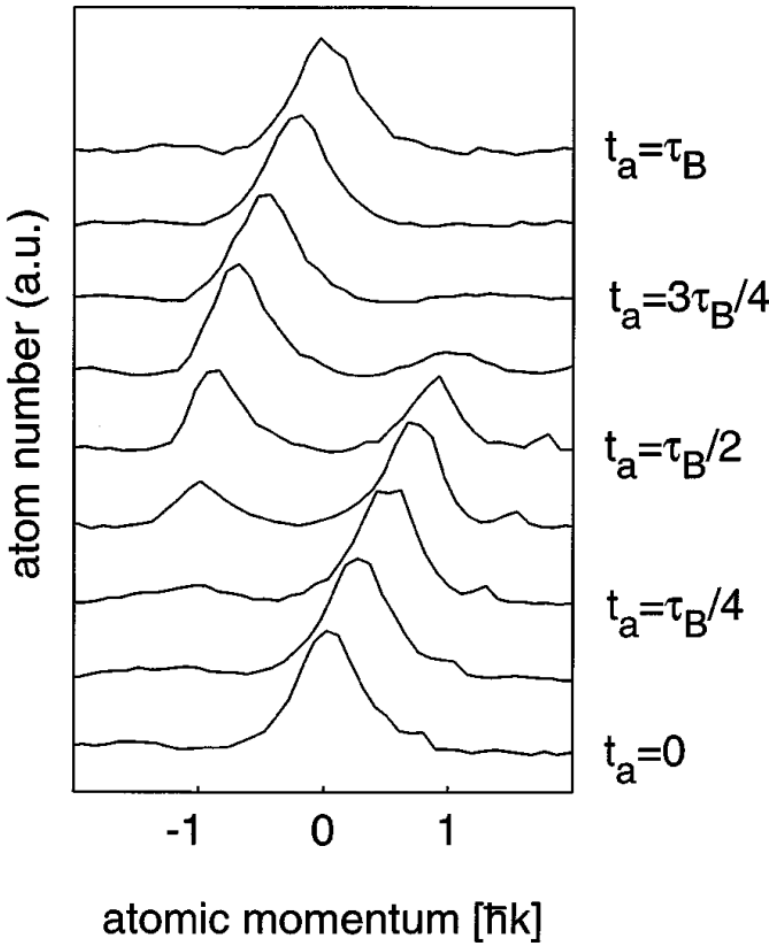
Bloch state $\psi(x, 0) = \mathrm{e}^{\mathrm{i}q_i x} u(x, 0) \quad \rightarrow \quad$ Bloch state $\psi(x, t) = \mathrm{e}^{\mathrm{i}q(t)x} u(x, t)$.

Bloch oscillations

If the force F is weak enough, the system will stay in the ground band, with

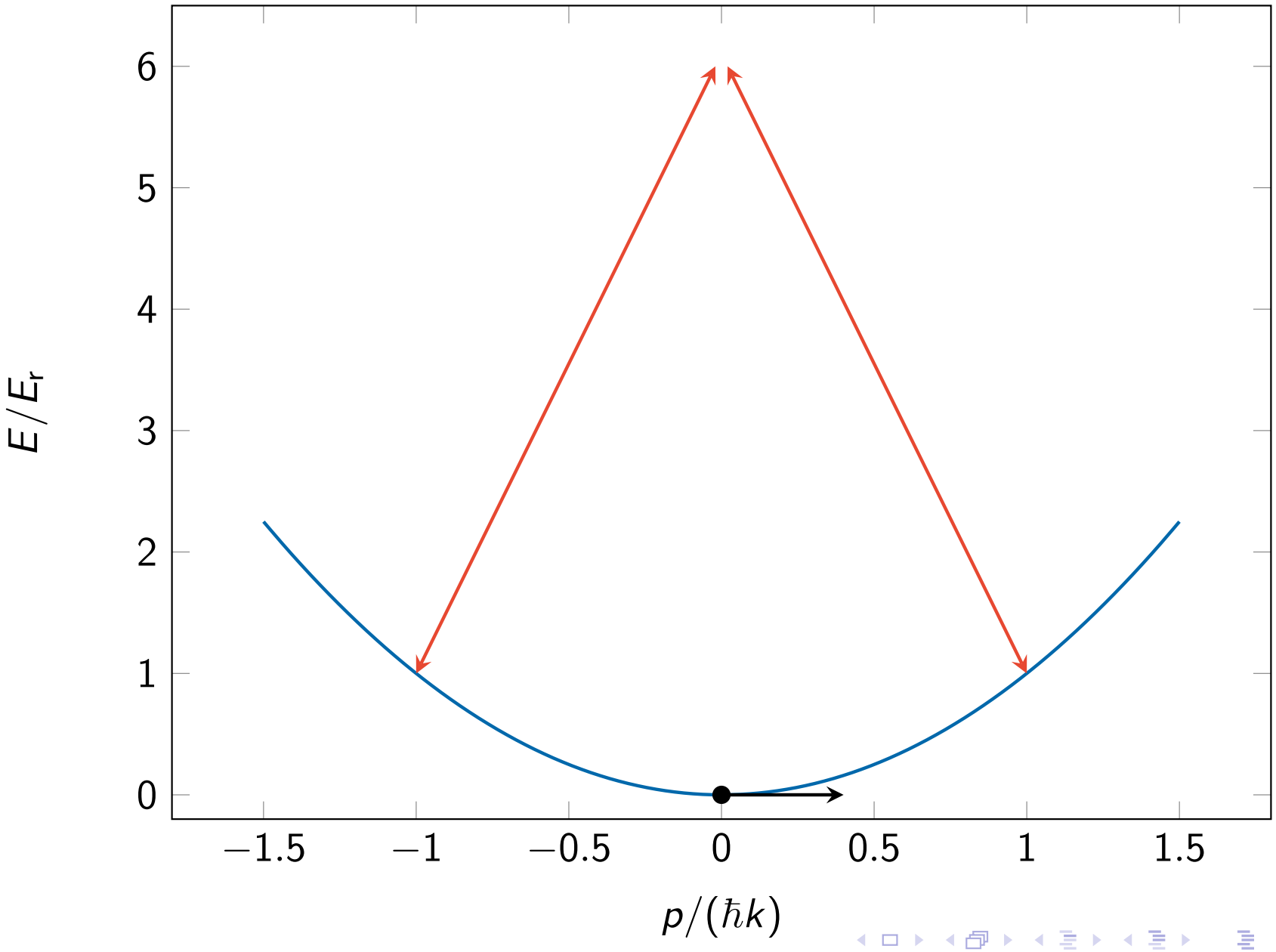
$$q(t) = q_i + Ft/\hbar.$$

The evolution is thus periodic, of period $T = 2\hbar k/F$.

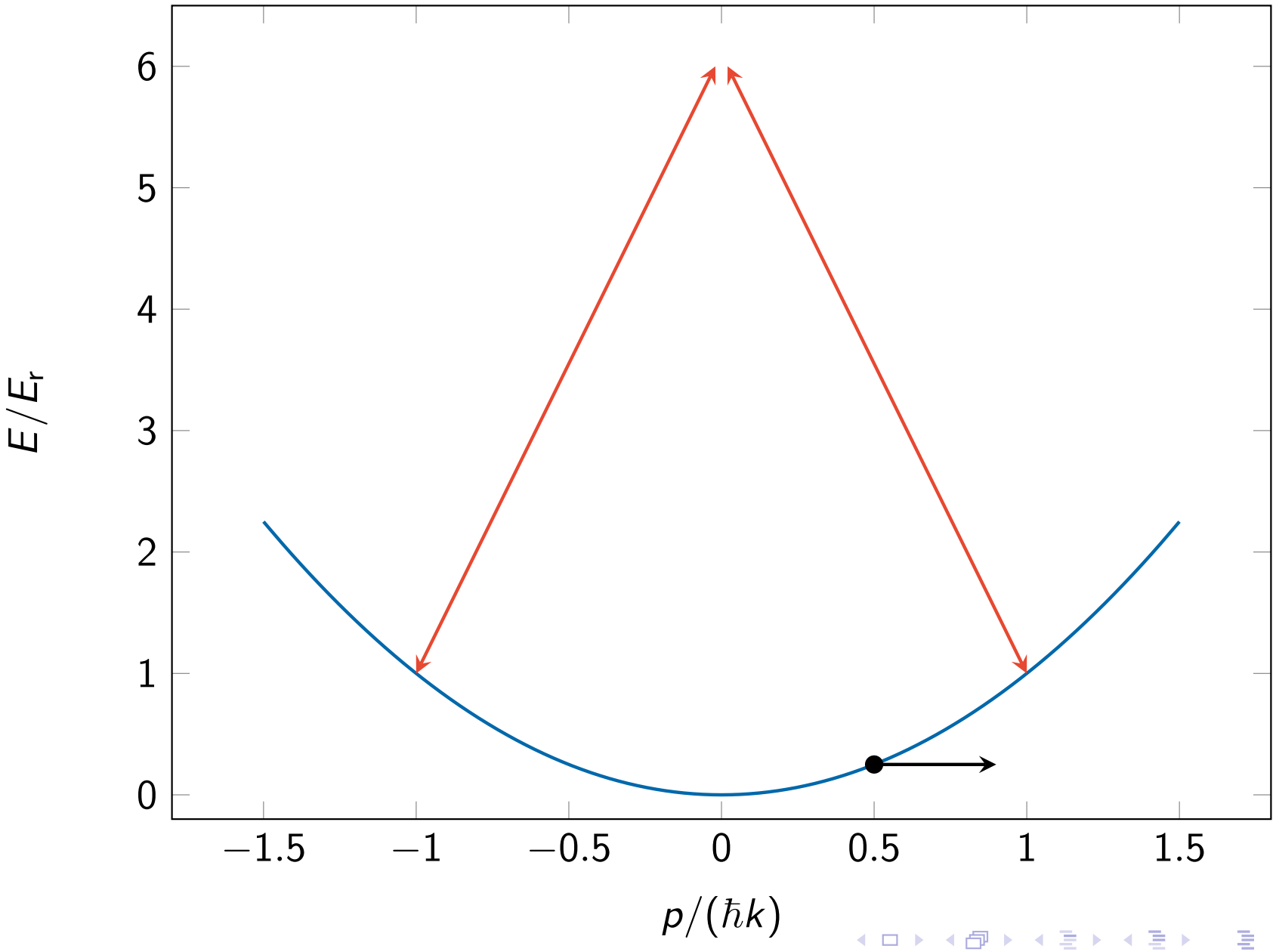


Ben Dahan et al, PRL 1996

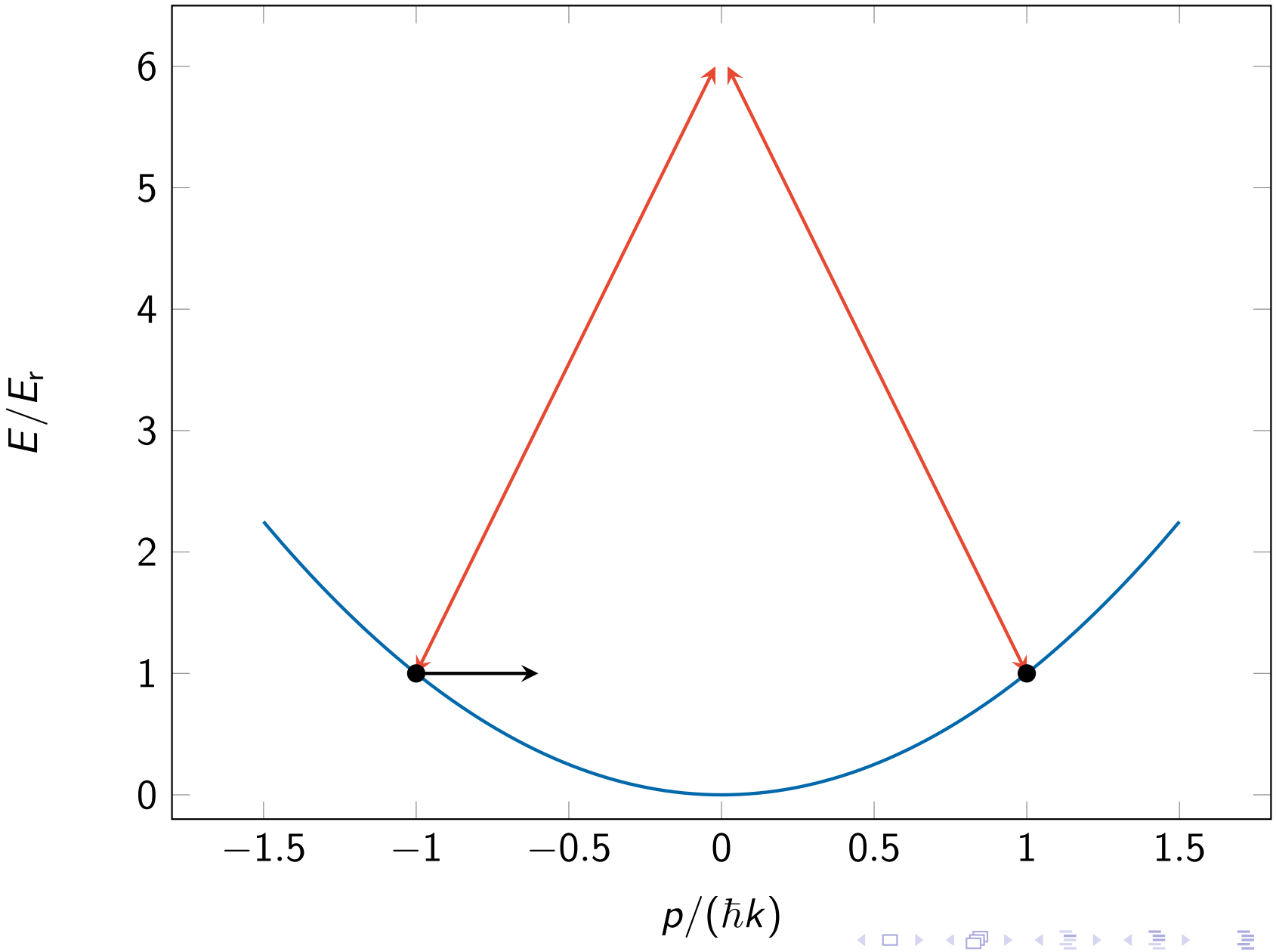
Interpretation in terms of Bragg scattering



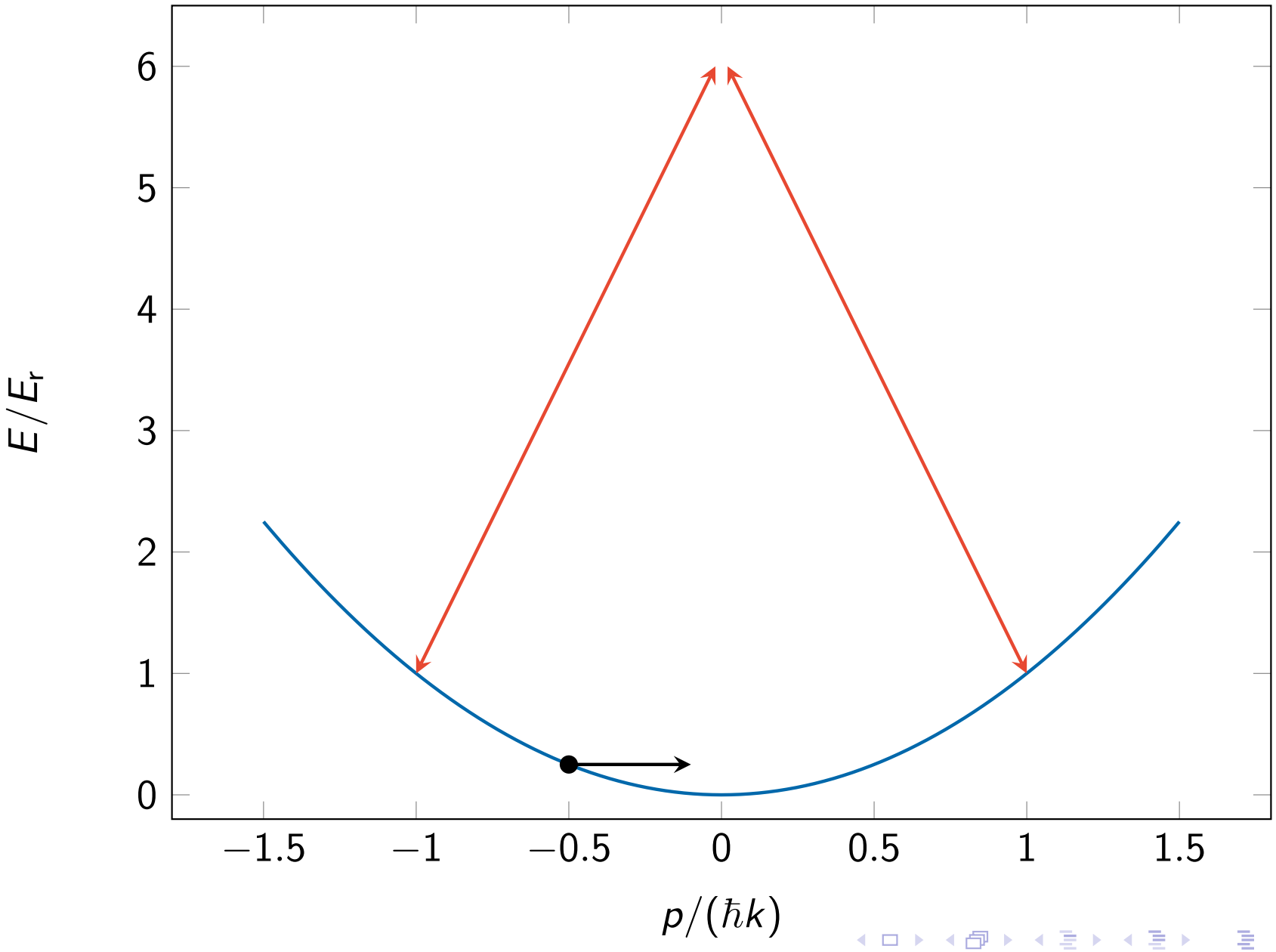
Interpretation in terms of Bragg scattering



Interpretation in terms of Bragg scattering



Interpretation in terms of Bragg scattering



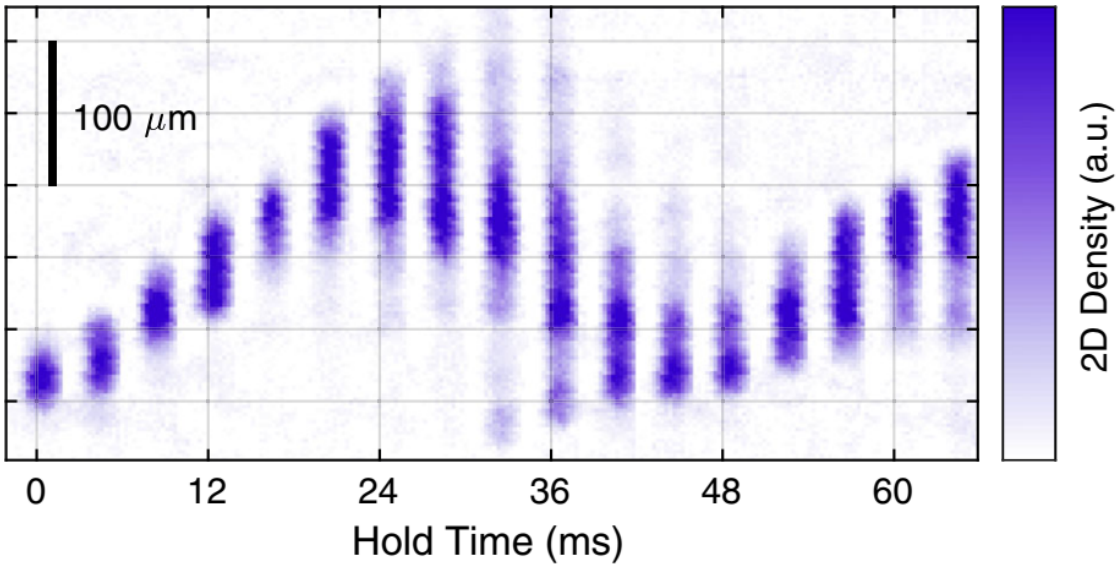
Amplitude in real space

The center of mass evolves as

$$\frac{\mathrm{d}\bar{x}}{\mathrm{d}t} = v_g = \frac{1}{\hbar}\frac{\mathrm{d}E_0(q)}{\mathrm{d}q}.$$

As $q(t)$ evolves as $q(t) = q_i + Ft/\hbar$ one obtains

$$\bar{x}(t) - \bar{x}(0) = \frac{1}{\hbar}\int_0^t \frac{\mathrm{d}E_0(q)}{\mathrm{d}q}\mathrm{d}t = \frac{1}{F}[E_0(q(t)) - E_0(q_i)].$$



Geiger et al, PRL 2018

For deep lattices: almost flat band → small real-space oscillation

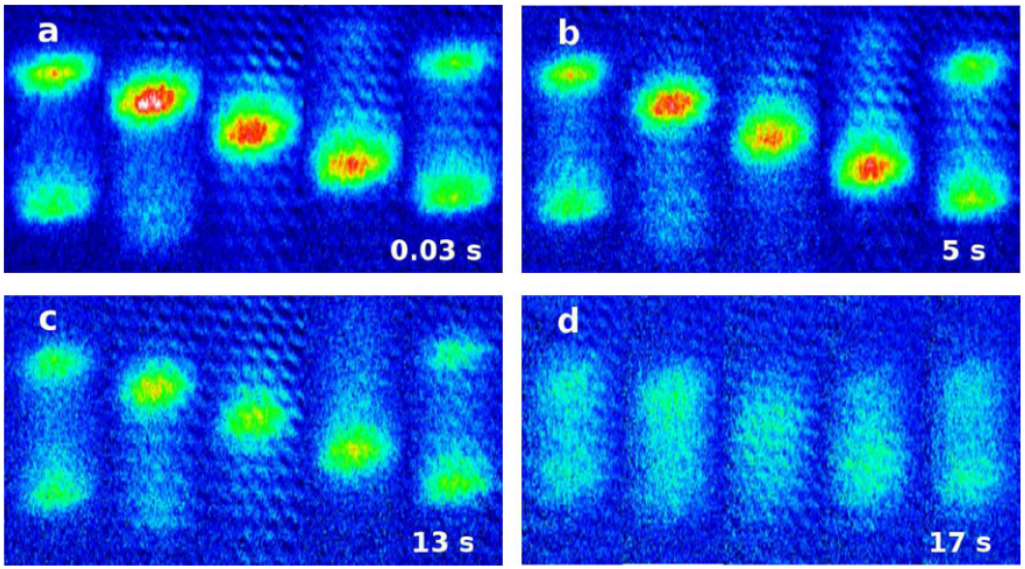
Metrology based on Bloch oscillations

Measuring the period of Bloch oscillations

$$T = 2\hbar k/F$$

is very efficient to measure a force with high precision.

Example of a gravimeter



Poli et al, PRL 2011

Up to 10^4 measured oscillations $\rightarrow$ uncertainty $\Delta g/g \sim 10^{-7}$.

Bloch oscillations in an accelerated lattice

The interference between two beams of different frequencies produces a moving optical lattice

$$V(x,t) = V_0 \sin^2(kx - (\omega - \omega')t/2).$$

Sweeping the frequency produces an accelerated lattice
$\rightarrow$ inertial force in the lattice frame of reference.

Bloch oscillations in an accelerated lattice

The interference between two beams of different frequencies produces a moving optical lattice

$$V(x,t) = V_0 \sin^2(kx - (\omega - \omega')t/2).$$

Sweeping the frequency produces an accelerated lattice
$\rightarrow$ inertial force in the lattice frame of reference.

Each Bloch oscillation corresponds to the gain of a momentum $2\hbar k$ in the laboratory frame.

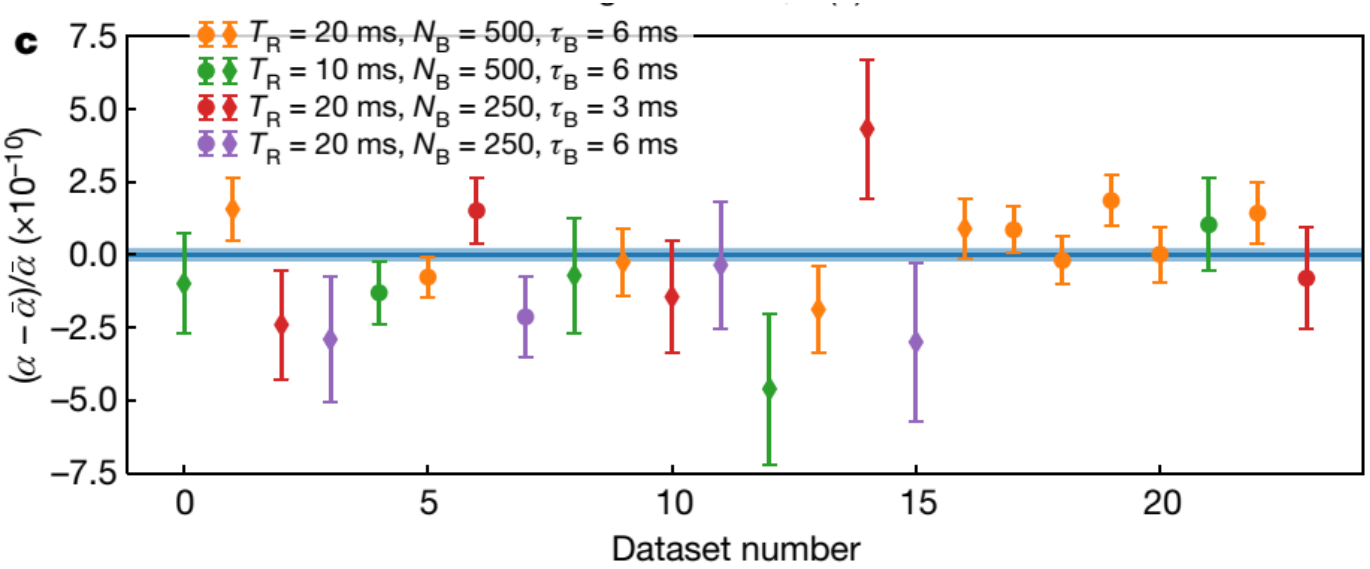
Bloch oscillations in an accelerated lattice

The interference between two beams of different frequencies produces a moving optical lattice

$$V(x,t) = V_0 \sin^2(kx - (\omega - \omega')t/2).$$

Sweeping the frequency produces an accelerated lattice
$\rightarrow$ inertial force in the lattice frame of reference.

Each Bloch oscillation corresponds to the gain of a momentum $2\hbar k$ in the laboratory frame.
Many cycles $\rightarrow$ high precision spectroscopy of $\hbar k/m$.



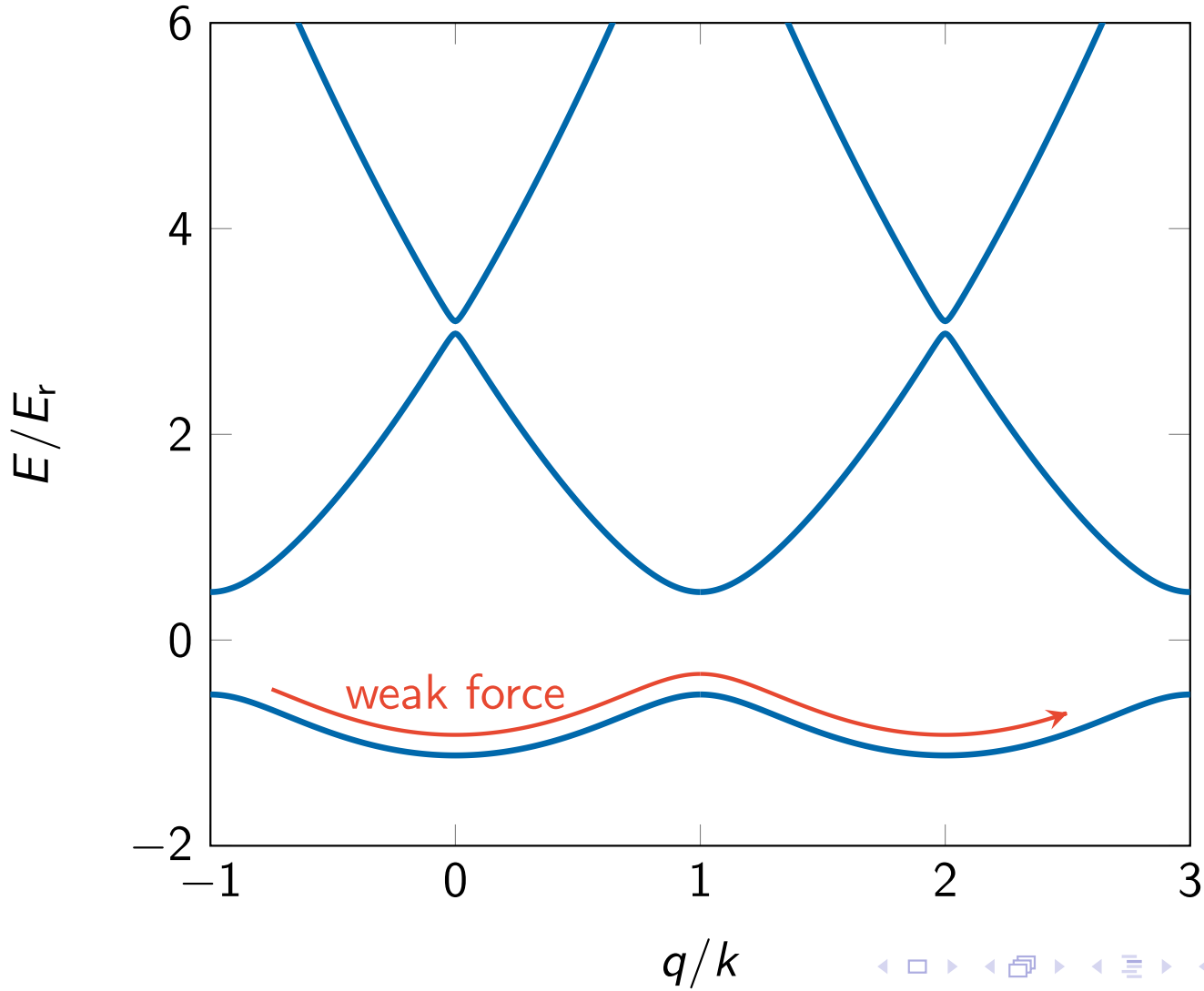
Morel et al, Nature 2020

allows measuring the fine structure constant $\alpha = 1/137.035999206(11)$.

Landau Zener transitions

If the force is too large the system will not remain in the lowest Bloch band.

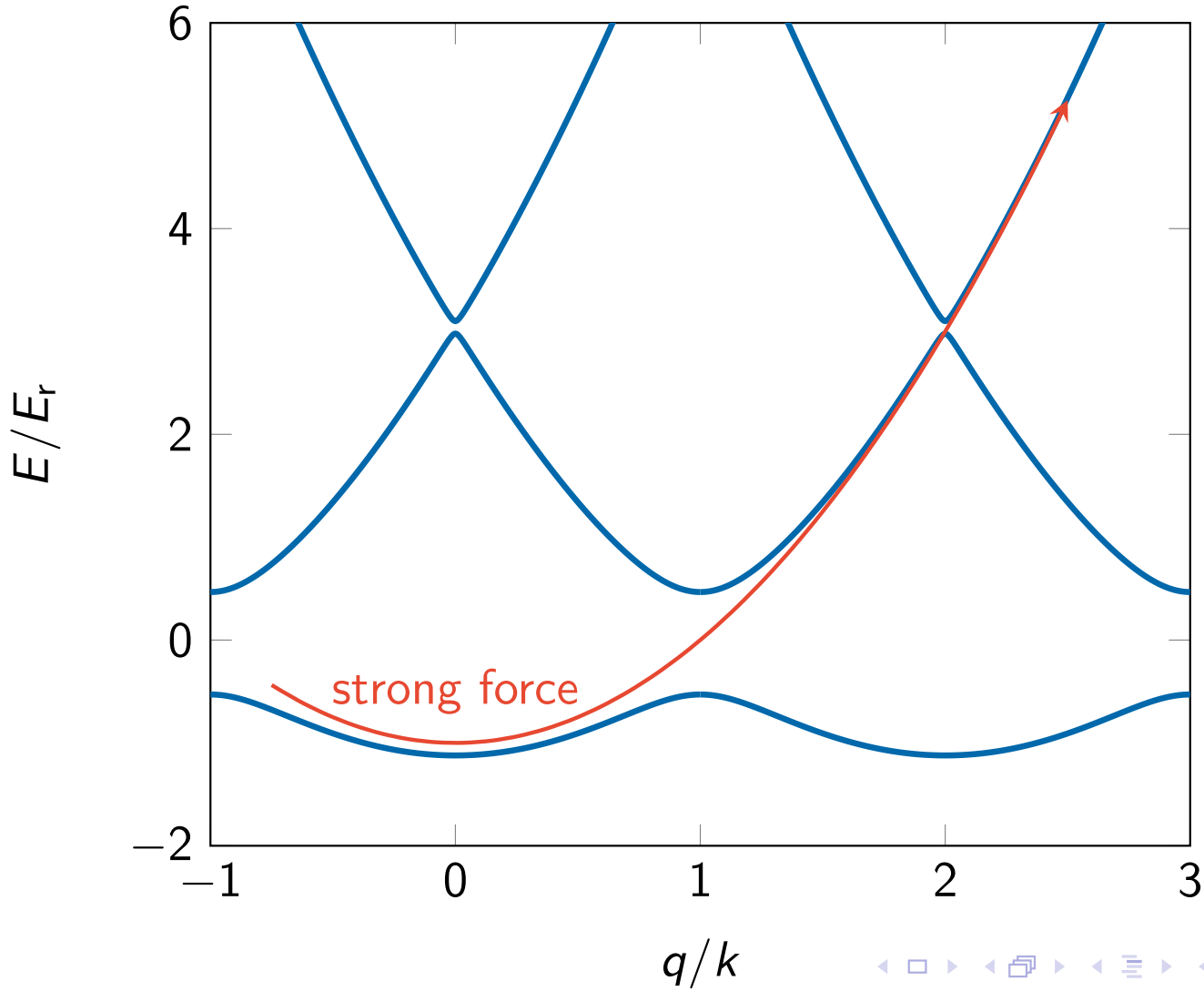
Example: bandstructure for $V_0 = 2E_r$.



Landau Zener transitions

If the force is too large the system will not remain in the lowest Bloch band.

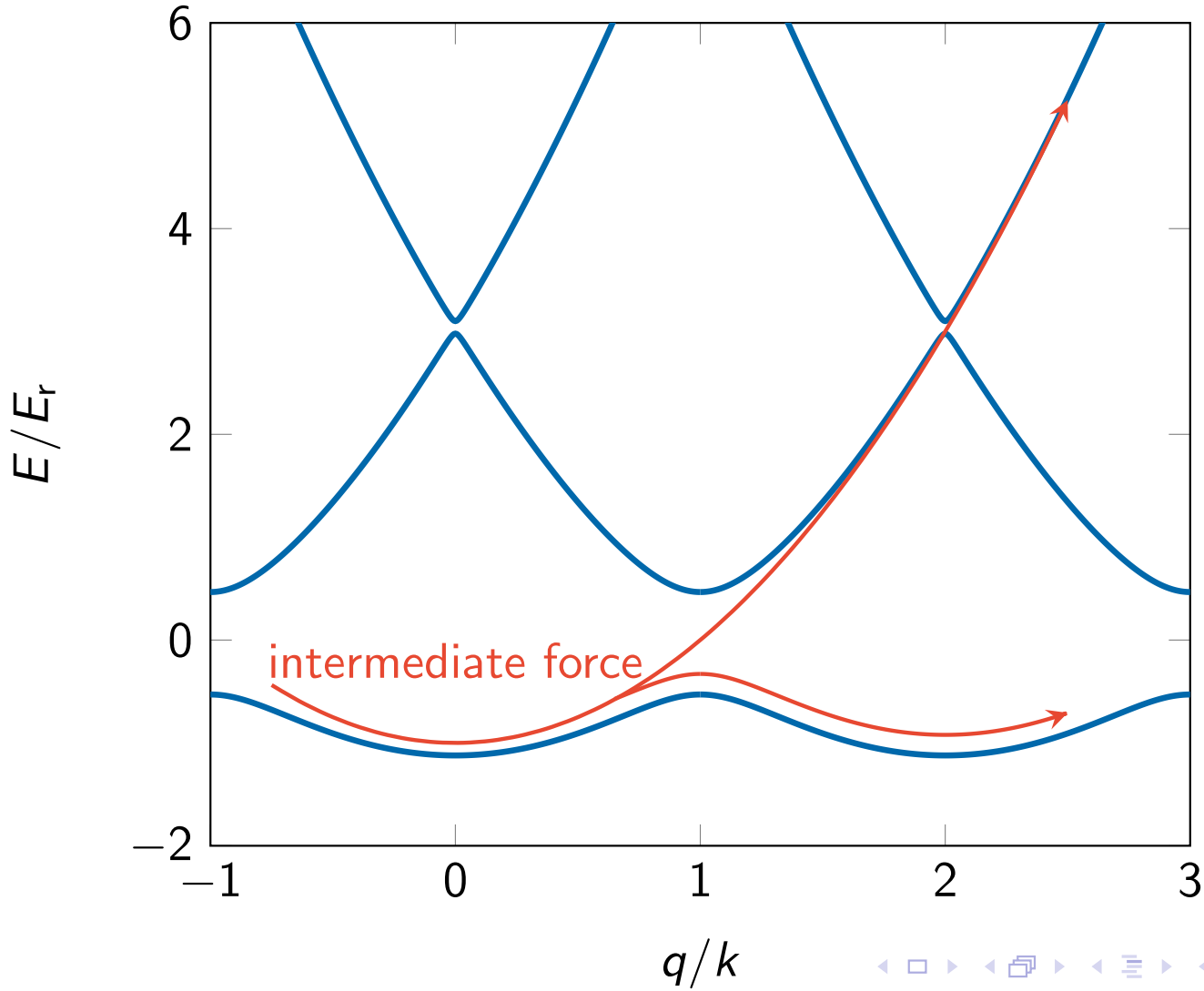
Example: bandstructure for $V_0 = 2E_r$.



Landau Zener transitions

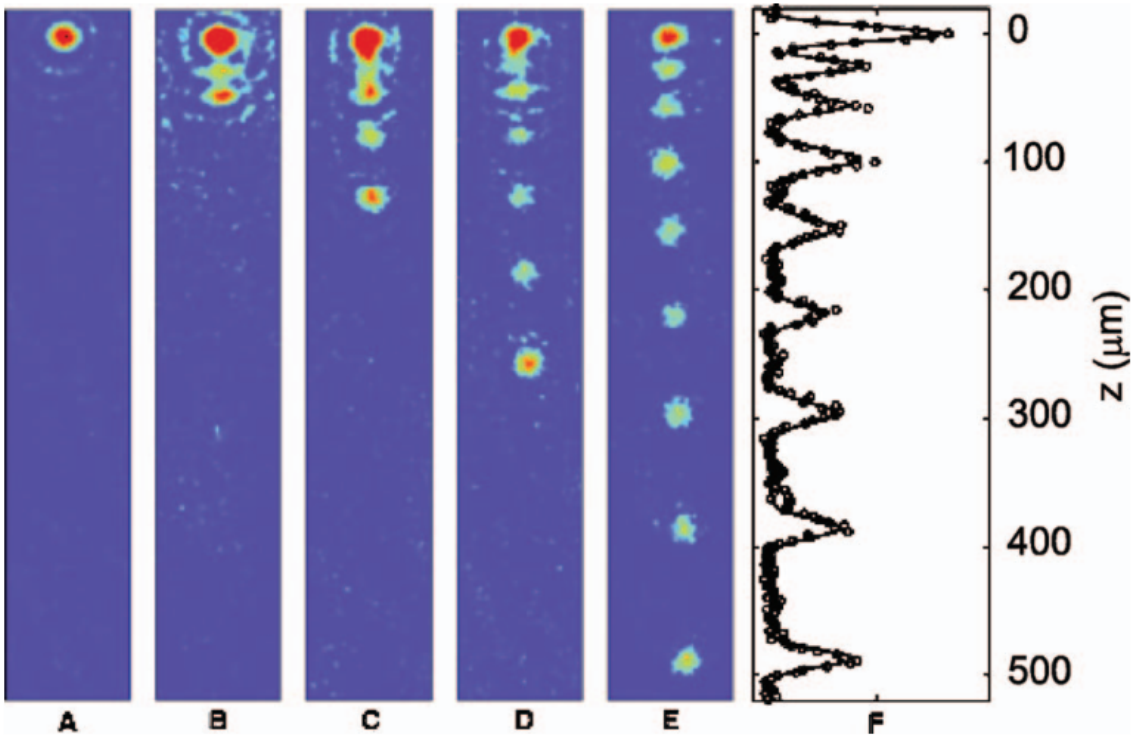
If the force is too large the system will not remain in the lowest Bloch band.

Example: bandstructure for $V_0 = 2E_r$.



Landau Zener transitions

Successive LZ transitions each time the avoided crossing is met.



Anderson et al, Science 1998

Other possibilites:

- preparing coherent superposition of Bloch bands,
- interference effect when the LZ transition can happen twice $\rightarrow$ Stückelberg oscillations.

Outline

1. Band structure and dynamics in optical lattices
   - Band structure in one dimension
   - Dynamics of a particle in an optical lattice
   - Wannier functions and tight-binding limit
   - Complex lattices in 1D: SSH model
   - Complex lattices in 2D: graphene and quantum Hall bands
2. Superfluid/Mott insulator transition
   - Hubbard Hamiltonian
   - Superfluid/Mott insulator: phase diagram
   - Gutzwiller variational approach
   - Interference experiments
   - Transport experiments
   - Mott shell structure
   - Low-energy excitations
3. Fermi-Hubbard model and quantum magnetism
   - Attractive Fermi-Hubbard model
   - Repulsive Fermi-Hubbard model and Mott insulator
   - Quantum magnetism

Wannier functions

- Bloch function are the equivalent of plane waves in a lattice potential.
- We want to define the equivalent of ‘position eigenstates’ within a given Bloch band.

Wannier functions

- Bloch function are the equivalent of plane waves in a lattice potential.
- We want to define the equivalent of 'position eigenstates' within a given Bloch band.

For a given Bloch band n, the most localized states corresponds to a Wannier function

$$w_{n,j}(x) = \frac{1}{\sqrt{2k}} \int_{-k}^{k} \psi_{n,q}(x) \mathrm{e}^{-\mathrm{i}jaq} \mathrm{d}q,$$

where $a = \lambda/2$. It corresponds to a state localized around $x_j = ja$.

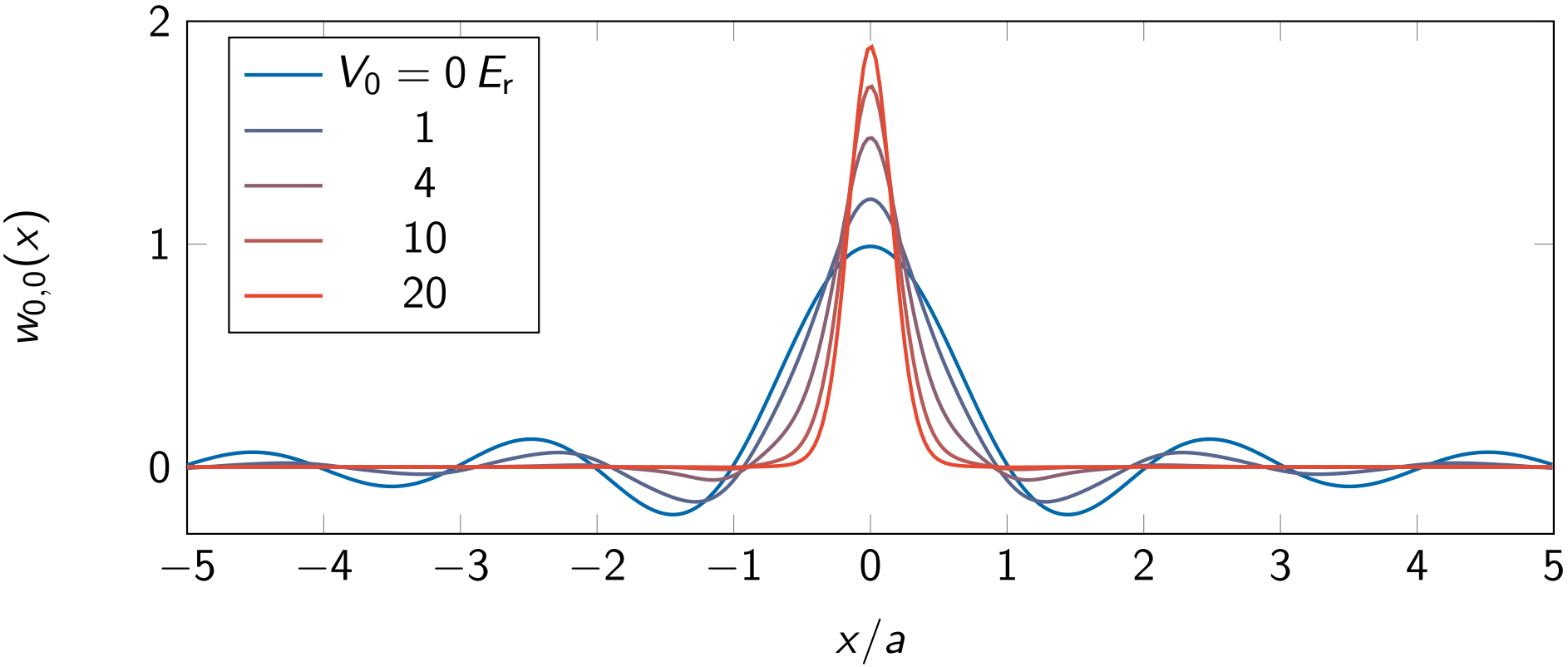
Orthogonality relation

$$\int w^*_{n,j}(x) w_{n',j'}(x) \mathrm{d}x = \delta_{n,n'} \delta_{j,j'}.$$

Wannier functions of the same band are related by a translation as

$$w_{n,j}(x) = w_{n,0}(x - ja).$$

Wannier functions



For $V_0 \gg E_r$ the Wannier function is mostly localized within a single lattice well.

Its shape is close to the gaussian ground state expected from a harmonic expansion of the well bottom.

Hamiltonian in the Wannier basis

The Hamiltonian can be written in the Wannier basis as

$$H = \sum_n \sum_{j,j'} J_n(j-j') a^\dagger_{n,j} a_{n,j'},$$

where $a_{n,j}$ annihilates a particle in the Wannier state $w_{n,j}$.

The Hamiltonian does not couple the different bands but couples a priori all Wannier states. The coefficient $J_n(j-j')$ is the tunneling amplitude between sites j and j'. It can be expressed as

$$J_n(j) = \int w^*_{n,j}(x) \left[\frac{-\hbar^2}{2m} \Delta + V(x) \right] w_{n,0}(x) \mathrm{d}x.$$

Tight-binding limit

For $V_0 \gg E_r$ the Wannier functions are strongly localized in a given well, and different Wannier functions are weakly coupled.

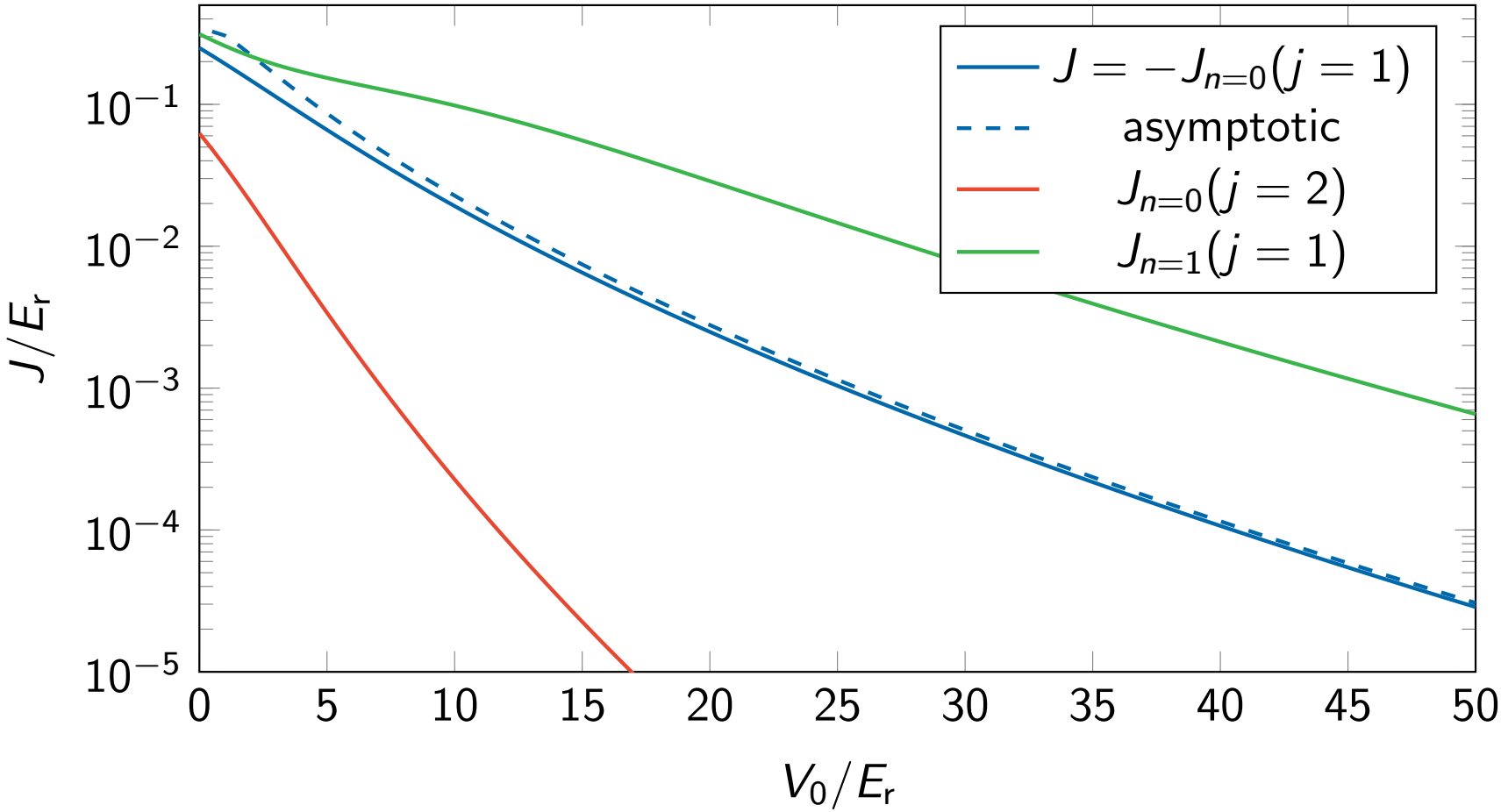
- The tunneling between nearest neighbours $J = -J_0(1) > 0$ dominates over longer-range tunneling.
- Asymptotic expression

$$J = \frac{4}{\sqrt{\pi}} \left(\frac{V_0}{E_r}\right)^{3/4} \exp\left[-2\left(\frac{V_0}{E_r}\right)^{1/2}\right] E_r.$$

  The exponential suppression is typical of quantum tunneling through a barrier.
- The tunneling is directly related to the band width, as the dispersion relation reads

$$E_{0,q} = -2J \cos(\pi q/k).$$

Tunneling rate in the tight-binding limit



For $V \gtrsim 5\,E_r$ the lowest-band dynamics can be restricted to

$$H = -J \sum_j \left(a^\dagger_{0,j} a_{0,j+1} + \text{h.c.} \right).$$

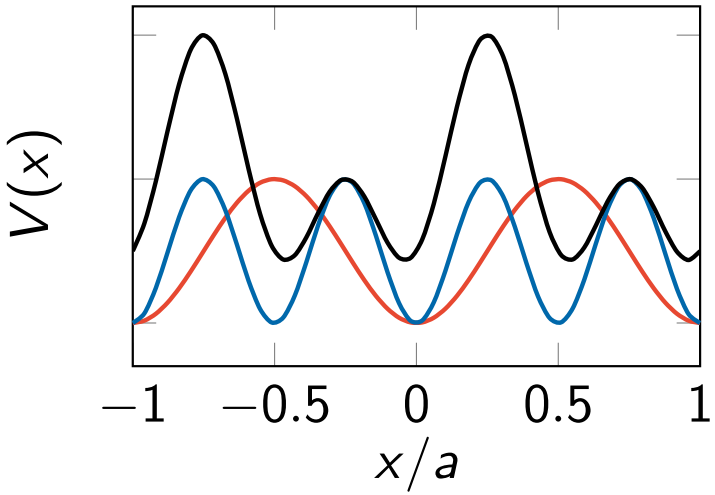
Outline

1. Band structure and dynamics in optical lattices
   - Band structure in one dimension
   - Dynamics of a particle in an optical lattice
   - Wannier functions and tight-binding limit
   - Complex lattices in 1D: SSH model
   - Complex lattices in 2D: graphene and quantum Hall bands
2. Superfluid/Mott insulator transition
   - Hubbard Hamiltonian
   - Superfluid/Mott insulator: phase diagram
   - Gutzwiller variational approach
   - Interference experiments
   - Transport experiments
   - Mott shell structure
   - Low-energy excitations
3. Fermi-Hubbard model and quantum magnetism
   - Attractive Fermi-Hubbard model
   - Repulsive Fermi-Hubbard model and Mott insulator
   - Quantum magnetism

1D superlattice potential

Can be obtained by summing two-color lattice potentials of wavelength λ and $\lambda/2$

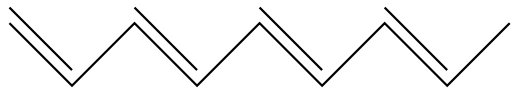
$$V(x) = V_1 \sin^2(kx) + V_2 \sin^2(2kx + \phi).$$

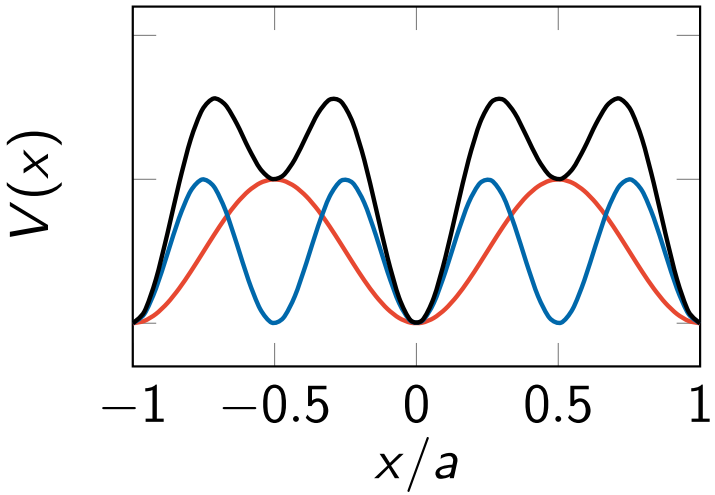


$\phi = \pi/2$

lattice of double-wells

analog of polyacetylene



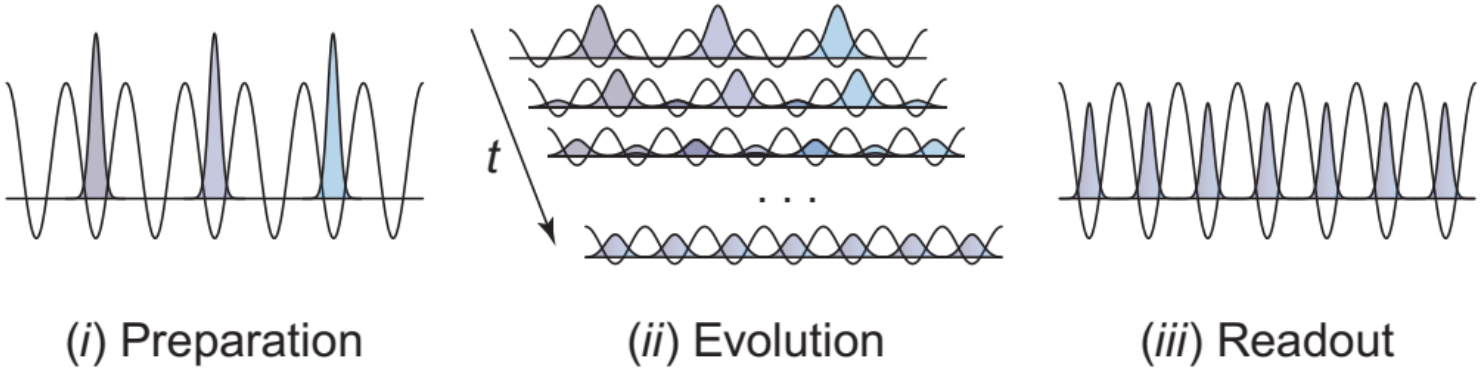


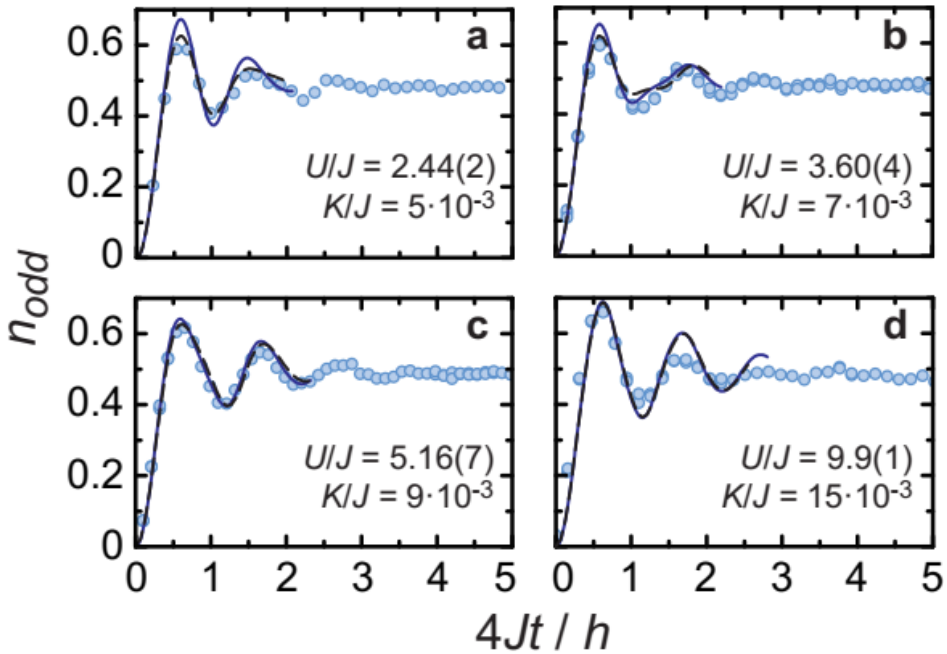
$\phi = 0$

staggered energy offsets

1D superlattice potential: application

Allows imprinting a density pattern and monitor its evolution.

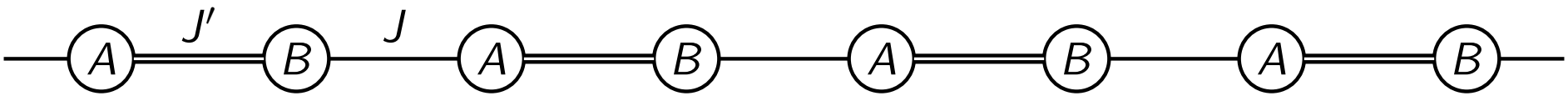




Trotzky et al, Nature Phys. 2012

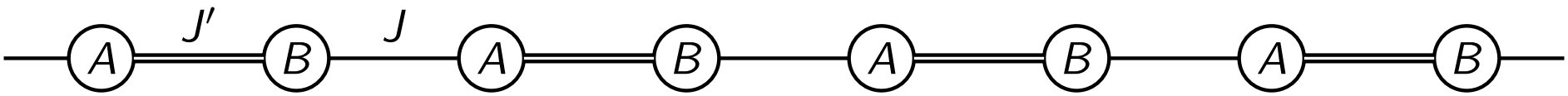
Band structure of the SSH model

We come back to the lattice of double-wells



Band structure of the SSH model

We come back to the lattice of double-wells



One looks for Bloch eigenstates

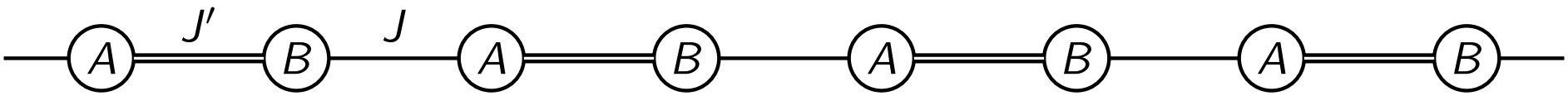
$$|\psi\rangle_q = \sum_j \mathrm{e}^{\mathrm{i}qja}(\alpha_q |A_j\rangle + \beta_q |B_j\rangle),$$

solutions of the eigensystem

$$-\begin{pmatrix} 0 & J' + J\mathrm{e}^{-\mathrm{i}qa} \\ J' + J\mathrm{e}^{\mathrm{i}qa} & 0 \end{pmatrix} \begin{pmatrix} \alpha_q \\ \beta_q \end{pmatrix} = E_q \begin{pmatrix} \alpha_q \\ \beta_q \end{pmatrix}.$$

Band structure of the SSH model

We come back to the lattice of double-wells



One looks for Bloch eigenstates

$$|\psi\rangle_q = \sum_j \mathrm{e}^{\mathrm{i}qja}(\alpha_q |A_j\rangle + \beta_q |B_j\rangle),$$

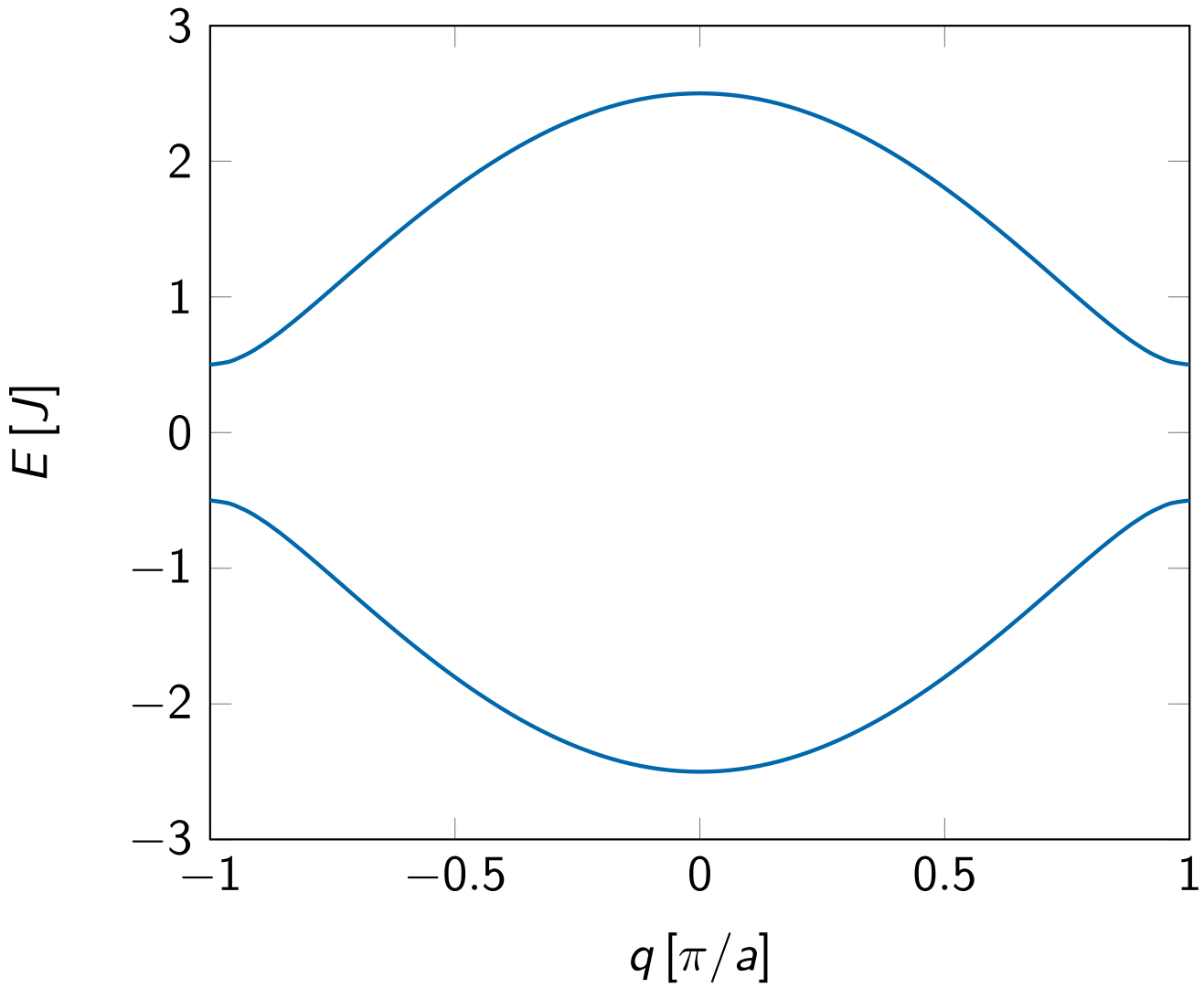
solutions of the eigensystem

$$-\begin{pmatrix} 0 & J' + J\mathrm{e}^{-\mathrm{i}qa} \\ J' + J\mathrm{e}^{\mathrm{i}qa} & 0 \end{pmatrix} \begin{pmatrix} \alpha_q \\ \beta_q \end{pmatrix} = E_q \begin{pmatrix} \alpha_q \\ \beta_q \end{pmatrix}.$$

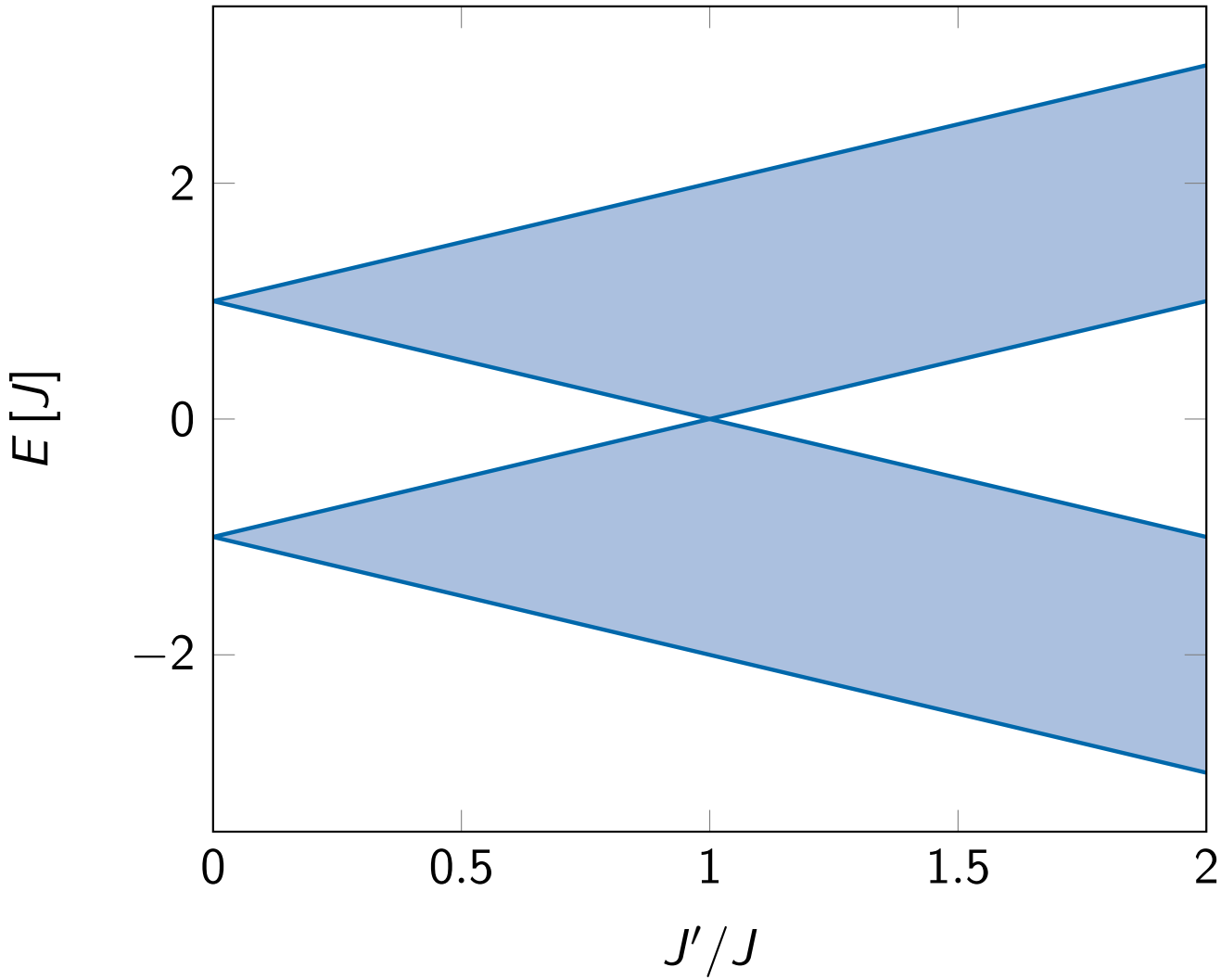
Dispersion relation

$$E_q = \pm\sqrt{J^2 + J'^2 + 2JJ'\cos(qa)}.$$

Example of dispersion relation ($J' = 1.5\,J$)



Spectrum versus J'/J

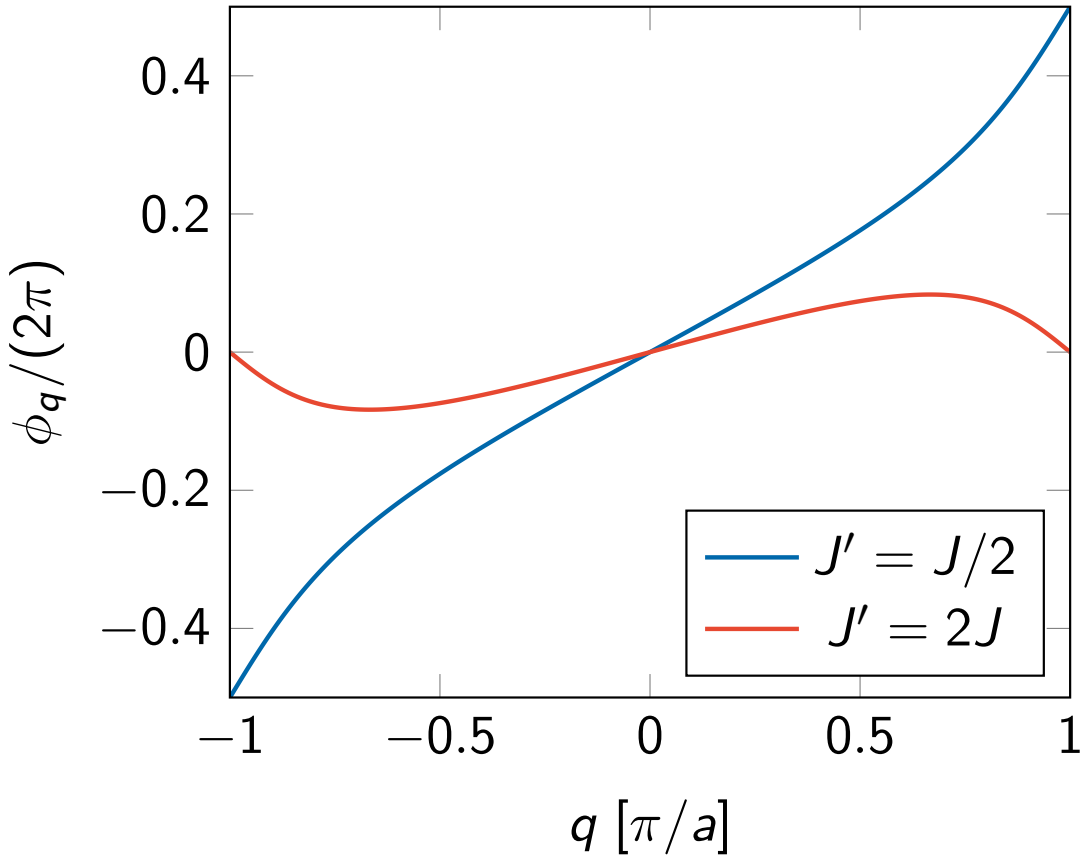


Topological Zak phase

The eigenstates can be written as

$$|u_q\rangle = \frac{1}{\sqrt{2}} \begin{pmatrix} 1 \\ e^{i\phi_q} \end{pmatrix}, \quad e^{i\phi_q} = \frac{J' + Je^{iqa}}{|J' + Je^{iqa}|}.$$

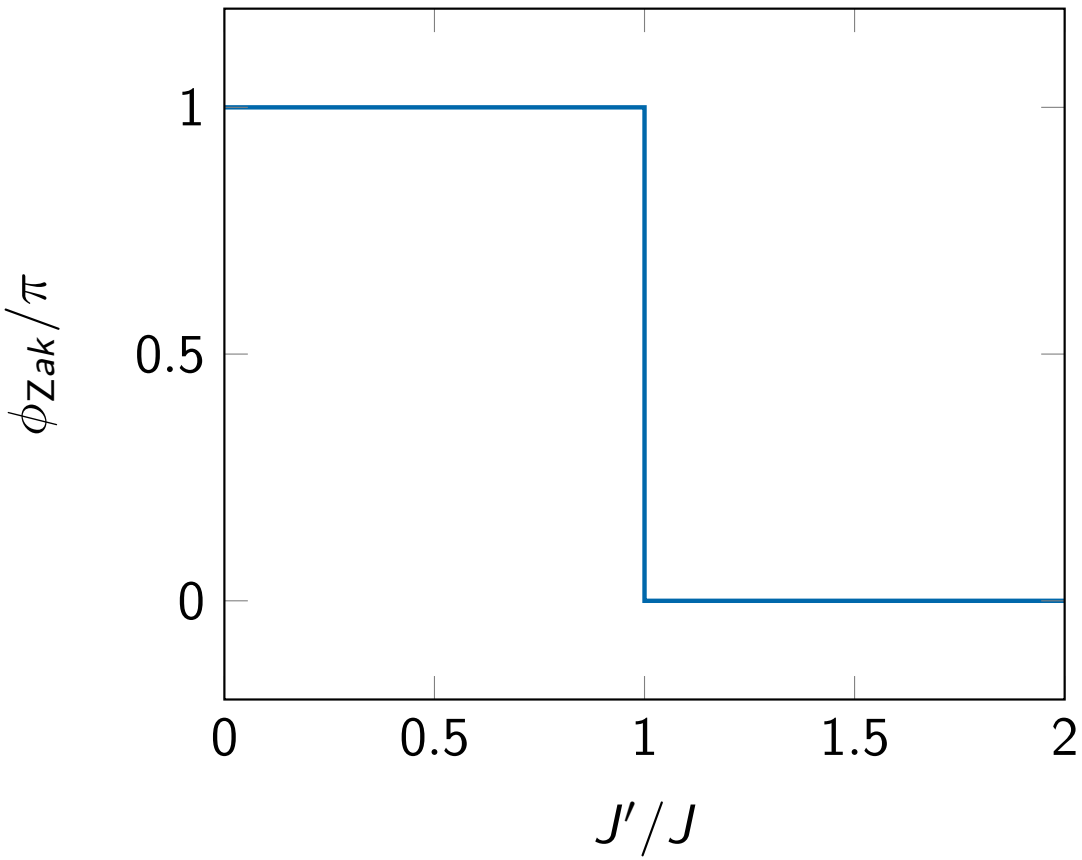
ϕ_q is well defined over the Brillouin Zone except for $J' = J$ (where the gap closes).



Topological Zak phase versus J'/J

Zak phase: Berry phase across the Brillouin zone, set by the winding number W of ϕ_q

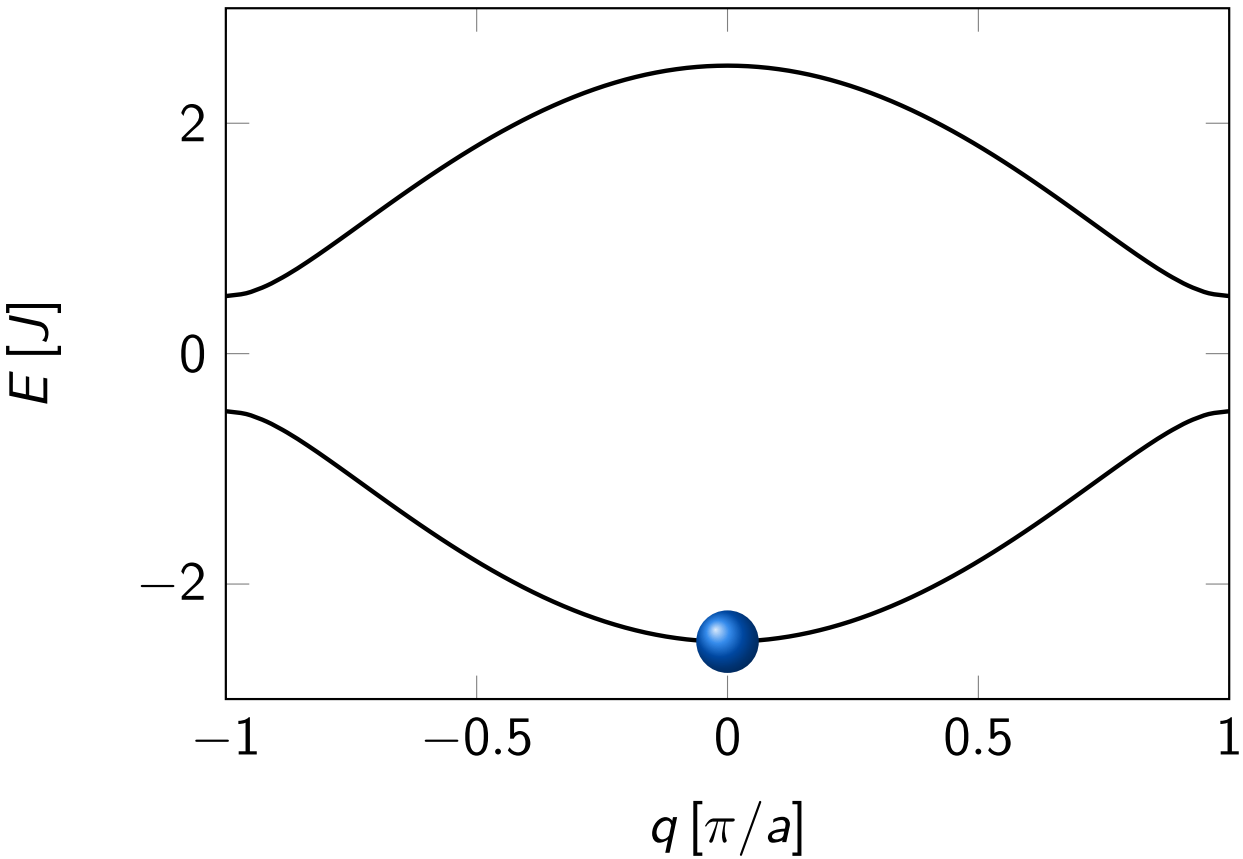
$$\phi_{\mathrm{Zak}} = \mathrm{i}\int \mathrm{d}q\,\langle u_q|\partial_q u_q\rangle = -\frac{1}{2}\int \mathrm{d}q\,\frac{\mathrm{d}\phi_q}{\mathrm{d}q} = \pi W \pmod{2\pi}.$$



Zak phase measurement

Mach-Zehnder interferometry

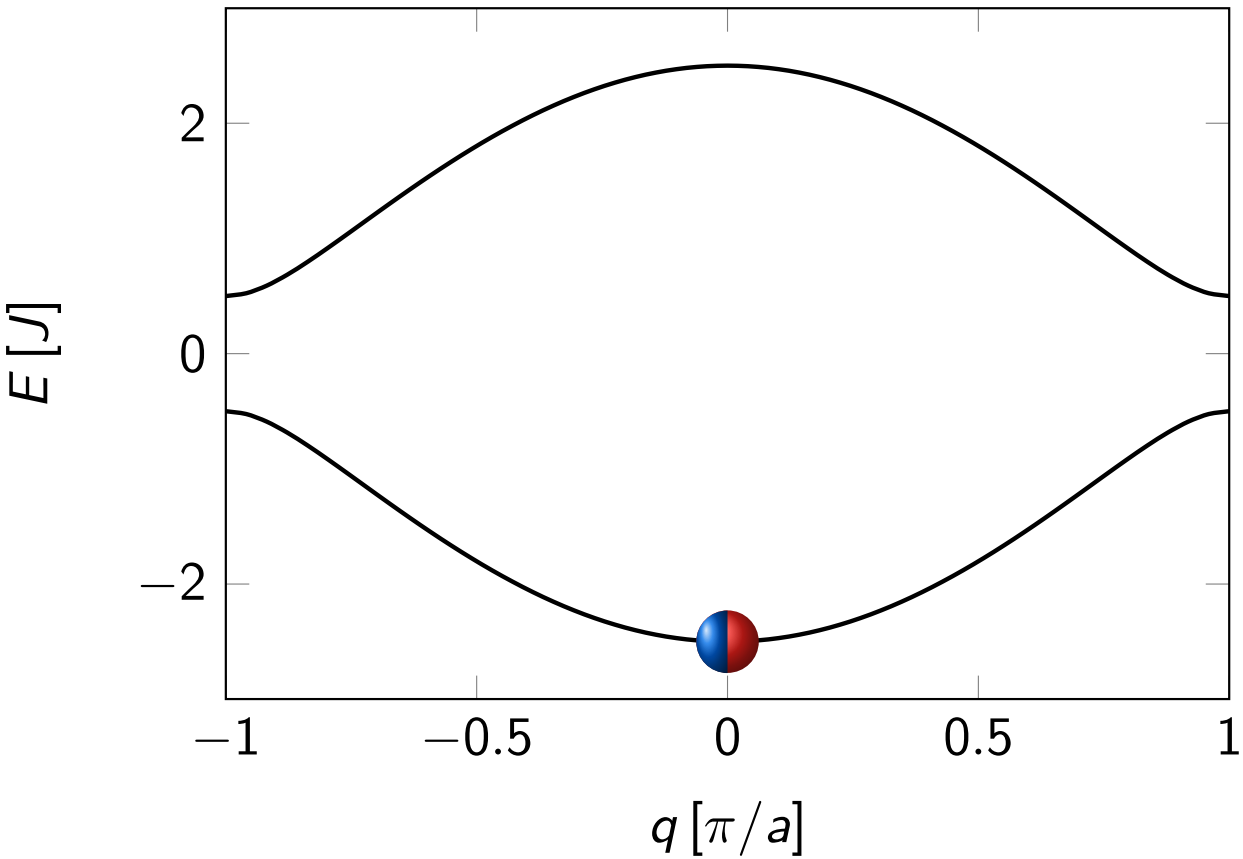
1. Initialize the system in $|q = 0, \uparrow\rangle$



Zak phase measurement

Mach-Zehnder interferometry

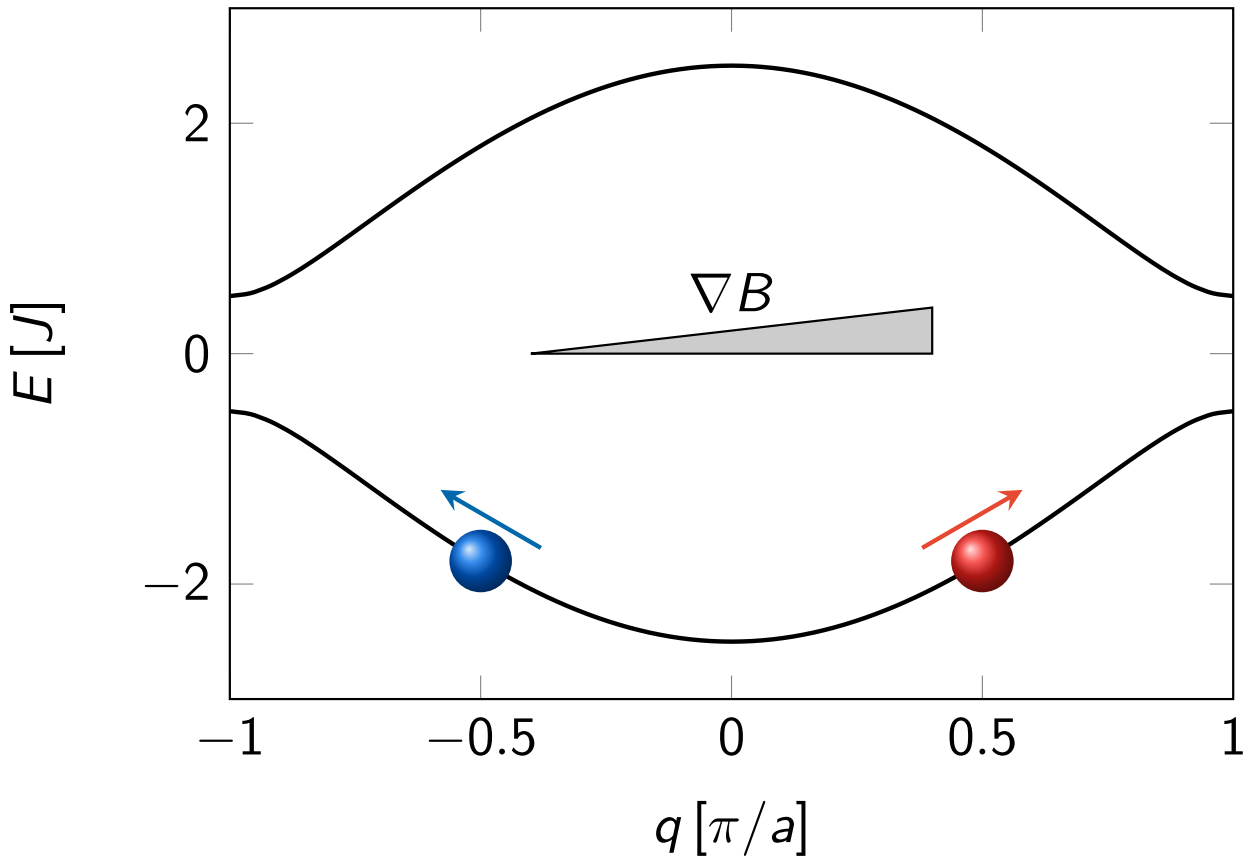
1. Initialize the system in $|q = 0, \uparrow\rangle$
2. $\pi/2$ pulse



Zak phase measurement

Mach-Zehnder interferometry

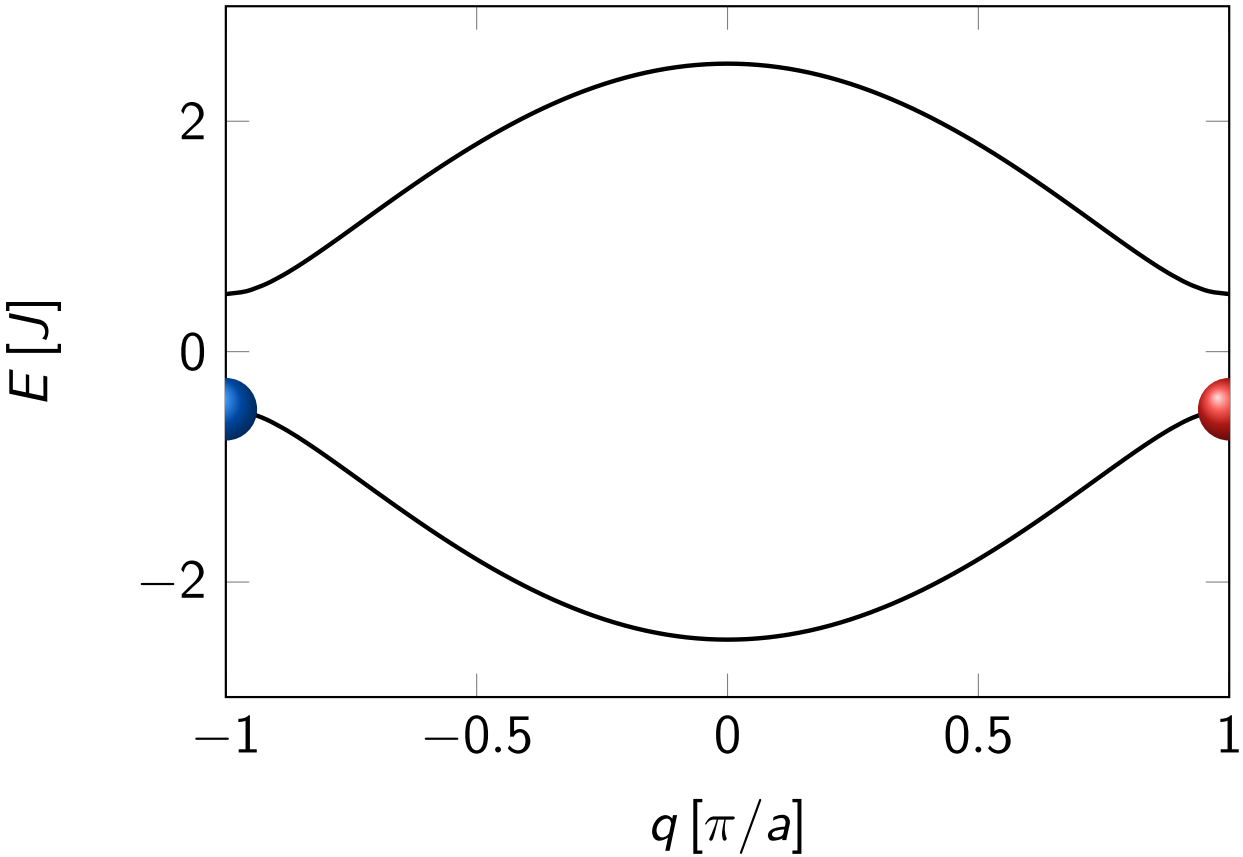
1. Initialize the system in $|q = 0, \uparrow\rangle$
2. $\pi/2$ pulse
3. Differential motion in the ground band using a magnetic field gradient



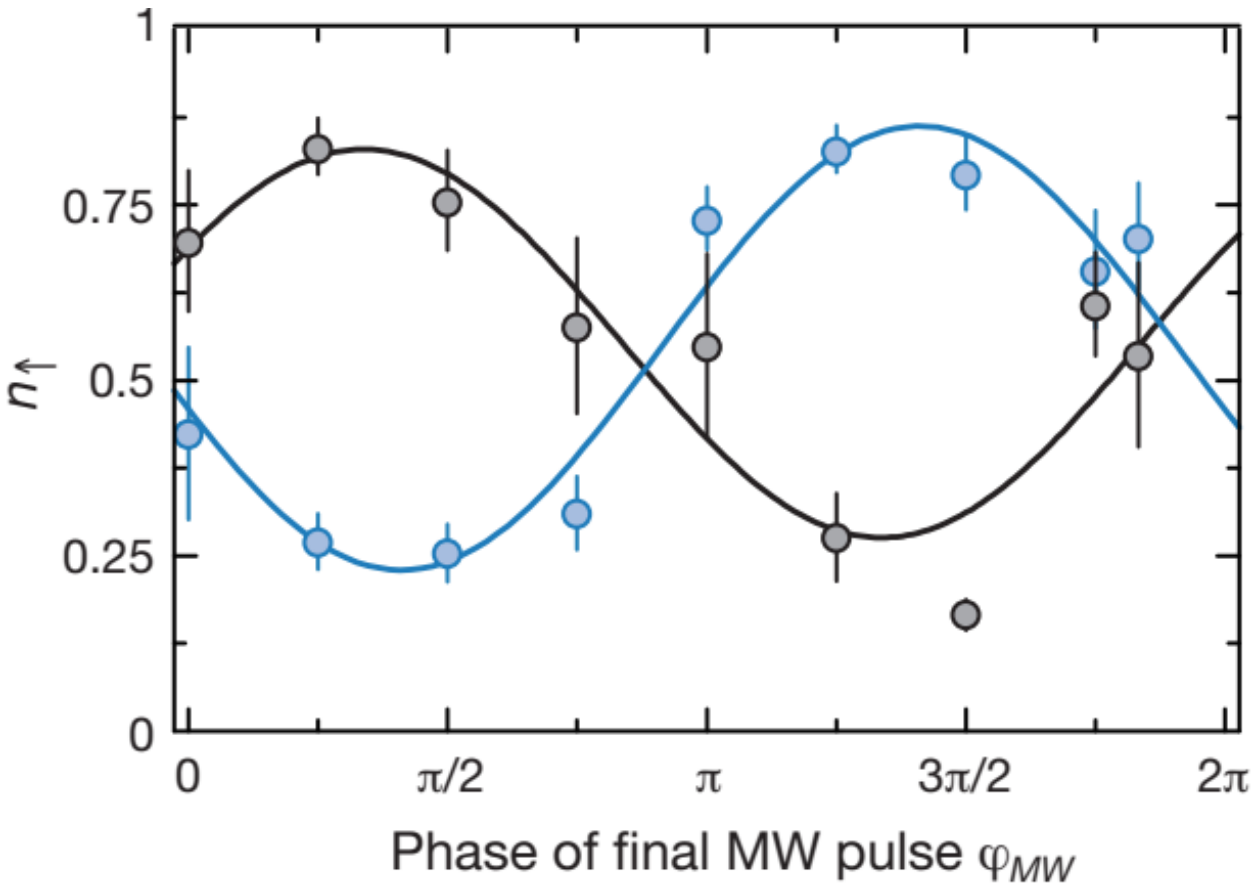
Zak phase measurement

Mach-Zehnder interferometry

1. Initialize the system in $|q = 0, \uparrow\rangle$
2. $\pi/2$ pulse
3. Differential motion in the ground band using a magnetic field gradient
4. $\pi/2$ pulse + measure population in $|\uparrow\rangle$



Zak phase measurement



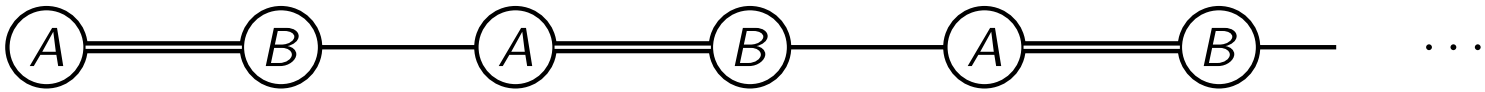
Phase shifts between the two phases $J > J'$ and $J < J'$

$$\delta\phi_{Zak} = 0.97(2)\pi.$$

Atala et al, Nature Phys. (2013)

Topological edge mode

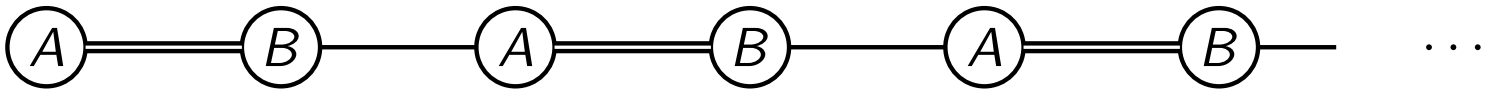
We cut the 1D lattice: semi-infinite geometry



What is the spectrum of eigenstates?

Topological edge mode

We cut the 1D lattice: semi-infinite geometry

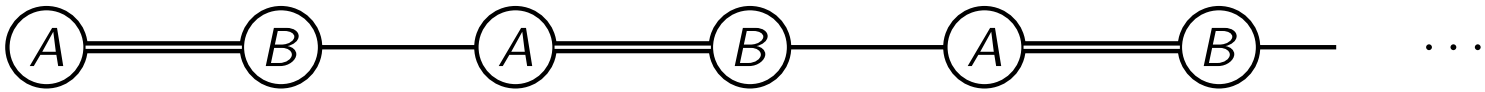


What is the spectrum of eigenstates?

- for E in the spectrum of the infinite chain: $E = E(q) = E(-q)$ the states $|\psi_q\rangle$ and $|\psi_{-q}\rangle$ can be combined to form an eigenstate

Topological edge mode

We cut the 1D lattice: semi-infinite geometry



What is the spectrum of eigenstates?

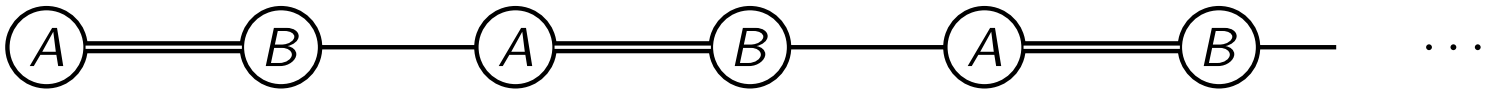
- for E in the spectrum of the infinite chain: $E = E(q) = E(-q)$ the states $|\psi_q\rangle$ and $|\psi_{-q}\rangle$ can be combined to form an eigenstate
- additional state at $E = 0$ (assuming $J' < J$)

$$a_j = (-J'/J)^j, \quad b_j = 0.$$

Exponentially localized at the end.

Topological edge mode

We cut the 1D lattice: semi-infinite geometry

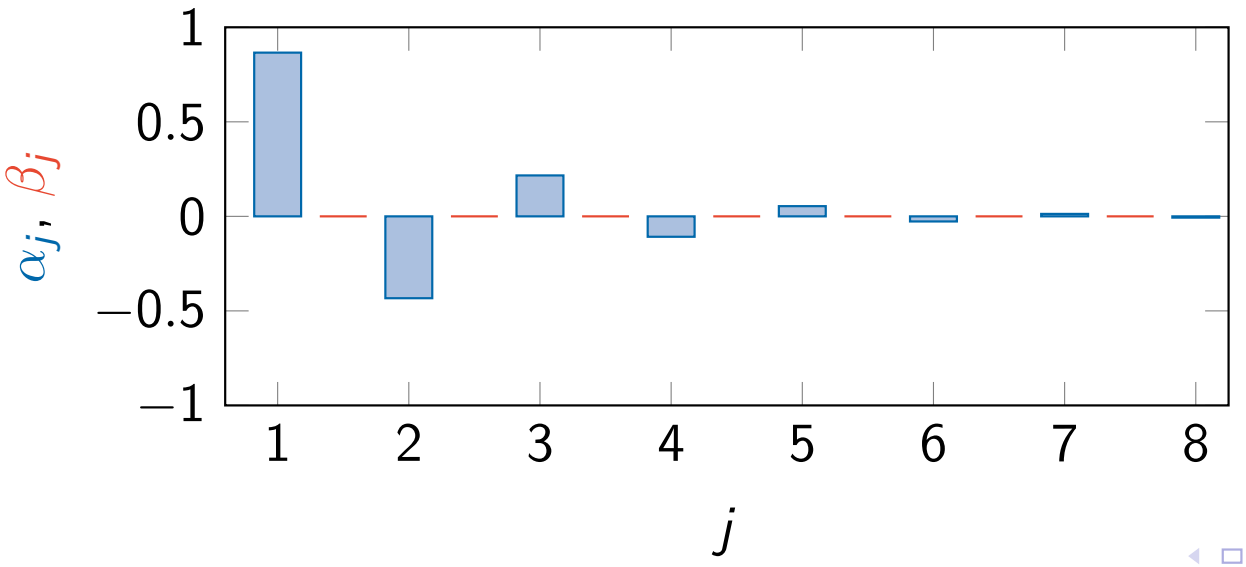


What is the spectrum of eigenstates?

- for E in the spectrum of the infinite chain: $E = E(q) = E(-q)$ the states $|\psi_q\rangle$ and $|\psi_{-q}\rangle$ can be combined to form an eigenstate
- additional state at $E = 0$ (assuming $J' < J$)

$$a_j = (-J'/J)^j, \quad b_j = 0.$$

Exponentially localized at the end.

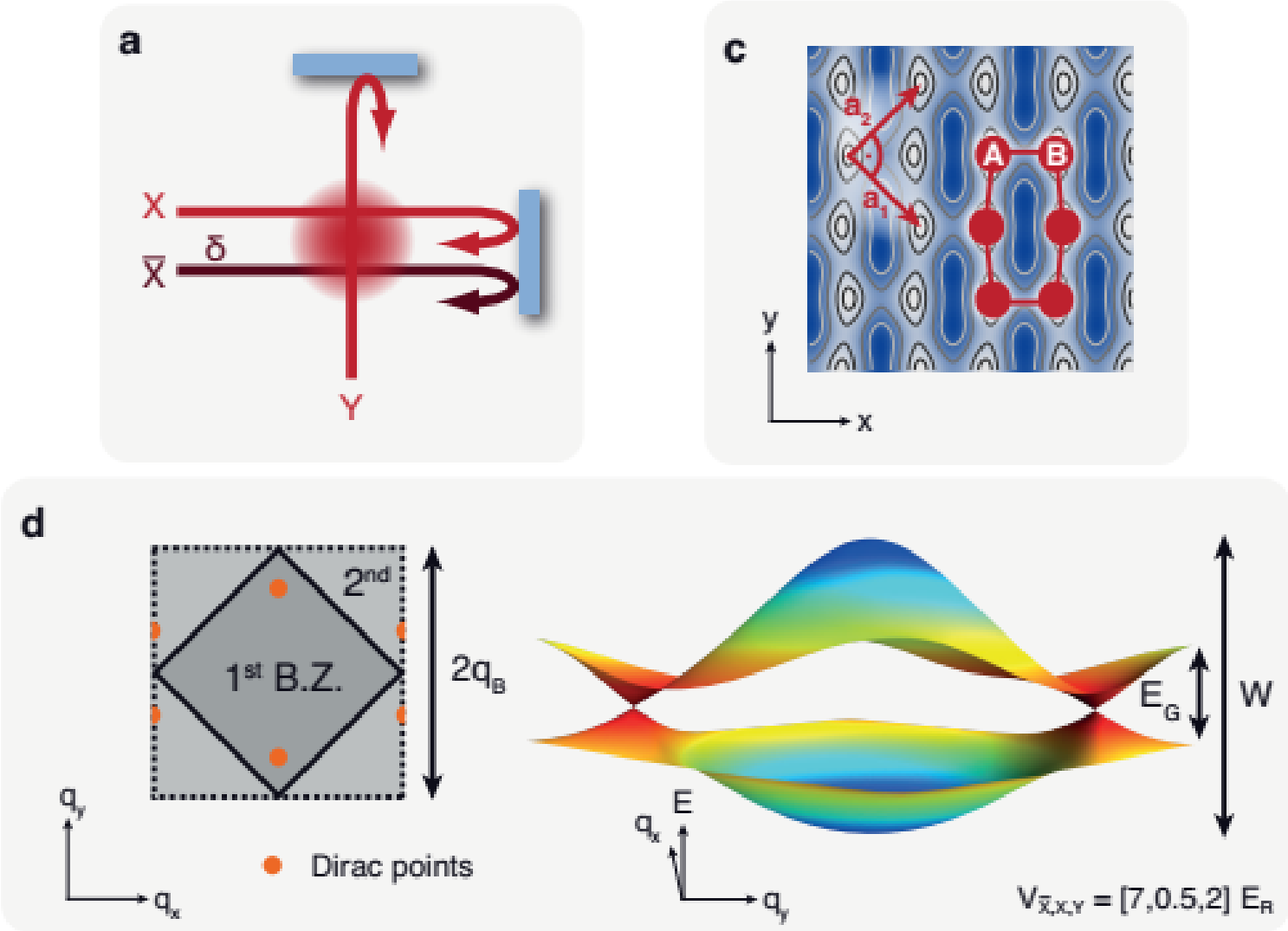


end mode for $J' = J/2$

Outline

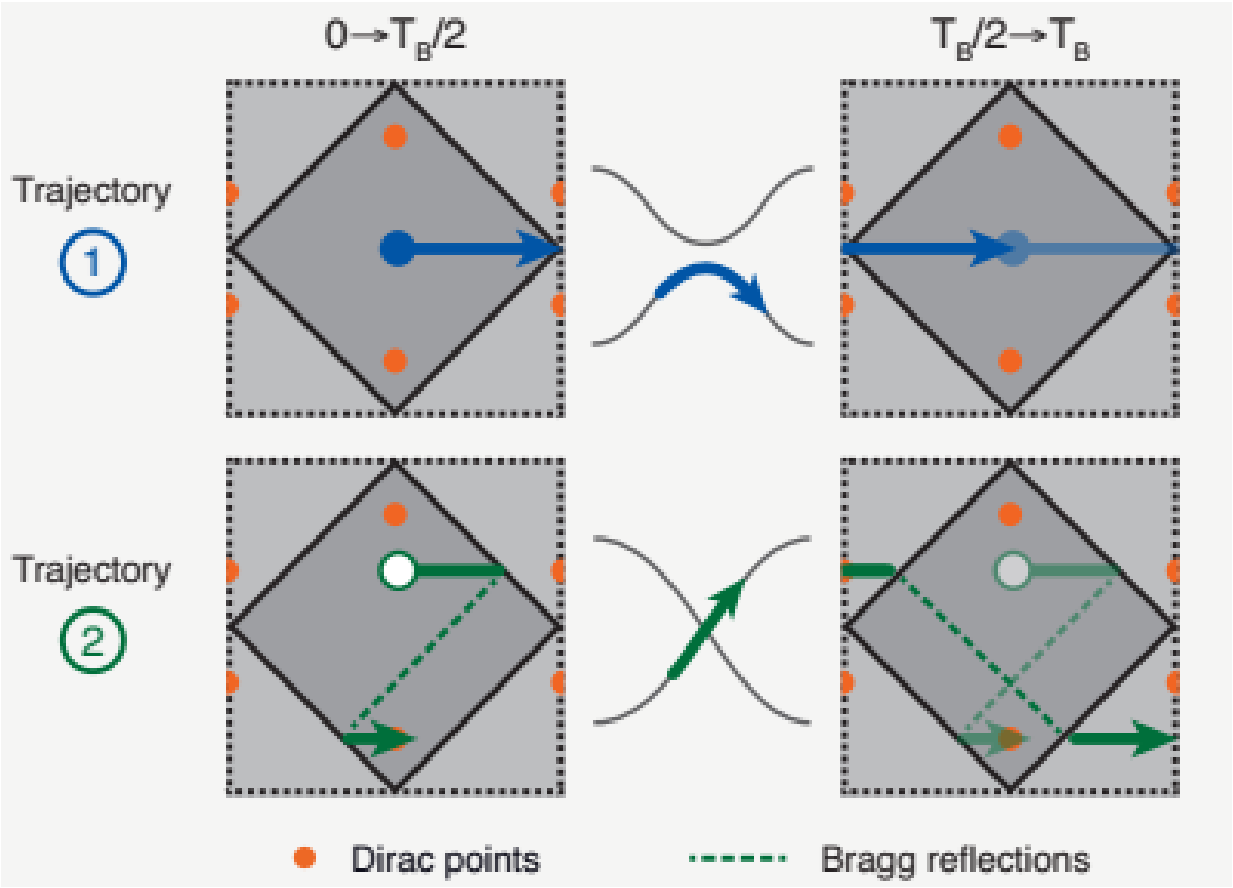
1. Band structure and dynamics in optical lattices
   - Band structure in one dimension
   - Dynamics of a particle in an optical lattice
   - Wannier functions and tight-binding limit
   - Complex lattices in 1D: SSH model
   - Complex lattices in 2D: graphene and quantum Hall bands
2. Superfluid/Mott insulator transition
   - Hubbard Hamiltonian
   - Superfluid/Mott insulator: phase diagram
   - Gutzwiller variational approach
   - Interference experiments
   - Transport experiments
   - Mott shell structure
   - Low-energy excitations
3. Fermi-Hubbard model and quantum magnetism
   - Attractive Fermi-Hubbard model
   - Repulsive Fermi-Hubbard model and Mott insulator
   - Quantum magnetism

Graphene-like 2D lattice

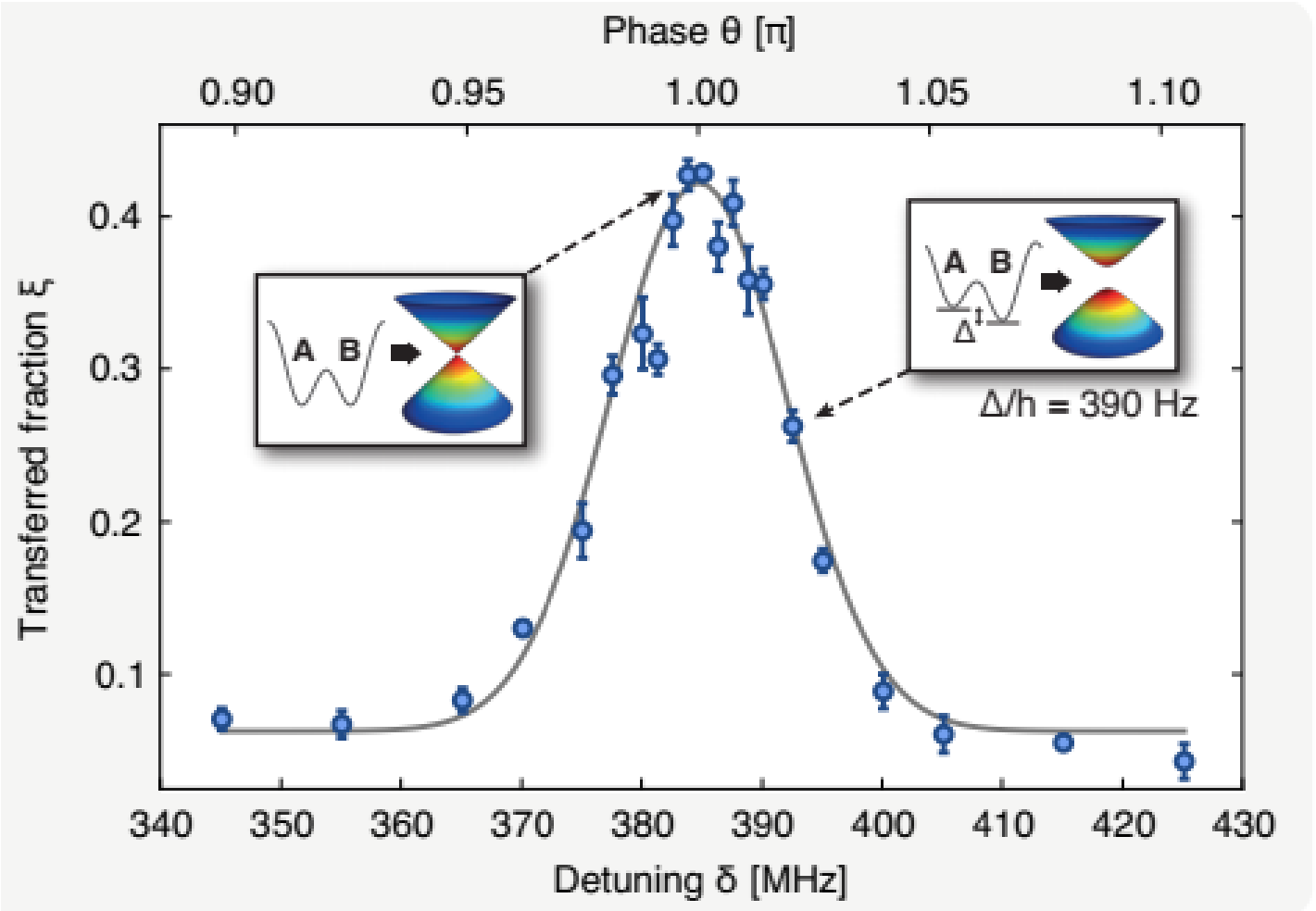


Tarruell et al, Nature 2012

Probing the Dirac points using Bloch oscillations

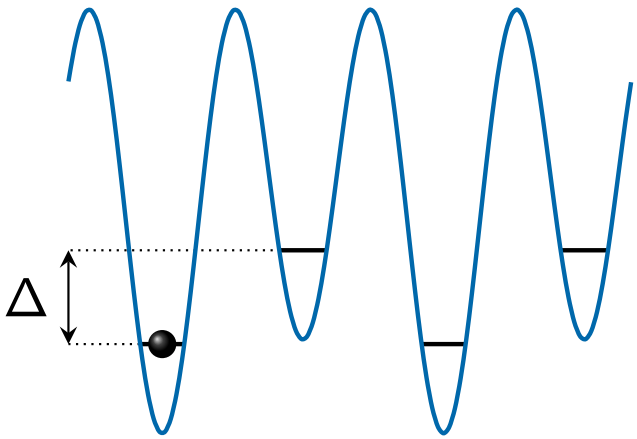


Probing the Dirac points using Bloch oscillations



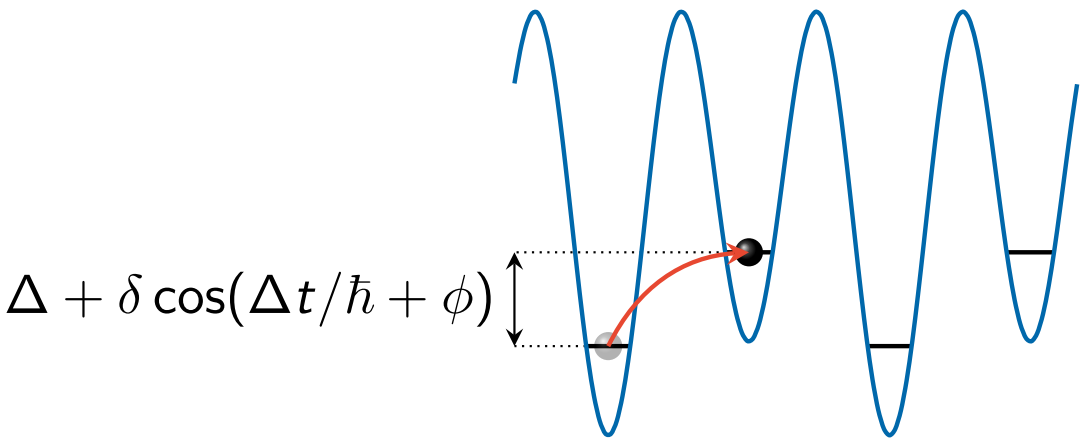
Optical lattices with complex-valued hoppings

- Suppress tunneling with an energy offset Δ,



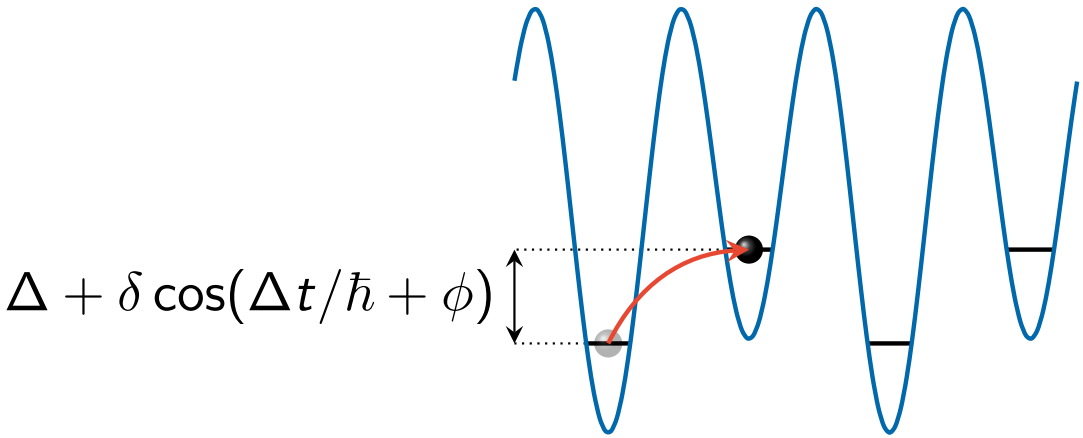
Optical lattices with complex-valued hoppings

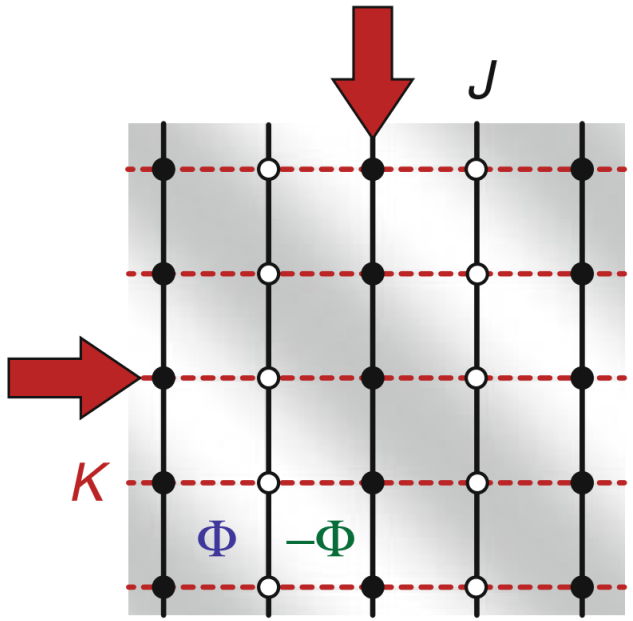
- Suppress tunneling with an energy offset Δ,
- Restore tunneling with a resonant modulation of the offset $\rightarrow$ effective tunneling $Je^{i\phi}$,



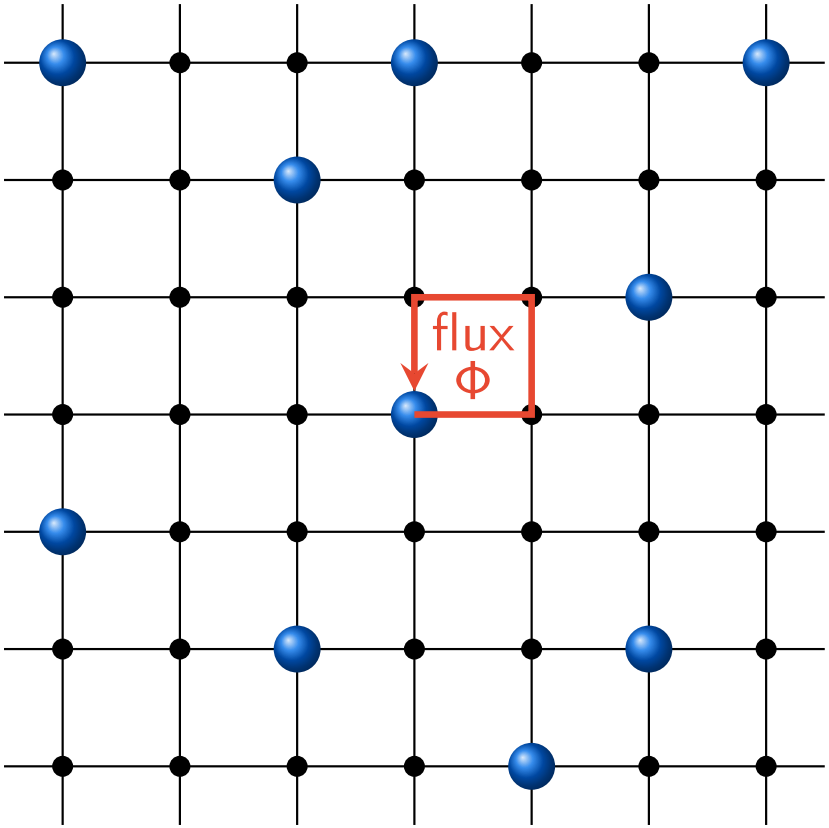
Optical lattices with complex-valued hoppings

- Suppress tunneling with an energy offset Δ,
- Restore tunneling with a resonant modulation of the offset $\rightarrow$ effective tunneling $Je^{i\phi}$,
- Spatial modulation leads to variation of the Peirls phases $\phi(\mathbf{r})$.



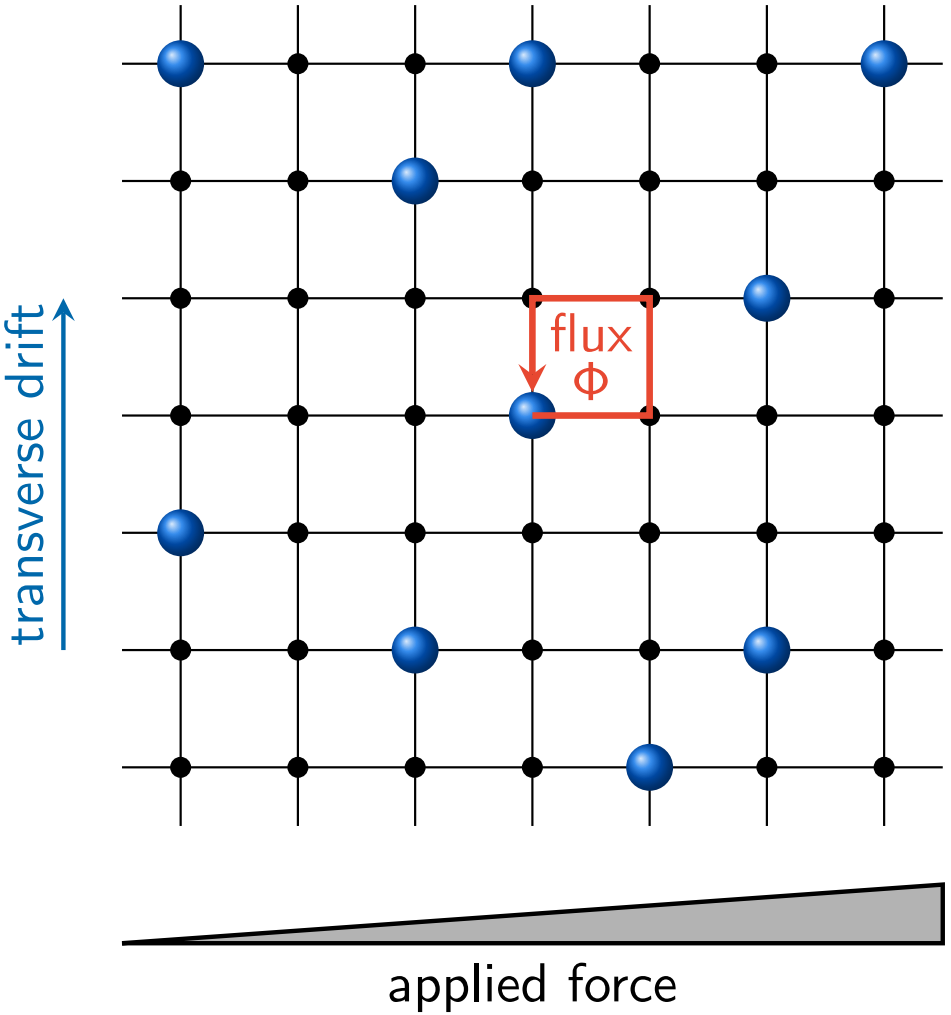


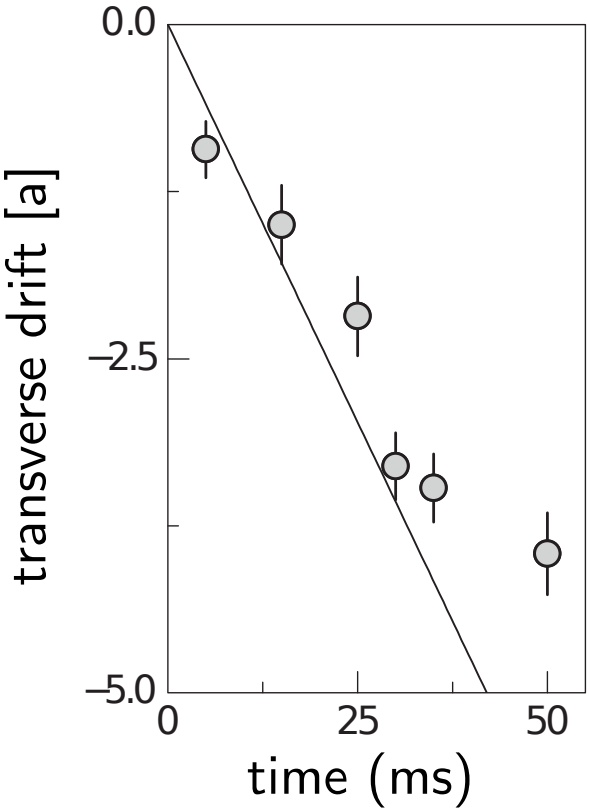
Hofstadter model and quantum Hall effect



Aidelsburger et al, Nature Phys. 2015

Hofstadter model and quantum Hall effect





Aidelsburger et al, Nature Phys. 2015

Outline

1. Band structure and dynamics in optical lattices
   - Band structure in one dimension
   - Dynamics of a particle in an optical lattice
   - Wannier functions and tight-binding limit
   - Complex lattices in 1D: SSH model
   - Complex lattices in 2D: graphene and quantum Hall bands
2. Superfluid/Mott insulator transition
   - Hubbard Hamiltonian
   - Superfluid/Mott insulator: phase diagram
   - Gutzwiller variational approach
   - Interference experiments
   - Transport experiments
   - Mott shell structure
   - Low-energy excitations
3. Fermi-Hubbard model and quantum magnetism
   - Attractive Fermi-Hubbard model
   - Repulsive Fermi-Hubbard model and Mott insulator
   - Quantum magnetism

Outline

1. Band structure and dynamics in optical lattices
   - Band structure in one dimension
   - Dynamics of a particle in an optical lattice
   - Wannier functions and tight-binding limit
   - Complex lattices in 1D: SSH model
   - Complex lattices in 2D: graphene and quantum Hall bands
2. Superfluid/Mott insulator transition
   - Hubbard Hamiltonian
   - Superfluid/Mott insulator: phase diagram
   - Gutzwiller variational approach
   - Interference experiments
   - Transport experiments
   - Mott shell structure
   - Low-energy excitations
3. Fermi-Hubbard model and quantum magnetism
   - Attractive Fermi-Hubbard model
   - Repulsive Fermi-Hubbard model and Mott insulator
   - Quantum magnetism

Hubbard Hamiltonian

- We consider a lattice system in the tight-binding regime, described by a non-interacting Hamiltonian

$$H = -J \sum_j \left(a_j^\dagger a_{j+1} + \text{h.c.} \right),$$

where a_j annihilates a particle in the lowest band at site j.

Hubbard Hamiltonian

- We consider a lattice system in the tight-binding regime, described by a non-interacting Hamiltonian

$$H = -J \sum_j \left(a_j^\dagger a_{j+1} + \text{h.c.} \right),$$

where a_j annihilates a particle in the lowest band at site j.

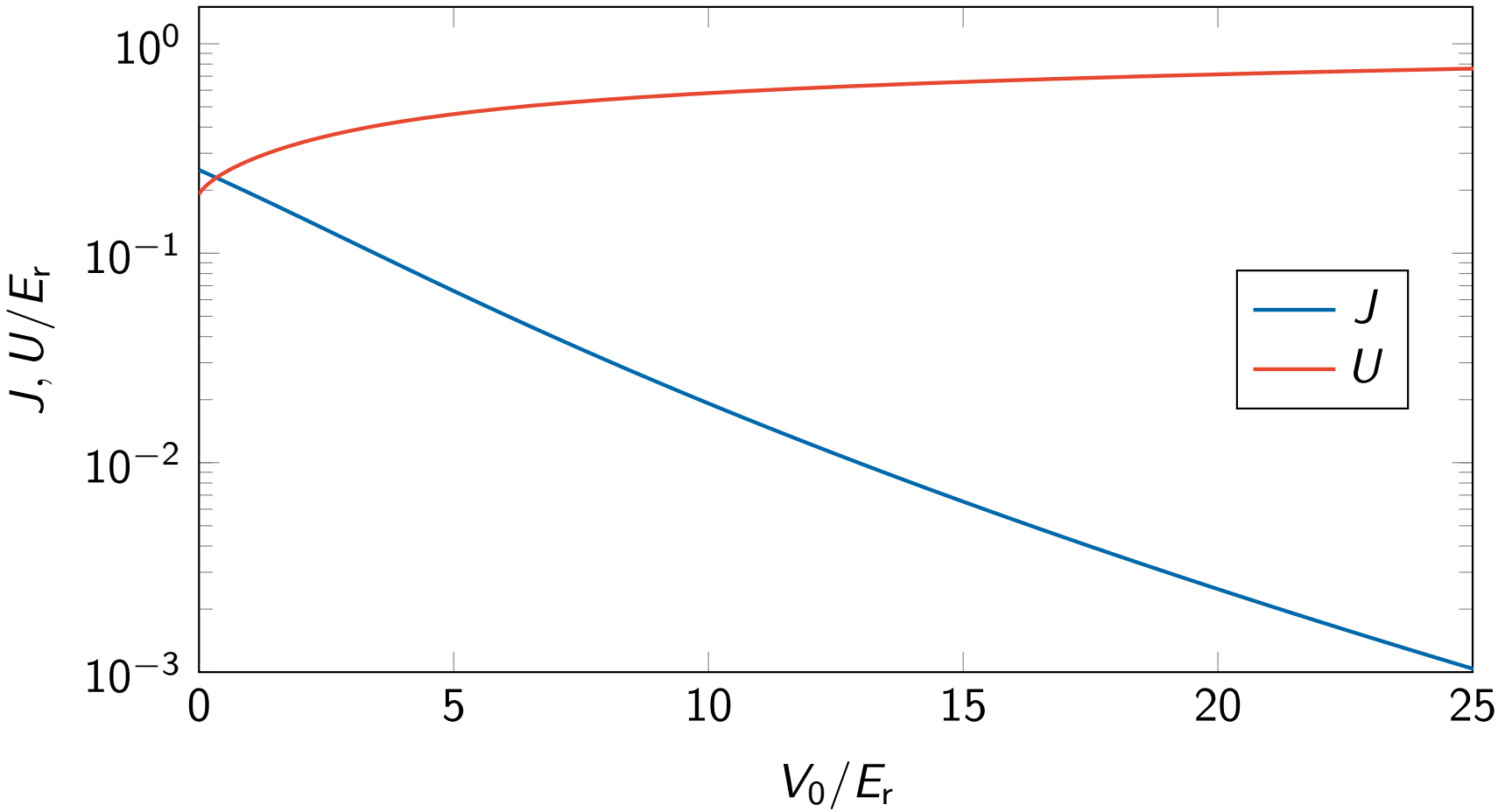
- We want to account for contact interactions (assume spin-polarized bosons)
  $\rightarrow$ The Bloch basis is not suited (extended wavefunctions)
  $\rightarrow$ In the Wannier basis: restriction to onsite interaction

$$H_{\text{int}} \simeq U \sum_j \frac{n_j(n_j - 1)}{2}, \quad n_j = a_j^\dagger a_j,$$

where we define

$$U = g \int |w_0(x)|^4 \mathrm{d}x.$$

Tunneling vs interaction



Calculation for ^{87}Rb atoms in a cubic lattice with $\lambda = 840\,\text{nm}$.

U increases as $V_0^{3/4}$ in a cubic lattice.

Outline

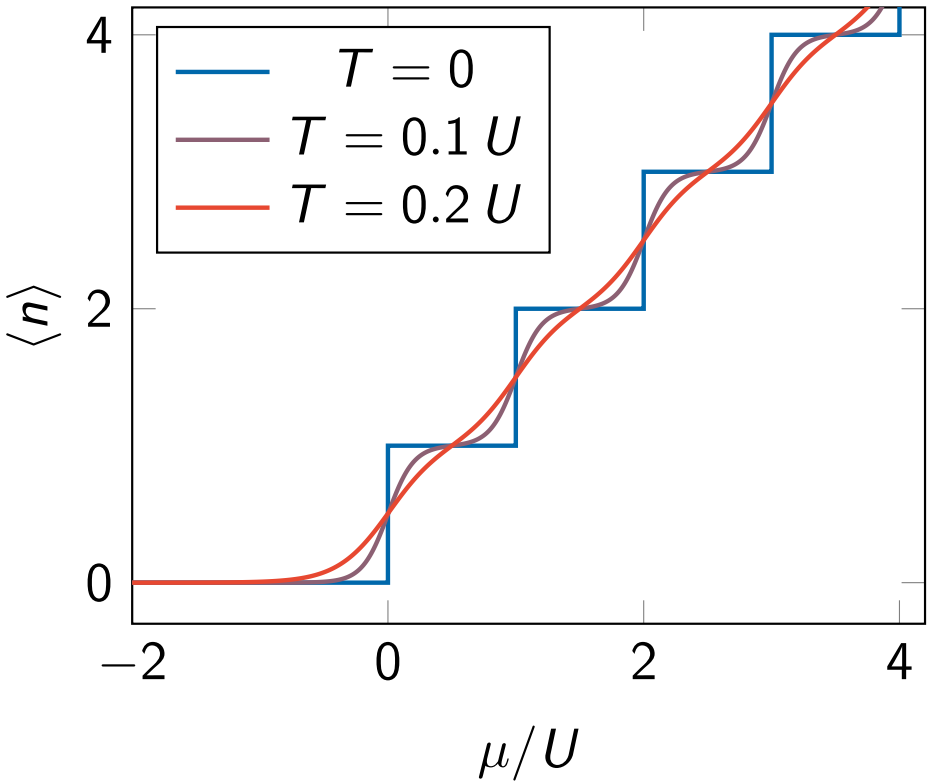
1. Band structure and dynamics in optical lattices
   - Band structure in one dimension
   - Dynamics of a particle in an optical lattice
   - Wannier functions and tight-binding limit
   - Complex lattices in 1D: SSH model
   - Complex lattices in 2D: graphene and quantum Hall bands
2. Superfluid/Mott insulator transition
   - Hubbard Hamiltonian
   - Superfluid/Mott insulator: phase diagram
   - Gutzwiller variational approach
   - Interference experiments
   - Transport experiments
   - Mott shell structure
   - Low-energy excitations
3. Fermi-Hubbard model and quantum magnetism
   - Attractive Fermi-Hubbard model
   - Repulsive Fermi-Hubbard model and Mott insulator
   - Quantum magnetism

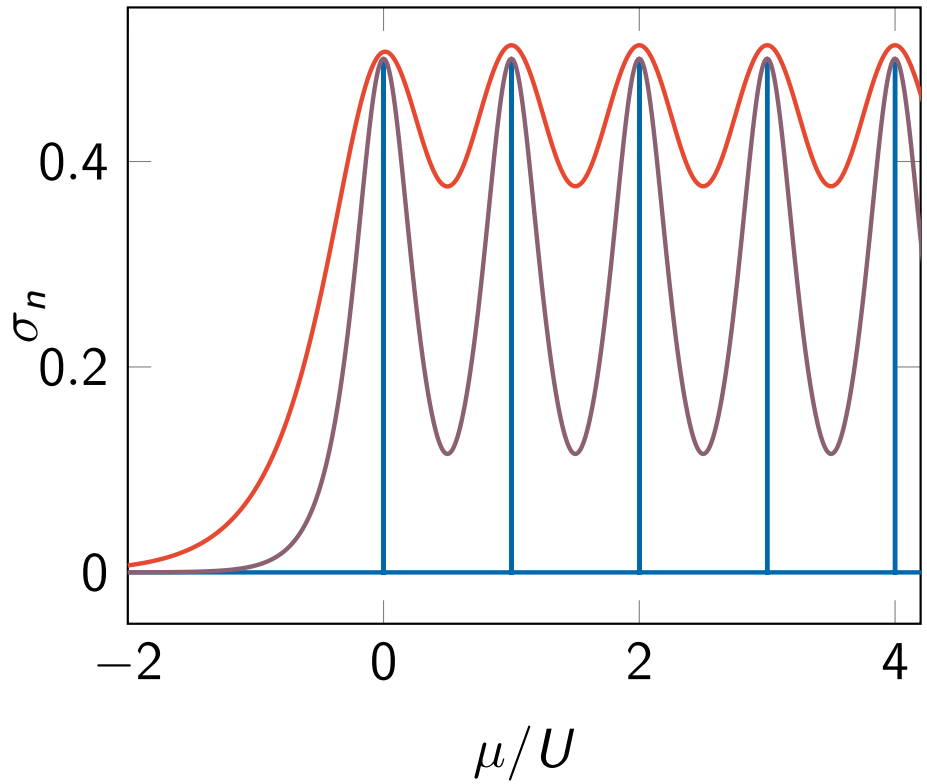
Atomic limit

For $V_0 \gtrsim 30\, E_\mathrm{r}$ the tunneling rate becomes negligible $\rightarrow$ independent wells

$$H - \mu n = \frac{U}{2} n(n-1) - \mu n.$$

Energy levels are Fock states of given atom number $n \in \mathbb{N}$.





Superfluid-Mott insulator transition: phase diagram

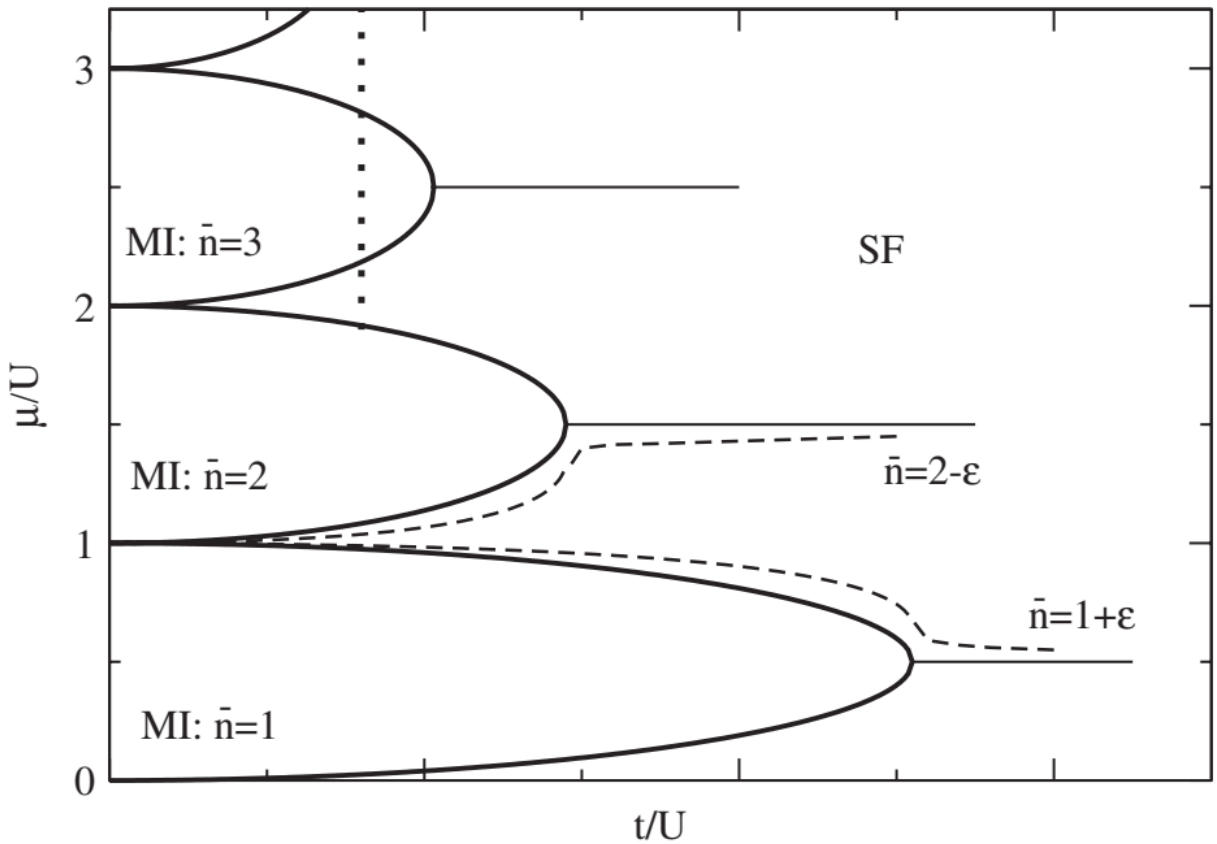
Main characteristics of the limiting cases:

- $U \to 0$: weakly interacting Bose-Einstein condensate. We expect interactions to lead to a depletion of the BEC, eventually to its disappearance. Does superfluidity survive?
- $J \to 0$: fixed integer occupation n, incompressible state. Does incompressibility resist to a finite J?

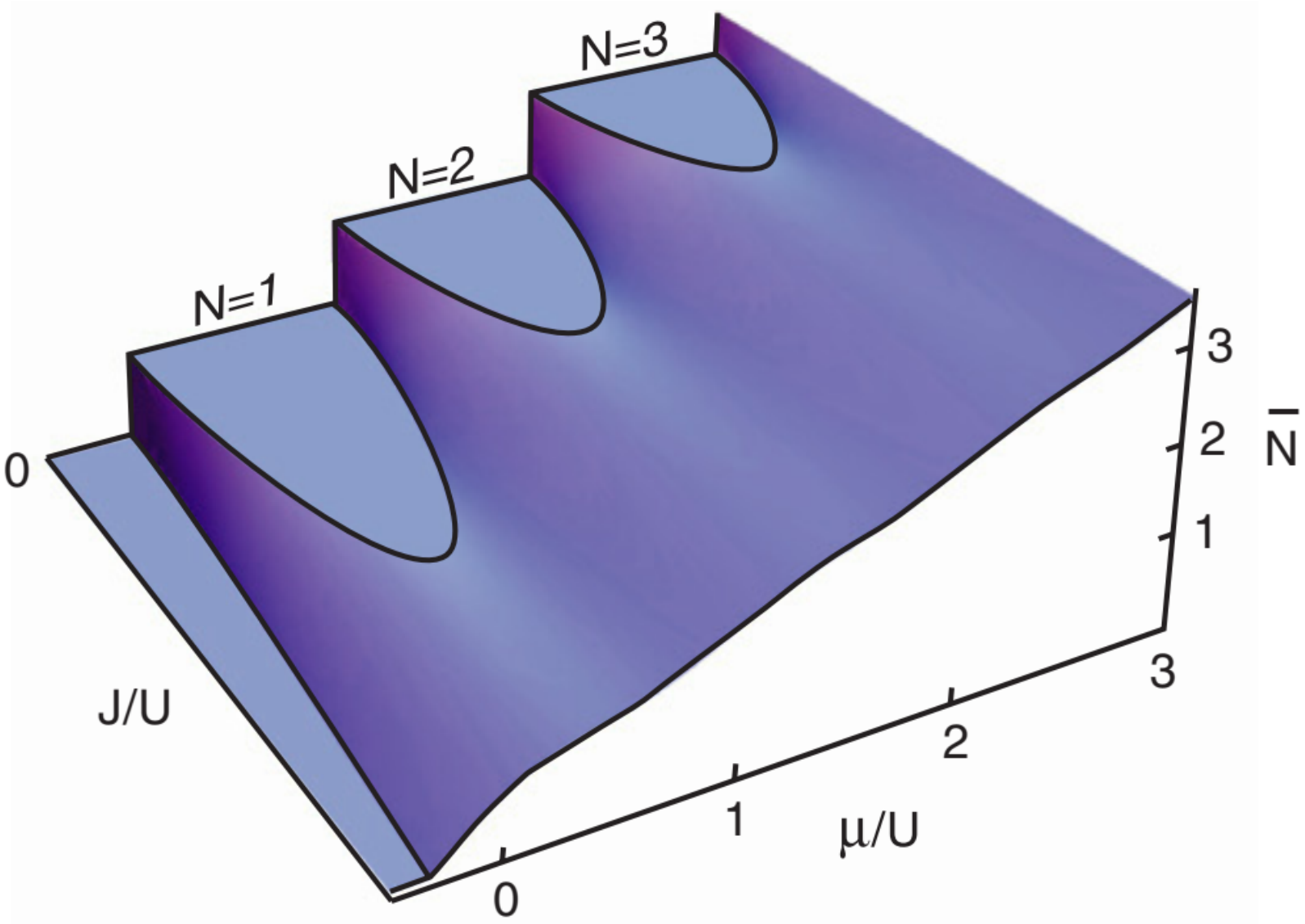
Superfluid-Mott insulator transition: phase diagram

Main characteristics of the limiting cases:

- $U \to 0$: weakly interacting Bose-Einstein condensate. We expect interactions to lead to a depletion of the BEC, eventually to its disappearance. Does superfluidity survive?
- $J \to 0$: fixed integer occupation n, incompressible state. Does incompressibility resist to a finite J?



Superfluid-Mott insulator transition: phase diagram



M. Greiner PhD thesis

Outline

1. Band structure and dynamics in optical lattices
   - Band structure in one dimension
   - Dynamics of a particle in an optical lattice
   - Wannier functions and tight-binding limit
   - Complex lattices in 1D: SSH model
   - Complex lattices in 2D: graphene and quantum Hall bands
2. Superfluid/Mott insulator transition
   - Hubbard Hamiltonian
   - Superfluid/Mott insulator: phase diagram
   - Gutzwiller variational approach
   - Interference experiments
   - Transport experiments
   - Mott shell structure
   - Low-energy excitations
3. Fermi-Hubbard model and quantum magnetism
   - Attractive Fermi-Hubbard model
   - Repulsive Fermi-Hubbard model and Mott insulator
   - Quantum magnetism

Gutzwiller ansatz

Analytical understanding of the superfluid/Mott insulator transition using a variational model

- Limiting case $U \to 0$: coherent BEC state

$$|\psi\rangle \propto \exp\left(\sqrt{N} b_{\mathbf{k}=0}^{\dagger}\right)|\emptyset\rangle \propto \prod_j \exp\left(\sqrt{\langle n\rangle} a_j^{\dagger}\right)|\emptyset\rangle_j \,,$$

Gutzwiller ansatz

Analytical understanding of the superfluid/Mott insulator transition using a variational model

- Limiting case $U \to 0$: coherent BEC state

$$|\psi\rangle \propto \exp\left(\sqrt{N} b_{\mathbf{k}=0}^{\dagger}\right)|\emptyset\rangle \propto \prod_j \exp\left(\sqrt{\langle n\rangle} a_j^{\dagger}\right)|\emptyset\rangle_j \,,$$

- Limiting case $J \to 0$: Mott insulator of integer filling n_0

$$|\psi\rangle = \prod_j |n_0\rangle_j \,.$$

Gutzwiller ansatz

Analytical understanding of the superfluid/Mott insulator transition using a variational model

- Limiting case $U \to 0$: coherent BEC state

$$|\psi\rangle \propto \exp\left(\sqrt{N} b_{\mathbf{k}=0}^{\dagger}\right)|\emptyset\rangle \propto \prod_j \exp\left(\sqrt{\langle n\rangle} a_j^{\dagger}\right)|\emptyset\rangle_j ,$$

- Limiting case $J \to 0$: Mott insulator of integer filling n_0

$$|\psi\rangle = \prod_j |n_0\rangle_j .$$

- General case: Gutzwiller trial wavefunction

$$|\psi\rangle = \prod_j |\phi\rangle_j , \quad |\phi\rangle = \sum_n c_n |n\rangle ,$$

where the c_n are chosen to minimize the energy with a fixed $\langle n\rangle = \sum_n n|c_n|^2$.

Gutzwiller energy functional

- The free energy per site reads

$$F = -Jz \left\langle a^\dagger \right\rangle \langle a \rangle + \frac{U}{2} \left\langle n^2 \right\rangle - \left(\mu + \frac{U}{2} \right) \langle n \rangle$$

Gutzwiller energy functional

- The free energy per site reads

$$F = -Jz \left\langle a^\dagger \right\rangle \langle a \rangle + \frac{U}{2} \left\langle n^2 \right\rangle - \left(\mu + \frac{U}{2} \right) \langle n \rangle$$

- We calculate the mean values

$$\langle a \rangle = \sum_n \sqrt{n+1} c^*(n) c(n+1),$$

$$\left\langle n^2 \right\rangle = \sum_n n^2 |c(n)|^2.$$

Gutzwiller energy functional

- The free energy per site reads

$$F = -Jz \left\langle a^\dagger \right\rangle \langle a \rangle + \frac{U}{2} \left\langle n^2 \right\rangle - \left(\mu + \frac{U}{2} \right) \langle n \rangle$$

- We calculate the mean values

$$\langle a \rangle = \sum_n \sqrt{n+1} c^*(n) c(n+1),$$

$$\left\langle n^2 \right\rangle = \sum_n n^2 |c(n)|^2.$$

- We minimize the free energy for a given value of the mean occupation $\langle n \rangle$.

Gutzwiller energy functional

- The free energy per site reads

$$F = -Jz \left\langle a^\dagger \right\rangle \langle a \rangle + \frac{U}{2} \left\langle n^2 \right\rangle - \left(\mu + \frac{U}{2} \right) \langle n \rangle$$

- We calculate the mean values

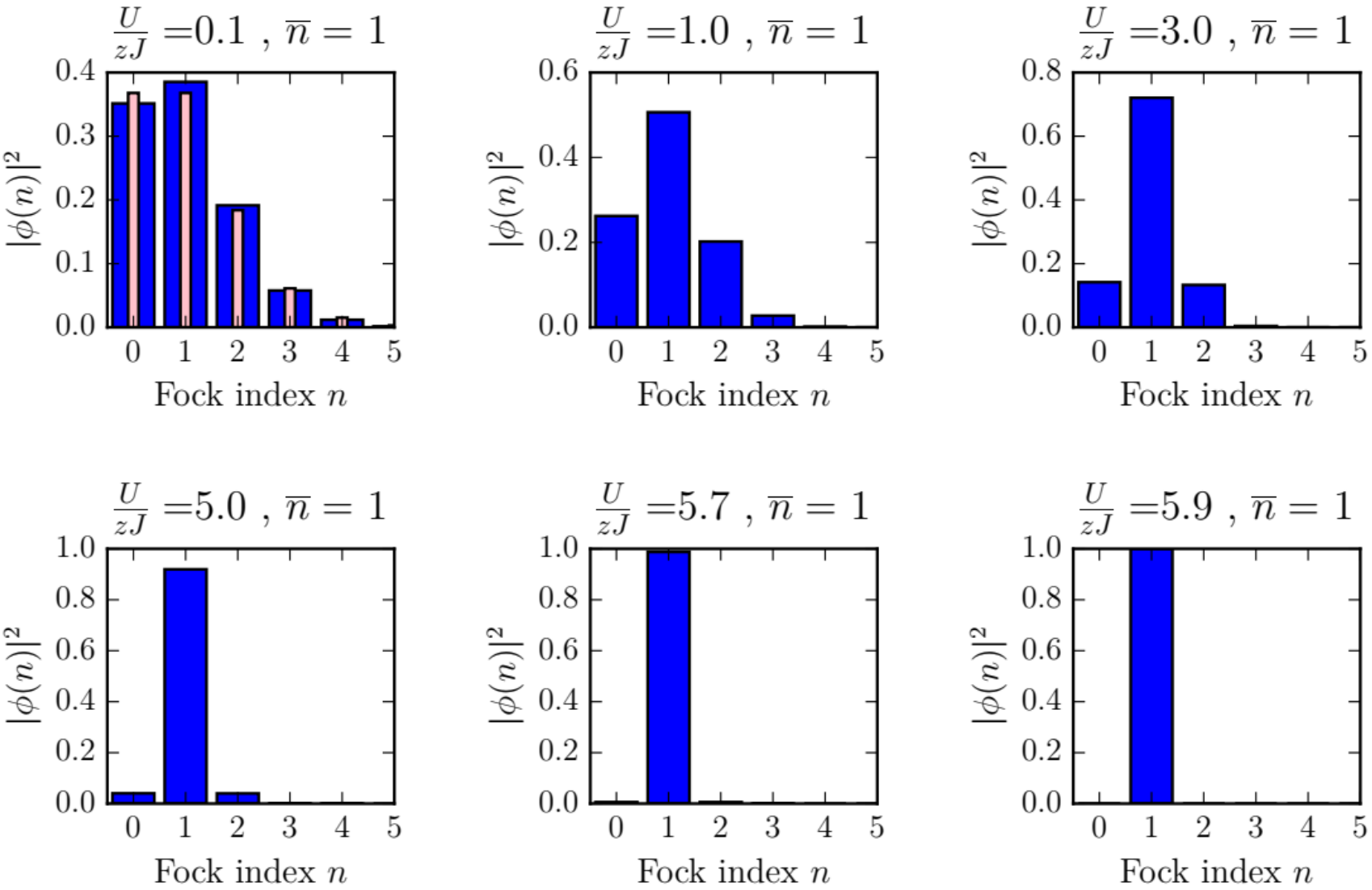
$$\langle a \rangle = \sum_n \sqrt{n+1} c^*(n) c(n+1),$$

$$\left\langle n^2 \right\rangle = \sum_n n^2 |c(n)|^2.$$

- We minimize the free energy for a given value of the mean occupation $\langle n \rangle$.
- Condensate fraction

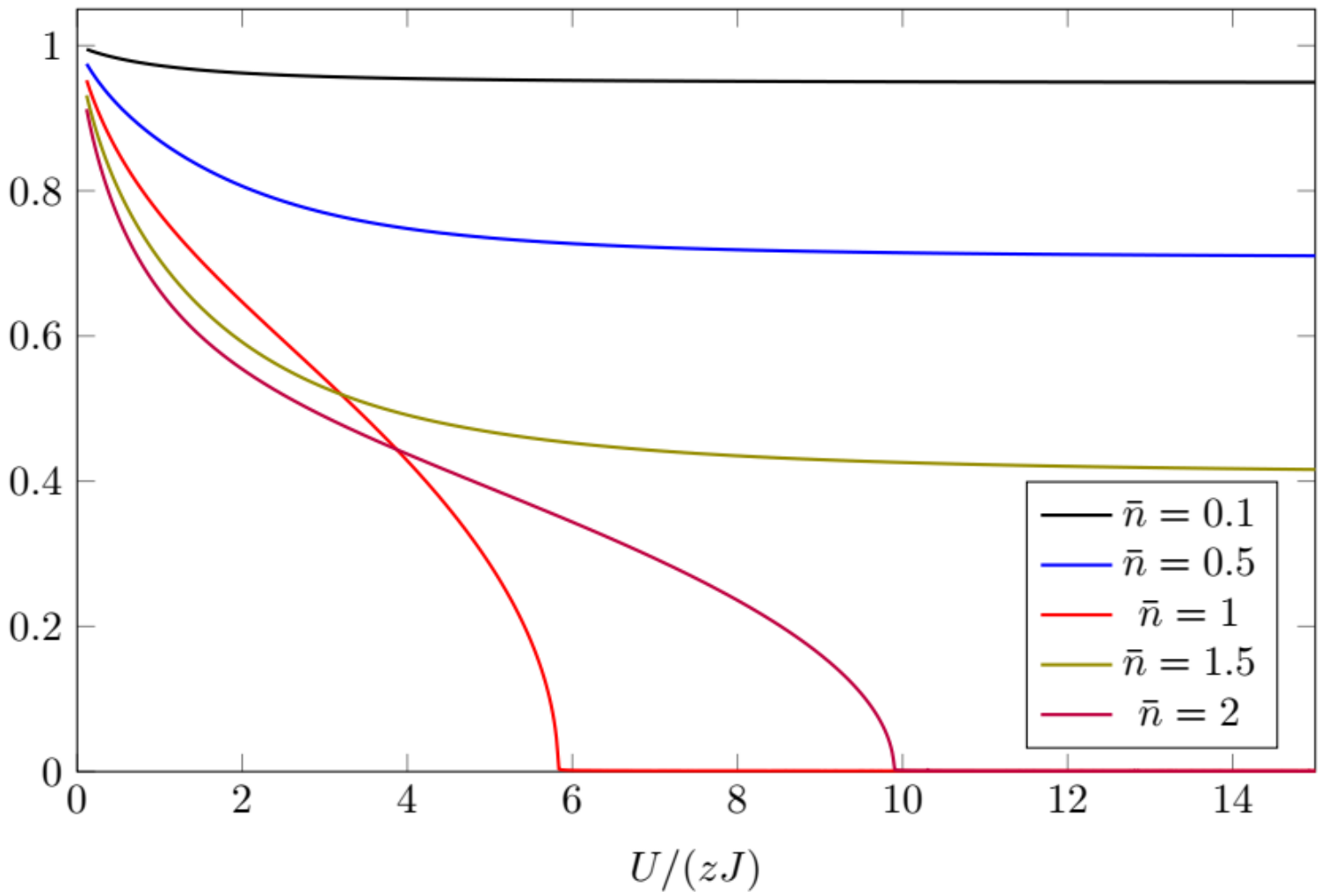
$$f_c = \frac{1}{N} \left\langle b_{\mathbf{q}}^\dagger b_{\mathbf{q}} \right\rangle_{\mathbf{q}=0} = \frac{|\langle a \rangle|^2}{\langle n \rangle}.$$

Gutzwiller ground state for $\langle n \rangle = 1$.



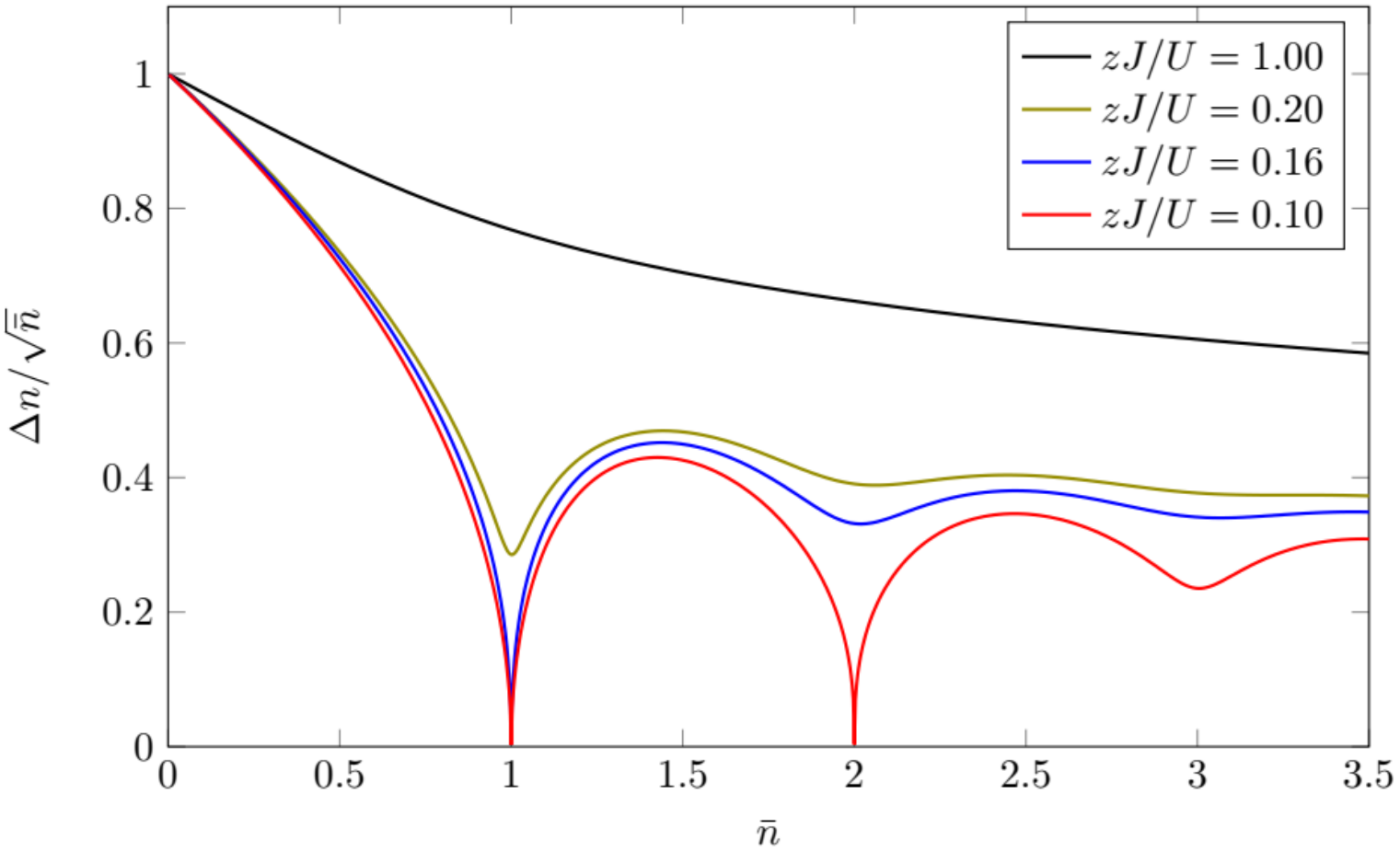
F. Gerbier, cours Atomes froids 2016

Number fluctuations for a fixed $\langle n \rangle$



J. Dalibard, cours Collège de France 2016

Number fluctuations versus $\langle n \rangle$



J. Dalibard, cours Collège de France 2016

Particle-hole approximation close to a Mott state

Analytical expressions can be written when restricting to three states only

$$|\phi\rangle = c(n_0 - 1)\,|n_0 - 1\rangle + c(n_0)\,|n_0\rangle + c(n_0 + 1)\,|n_0 + 1\rangle\,.$$

We parametrize the coefficients as

$$\begin{aligned} c(n_0 - 1) &= \cos\chi\, \sin\theta\, \mathrm{e}^{\mathrm{i}\phi_-}, \\ c(n_0) &= \cos\theta, \\ c(n_0 + 1) &= \sin\chi\, \sin\theta\, \mathrm{e}^{\mathrm{i}\phi_+}. \end{aligned}$$

The average filling reads

$$\langle n\rangle = n_0 - \sin^2\theta\, \cos(2\chi).$$

Ground state in the particle-hole approximation ($\langle n \rangle = n_0$)

In case of commensurate filling $\langle n \rangle = n_0$ (i.e. $\chi = \pi/4$), one obtains

$$F = \frac{U}{2} \sin^2\theta - \frac{zJ}{8} \sin^2(2\theta) \left[2n_0 + 1 + 2\sqrt{n_0(n_0+1)} \cos(\phi_+ + \phi_-) \right].$$

Ground state in the particle-hole approximation ($\langle n \rangle = n_0$)

In case of commensurate filling $\langle n \rangle = n_0$ (i.e. $\chi = \pi/4$), one obtains

$$F = \frac{U}{2} \sin^2\theta - \frac{zJ}{8} \sin^2(2\theta) \left[2n_0 + 1 + 2\sqrt{n_0(n_0+1)} \cos(\phi_+ + \phi_-) \right].$$

The energy is obviously minimized for $\cos(\phi_+ + \phi_-) = 1$. Then

$$F = \frac{U}{2} \sin^2\theta - \frac{zJ}{8} (\sqrt{n_0} + \sqrt{n_0+1})^2 \sin^2(2\theta).$$

Ground state in the particle-hole approximation ($\langle n \rangle = n_0$)

In case of commensurate filling $\langle n \rangle = n_0$ (i.e. $\chi = \pi/4$), one obtains

$$F = \frac{U}{2}\sin^2\theta - \frac{zJ}{8}\sin^2(2\theta)\left[2n_0 + 1 + 2\sqrt{n_0(n_0+1)}\cos(\phi_+ + \phi_-)\right].$$

The energy is obviously minimized for $\cos(\phi_+ + \phi_-) = 1$. Then

$$F = \frac{U}{2}\sin^2\theta - \frac{zJ}{8}(\sqrt{n_0} + \sqrt{n_0+1})^2\sin^2(2\theta).$$

- for $U \leq U_c = zJ(\sqrt{n_0} + \sqrt{n_0+1})^2$, one gets

  $$\theta = \arccos(U/U_c)/2.$$

  This state is superfluid as

  $$f_c = \frac{(\sqrt{n_0} + \sqrt{n_0+1})^2}{8n_0}\left(1 - (U/U_c)^2\right).$$

Ground state in the particle-hole approximation ($\langle n \rangle = n_0$)

In case of commensurate filling $\langle n \rangle = n_0$ (i.e. $\chi = \pi/4$), one obtains

$$F = \frac{U}{2}\sin^2\theta - \frac{zJ}{8}\sin^2(2\theta)\left[2n_0 + 1 + 2\sqrt{n_0(n_0+1)}\cos(\phi_+ + \phi_-)\right].$$

The energy is obviously minimized for $\cos(\phi_+ + \phi_-) = 1$. Then

$$F = \frac{U}{2}\sin^2\theta - \frac{zJ}{8}(\sqrt{n_0} + \sqrt{n_0+1})^2\sin^2(2\theta).$$

- for $U \leq U_c = zJ(\sqrt{n_0} + \sqrt{n_0+1})^2$, one gets

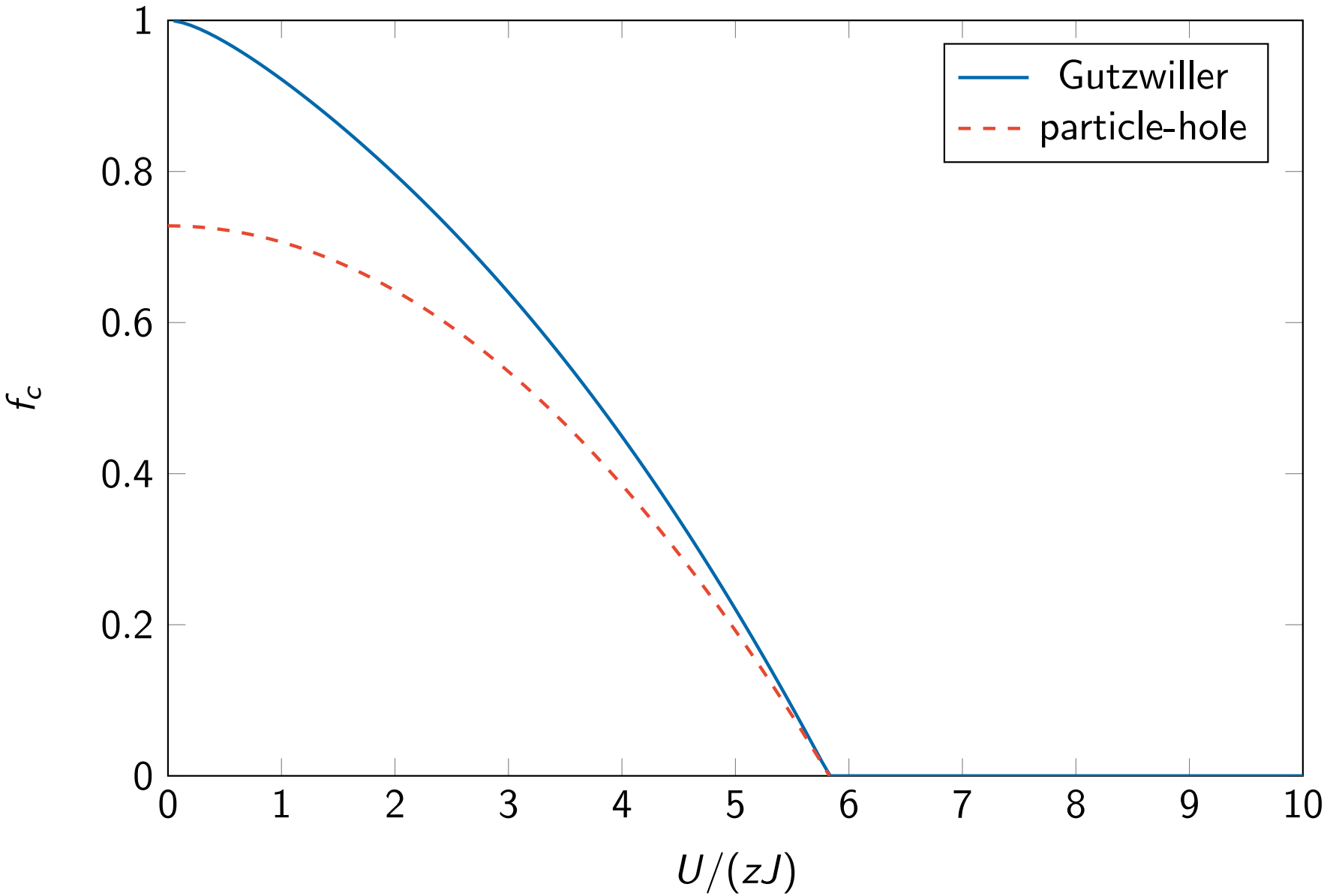
  $$\theta = \arccos(U/U_c)/2.$$

  This state is superfluid as

  $$f_c = \frac{(\sqrt{n_0} + \sqrt{n_0+1})^2}{8n_0}\left(1 - (U/U_c)^2\right).$$

- for $U > U_c$ one gets a Mott insulator with $c(n_0 - 1) = c(n_0 + 1) = 0$. No superfluidity.

Condensed fraction ($\langle n \rangle = 1$)



Mott phase boundary

The boundary of the Mott phases can be found using perturbation theory, as

$$|\phi\rangle = |n_0\rangle + \frac{zJ\alpha\sqrt{n_0}}{\mu - U(n_0-1)}|n_0-1\rangle + \frac{zJ\alpha\sqrt{n_0+1}}{Un_0-\mu}|n_0+1\rangle,$$

where $\alpha \equiv \langle a \rangle$ is determined self-consistently as

$$\alpha = zJ\alpha\left(\frac{n_0}{\mu - U(n_0-1)} + \frac{n_0+1}{Un_0-\mu}\right).$$

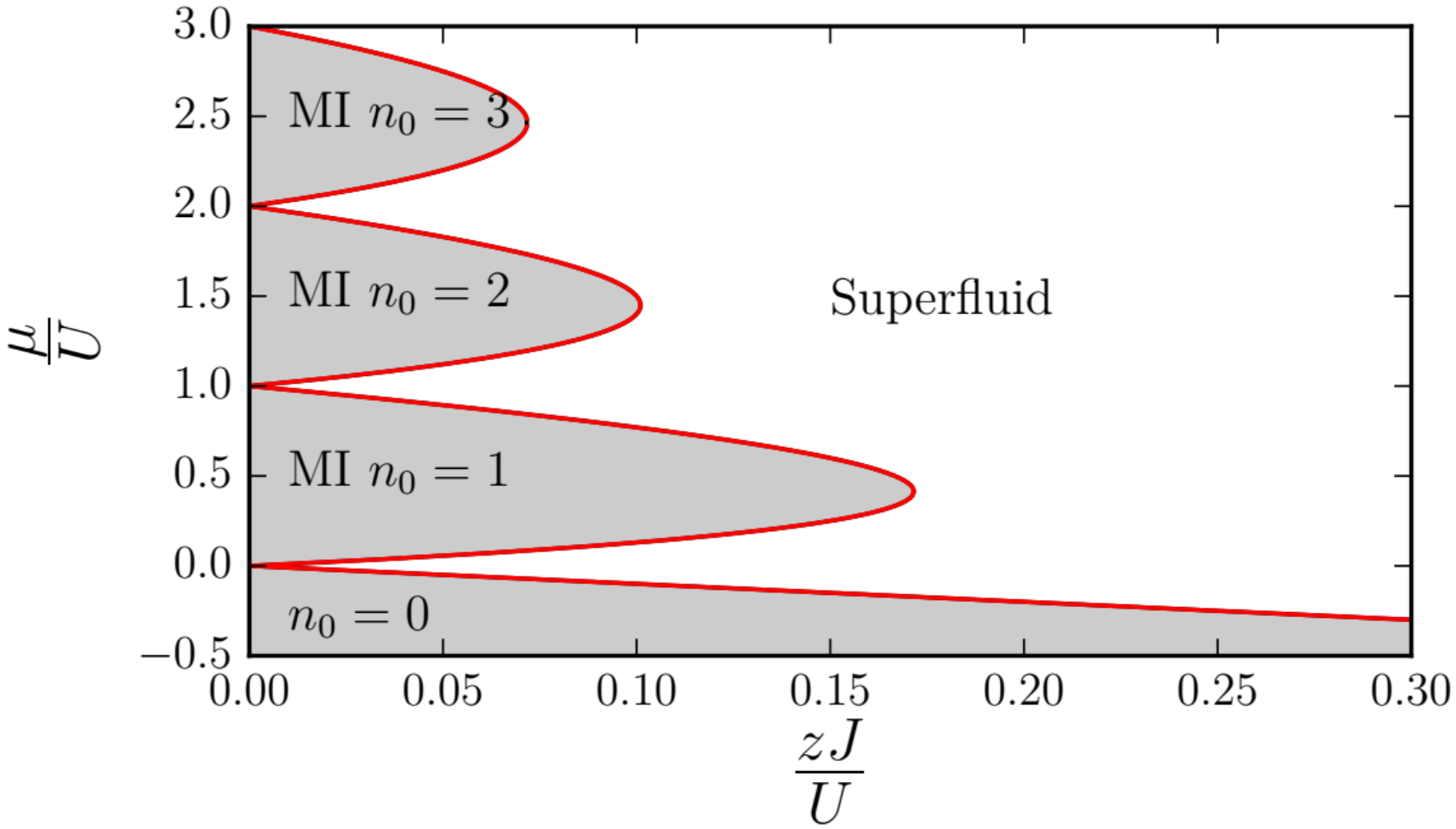
The solution $\alpha = 0$ corresponds to the Mott phase. The superfluid becomes stable when $\alpha \neq 0$, and

$$\frac{1}{zJ} = \frac{n_0}{\mu - U(n_0-1)} + \frac{n_0+1}{Un_0-\mu},$$

i.e.

$$\frac{\mu_\pm}{U} = n_0 - \frac{1}{2} - \frac{zJ}{2U} \pm \frac{1}{2}\sqrt{1 - 2(2n_0+1)\frac{zJ}{U} + \left(\frac{zJ}{U}\right)^2}.$$

Superfluid/Mott insulator boundaries



F. Gerbier, cours Atomes froids 2016

Outline

1. Band structure and dynamics in optical lattices
   - Band structure in one dimension
   - Dynamics of a particle in an optical lattice
   - Wannier functions and tight-binding limit
   - Complex lattices in 1D: SSH model
   - Complex lattices in 2D: graphene and quantum Hall bands
2. Superfluid/Mott insulator transition
   - Hubbard Hamiltonian
   - Superfluid/Mott insulator: phase diagram
   - Gutzwiller variational approach
   - Interference experiments
   - Transport experiments
   - Mott shell structure
   - Low-energy excitations
3. Fermi-Hubbard model and quantum magnetism
   - Attractive Fermi-Hubbard model
   - Repulsive Fermi-Hubbard model and Mott insulator
   - Quantum magnetism

Phase coherence from time-of-flight experiments

Field operator in Wannier basis

$$\psi(\mathbf{r}) = \sum_j w(\mathbf{r} - \mathbf{r}_j) a_j.$$

After time-of-flight

$$w(\mathbf{r} - \mathbf{r}_j) \to \tilde{w}\left(\mathbf{k} = \frac{m\mathbf{r}}{\hbar t}\right) \mathrm{e}^{\mathrm{i}m\mathbf{r}\cdot\mathbf{r}_j/(\hbar t)}.$$

The density then reads

$$n(\mathbf{k}) = G(\mathbf{k}) S(\mathbf{k}),$$

$$G(\mathbf{k}) = \left(\frac{m}{\hbar t}\right)^3 |w(\mathbf{k})|^2,$$

$$S(\mathbf{k}) = \sum_{i,j} \mathrm{e}^{\mathrm{i}\mathbf{k}\cdot(\mathbf{r}_i - \mathbf{r}_j)} \langle a_i^\dagger a_j \rangle,$$

where $S(\mathbf{k})$ is the structure factor and $G(\mathbf{k})$ is a smooth enveloppe.
The structure factor is the Fourier transform of the *site* correlation function

$$C(i,j) = \langle a_i^\dagger a_j \rangle.$$

Phase coherence in the superfluid/Mott phases

- Superfluid phase. For a fully condensed BEC one finds

$$C(i,j) = \langle n \rangle, \quad S(\mathbf{k}) = \langle n \rangle \left| \sum_j e^{i\mathbf{k}\cdot\mathbf{r}_j} \right|^2.$$

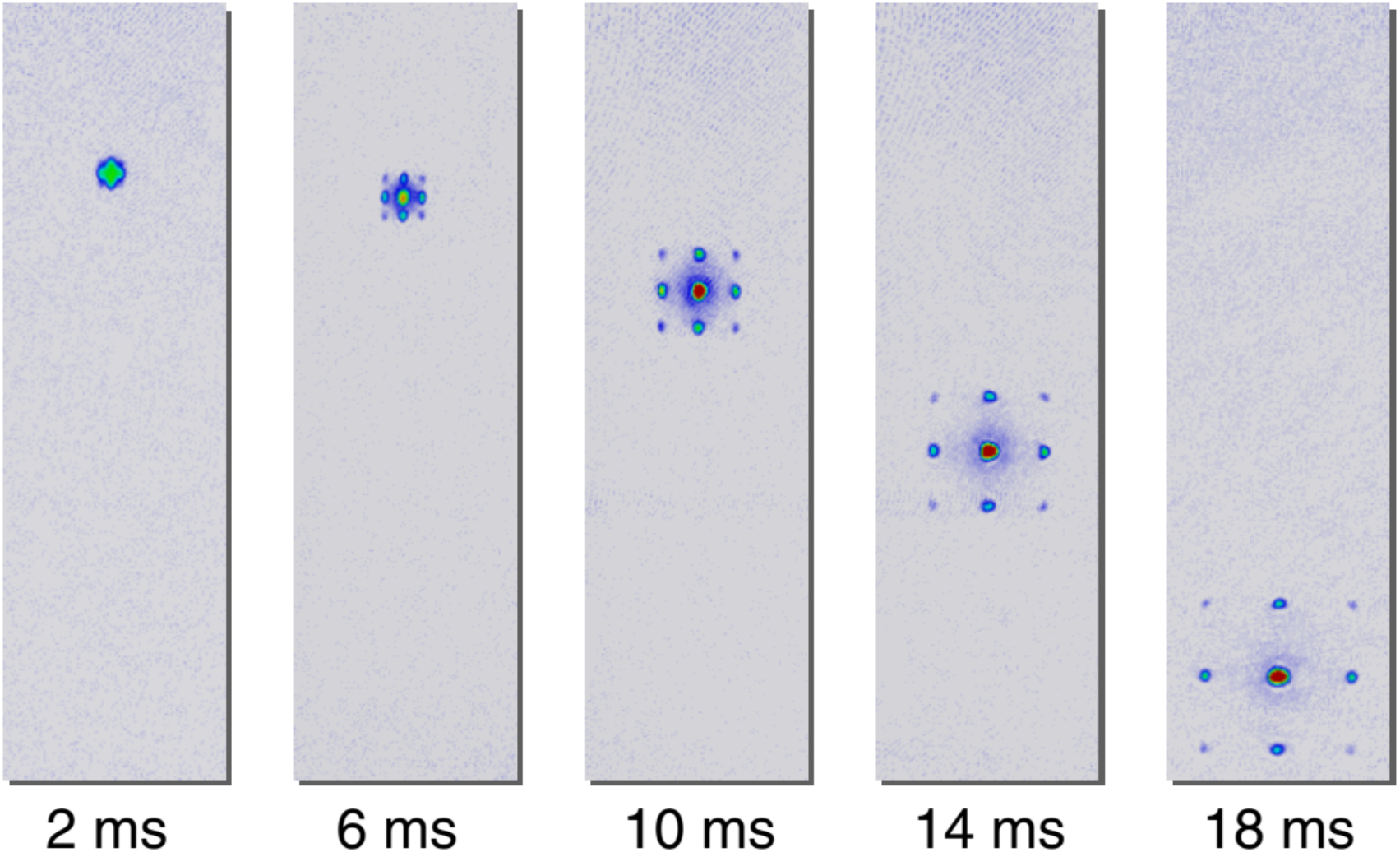
  We expect sharp peaks at the lattice reciprocal lattice (analog of x-ray Bragg diffraction in solids).

- Mott insulator

$$C(i,j) = n_0\, \delta_{i,j}, \quad S(\mathbf{k}) = N.$$

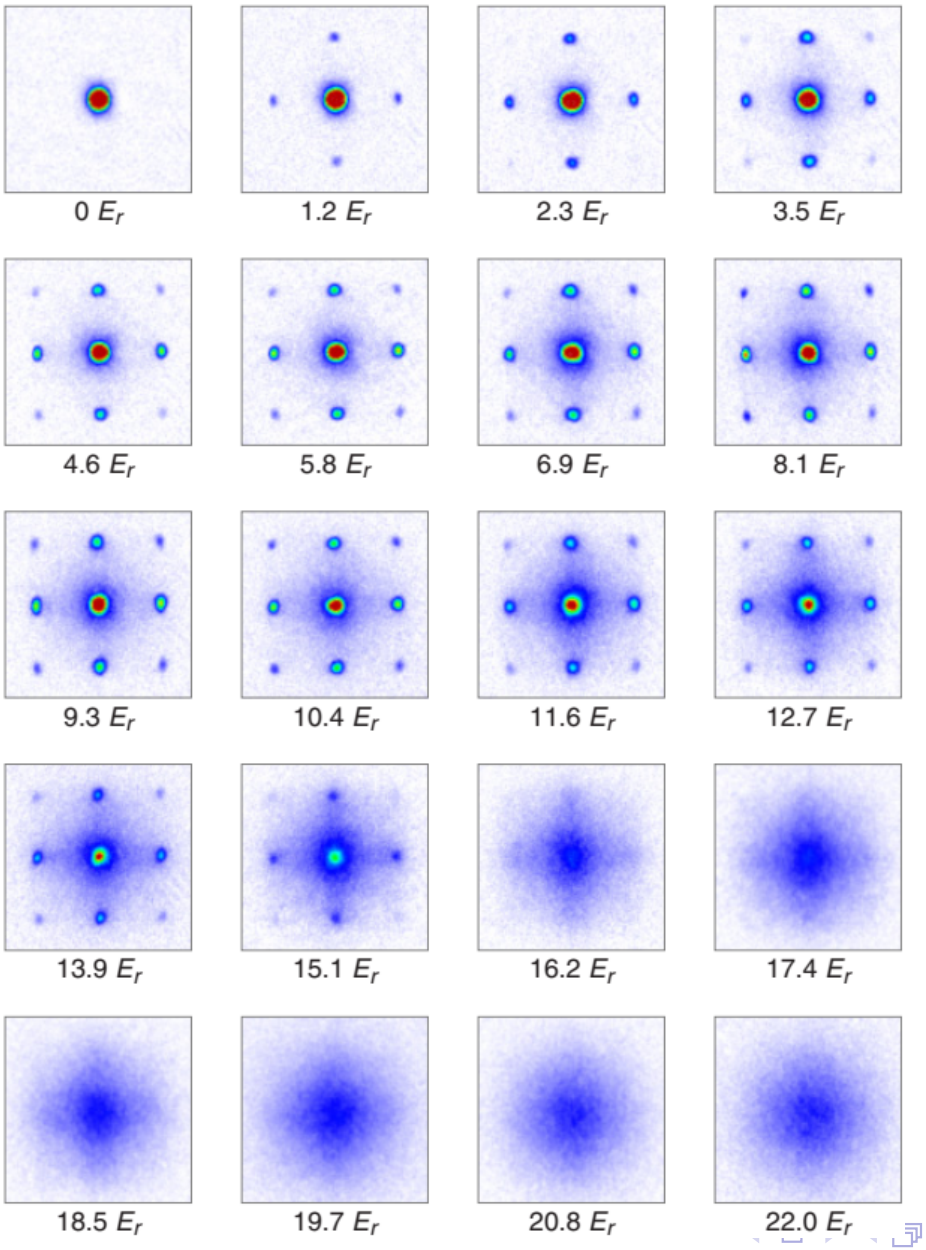
  No more diffraction peak.

Expansion of a superfluid gas



PhD Greiner, 2003

TOF images in the superfluid/Mott transition



Particle-hole excitations and coherence

Starting in a Mott insulator of filling n_0, we treat the tunneling perturbatively.

$$|\psi\rangle = |\psi_0\rangle + \frac{J\sqrt{n_0(n_0+1)}}{U} \sum_{\langle i,j\rangle} |\mathrm{p}: i, \mathrm{h}, j\rangle \,,$$

where $|\mathrm{p}: i, \mathrm{h}, j\rangle$ has a particle excitation at i and a hole at j. This state has a short-range correlation function

$$C(i,j) = n_0\delta_{ij} + 2\frac{Jn_0(n_0+1)}{U}\delta_{\langle i,j\rangle},$$

leading to a modulated structure factor (in 1D)

$$S(k) = n_0 + 4\frac{Jn_0(n_0+1)}{U}\cos(ka).$$

Particle-hole excitations and coherence

Starting in a Mott insulator of filling n_0, we treat the tunneling perturbatively.

$$|\psi\rangle = |\psi_0\rangle + \frac{J\sqrt{n_0(n_0+1)}}{U}\sum_{\langle i,j\rangle}|\mathrm{p}:i,\mathrm{h},j\rangle\,,$$

where $|\mathrm{p}:i,\mathrm{h},j\rangle$ has a particle excitation at i and a hole at j. This state has a short-range correlation function

$$C(i,j) = n_0\delta_{ij} + 2\frac{Jn_0(n_0+1)}{U}\delta_{\langle i,j\rangle},$$

leading to a modulated structure factor (in 1D)

$$S(k) = n_0 + 4\frac{Jn_0(n_0+1)}{U}\cos(ka).$$

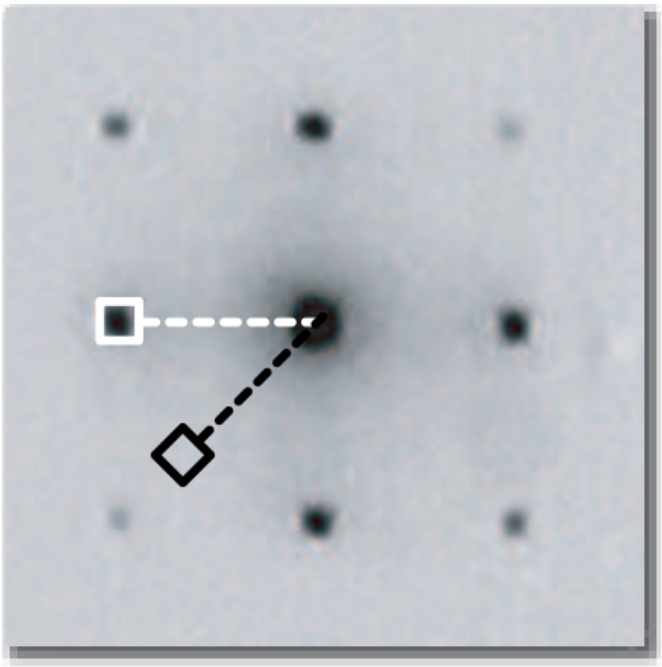
Non-perturbative treatment leads to a correlation function decaying exponentially

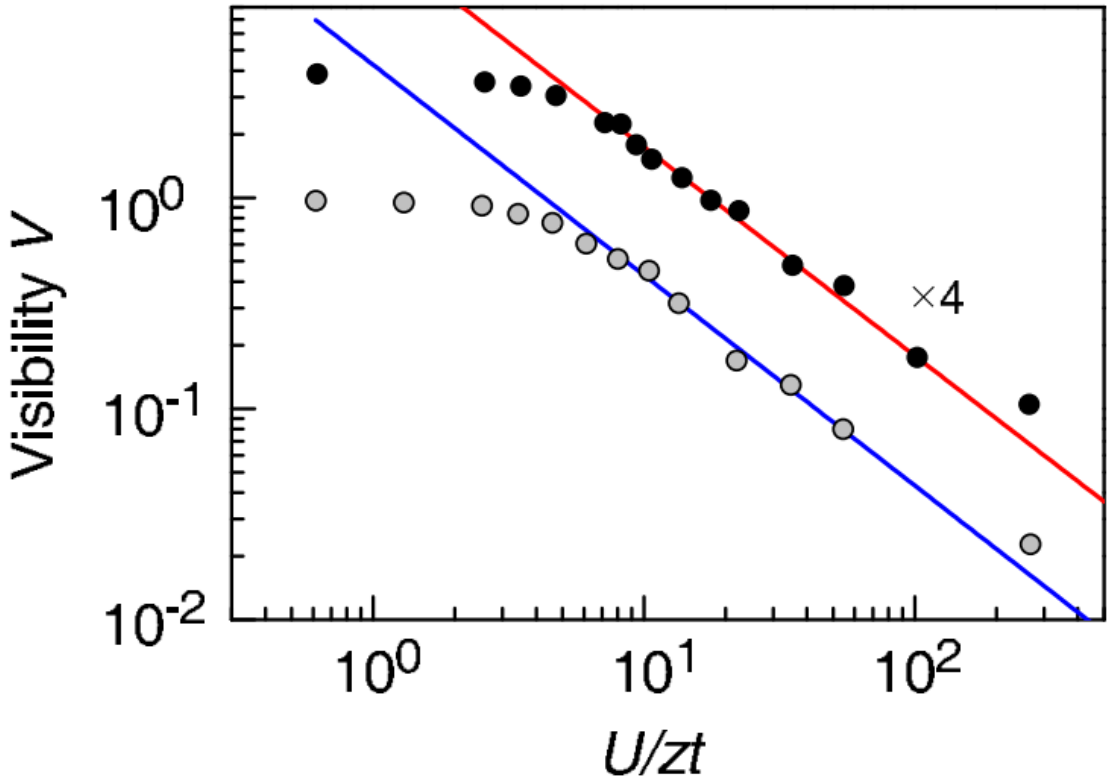
$$C(i,j) \sim \left(\frac{J}{U}\right)^{|i-j|}.$$

Correlation length

$$\xi = \frac{a}{\log(U/J)}.$$

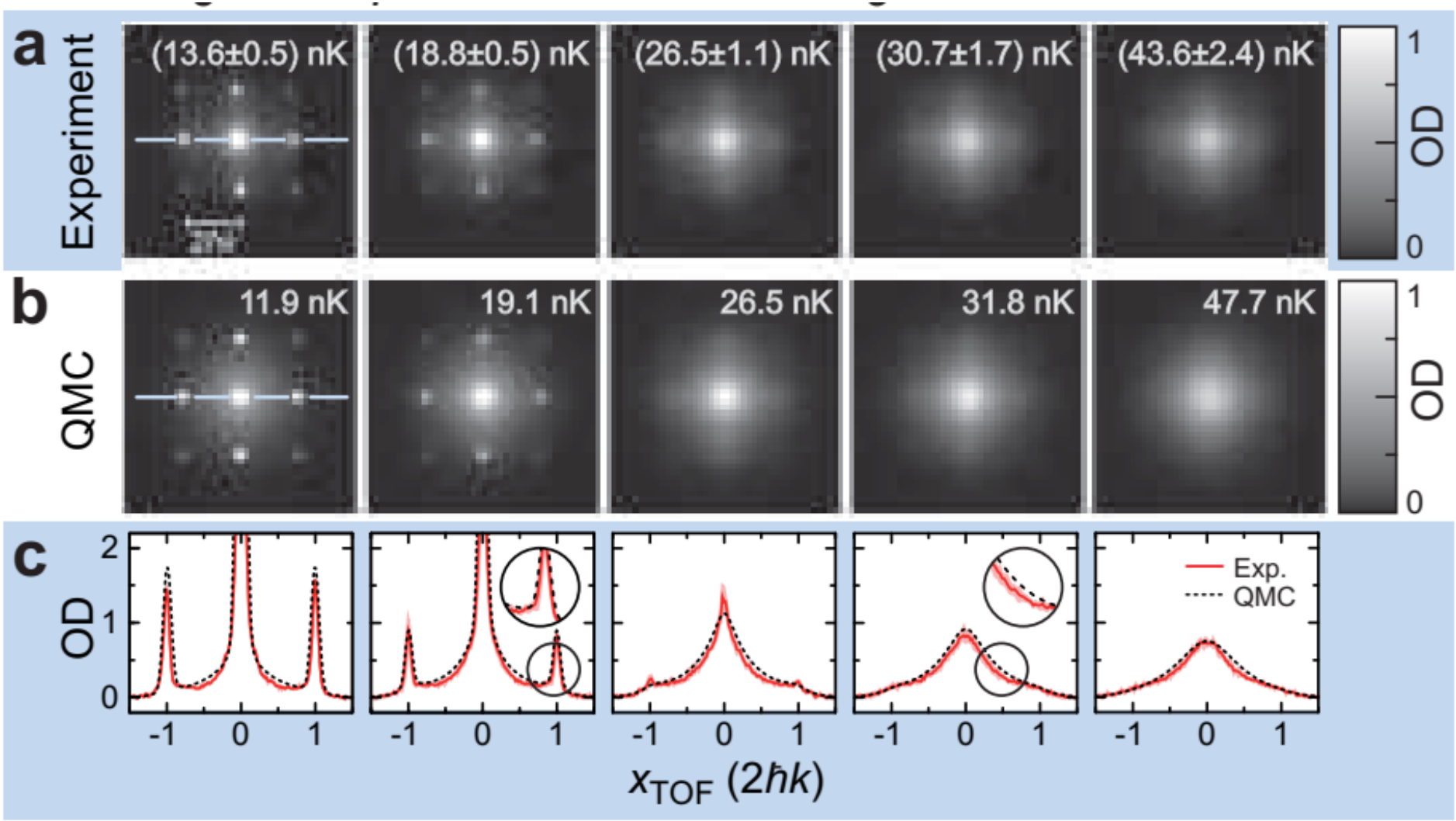
Signature of particle-hole excitations





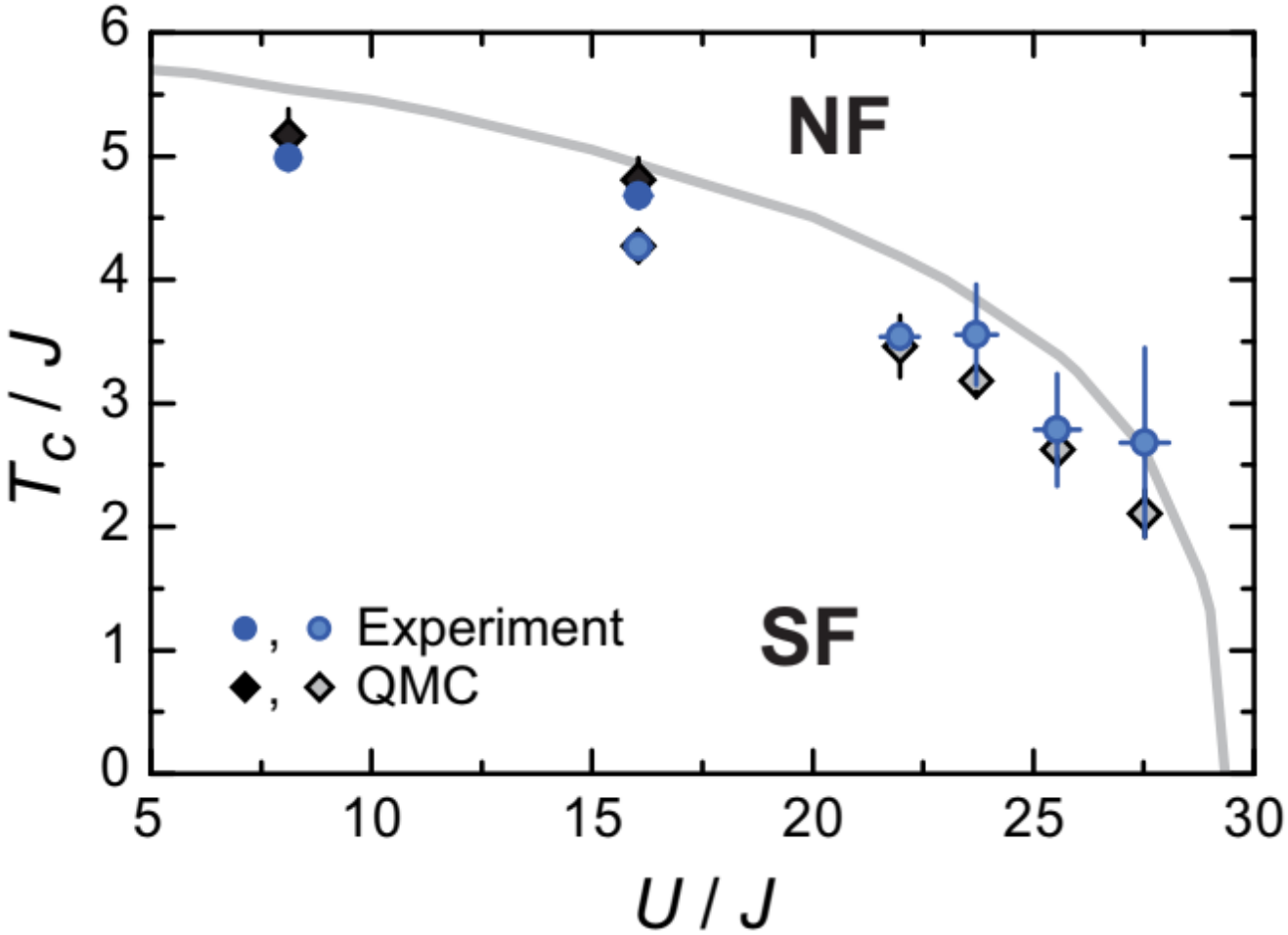
Gerbier et al, PRL 2005

Finite temperature: comparison with Monte-Carlo theory



Trotzky et al, Nature Phys. 2010

Superfluid critical temperature

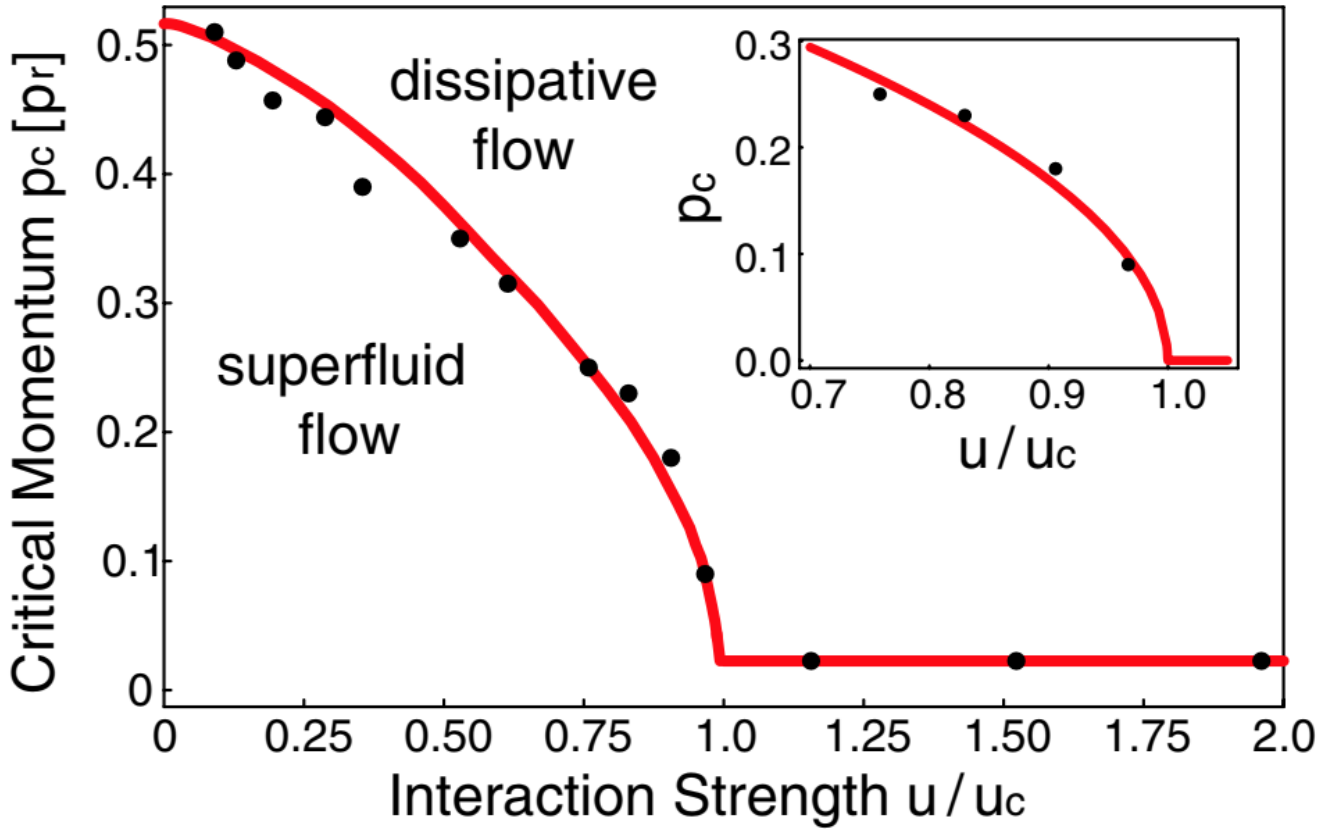


Trotzky et al, Nature Phys. 2010

Outline

1. Band structure and dynamics in optical lattices
   - Band structure in one dimension
   - Dynamics of a particle in an optical lattice
   - Wannier functions and tight-binding limit
   - Complex lattices in 1D: SSH model
   - Complex lattices in 2D: graphene and quantum Hall bands
2. Superfluid/Mott insulator transition
   - Hubbard Hamiltonian
   - Superfluid/Mott insulator: phase diagram
   - Gutzwiller variational approach
   - Interference experiments
   - Transport experiments
   - Mott shell structure
   - Low-energy excitations
3. Fermi-Hubbard model and quantum magnetism
   - Attractive Fermi-Hubbard model
   - Repulsive Fermi-Hubbard model and Mott insulator
   - Quantum magnetism

Superfluid critical velocity



Mun et al, PRL 2007

Outline

1. Band structure and dynamics in optical lattices
   - Band structure in one dimension
   - Dynamics of a particle in an optical lattice
   - Wannier functions and tight-binding limit
   - Complex lattices in 1D: SSH model
   - Complex lattices in 2D: graphene and quantum Hall bands
2. Superfluid/Mott insulator transition
   - Hubbard Hamiltonian
   - Superfluid/Mott insulator: phase diagram
   - Gutzwiller variational approach
   - Interference experiments
   - Transport experiments
   - Mott shell structure
   - Low-energy excitations
3. Fermi-Hubbard model and quantum magnetism
   - Attractive Fermi-Hubbard model
   - Repulsive Fermi-Hubbard model and Mott insulator
   - Quantum magnetism

Gaussian laser beams an additional potential

We consider an optical lattice produced by two counter-propagating gaussian beams (red-detuned)

$$V(\mathbf{r}) = -V_0[1 - \sin^2(kx)]\mathrm{e}^{-2(y^2+z^2)/w^2}.$$

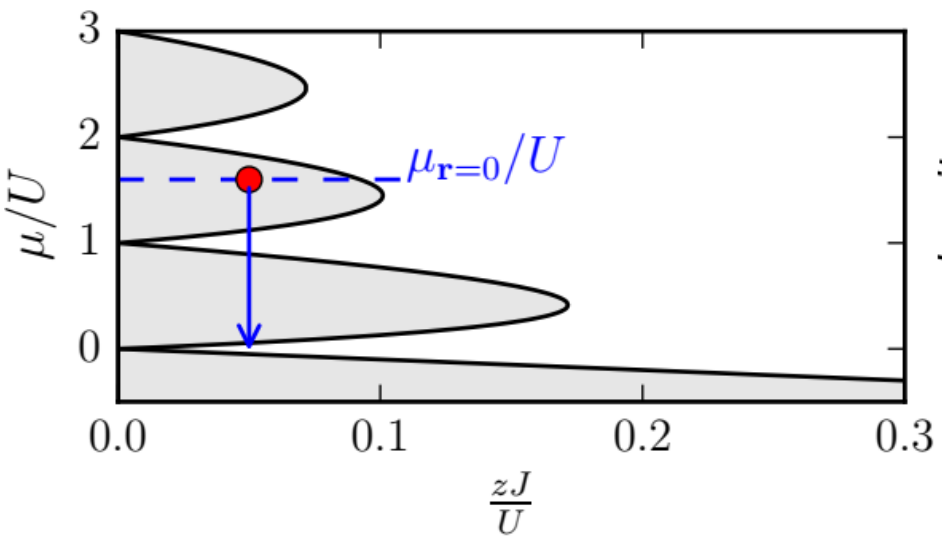
It can be approximated by the sum of

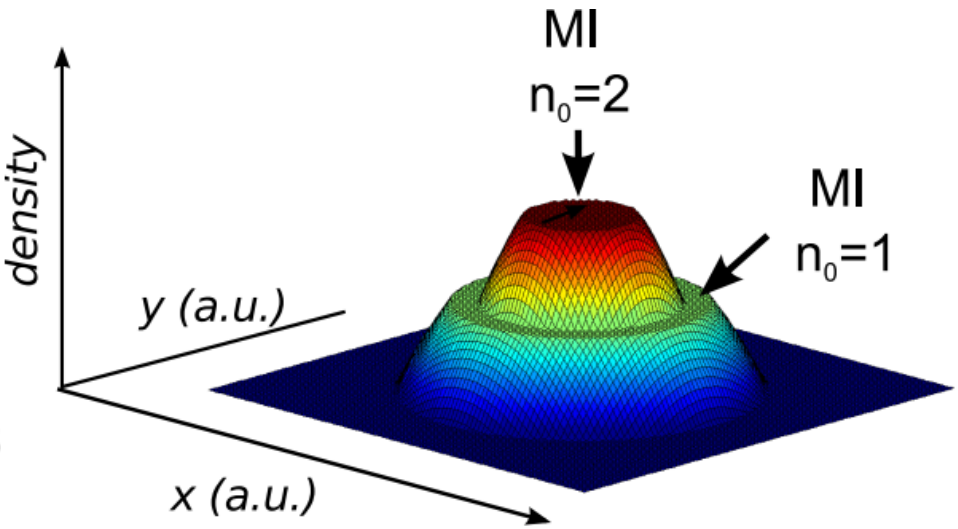
- a lattice of uniform depth V_0,
- an additional harmonic confinement of frequency $\Omega = \sqrt{4V_0/mw^2}$.

Consequence: gradual variation of the local chemical potential

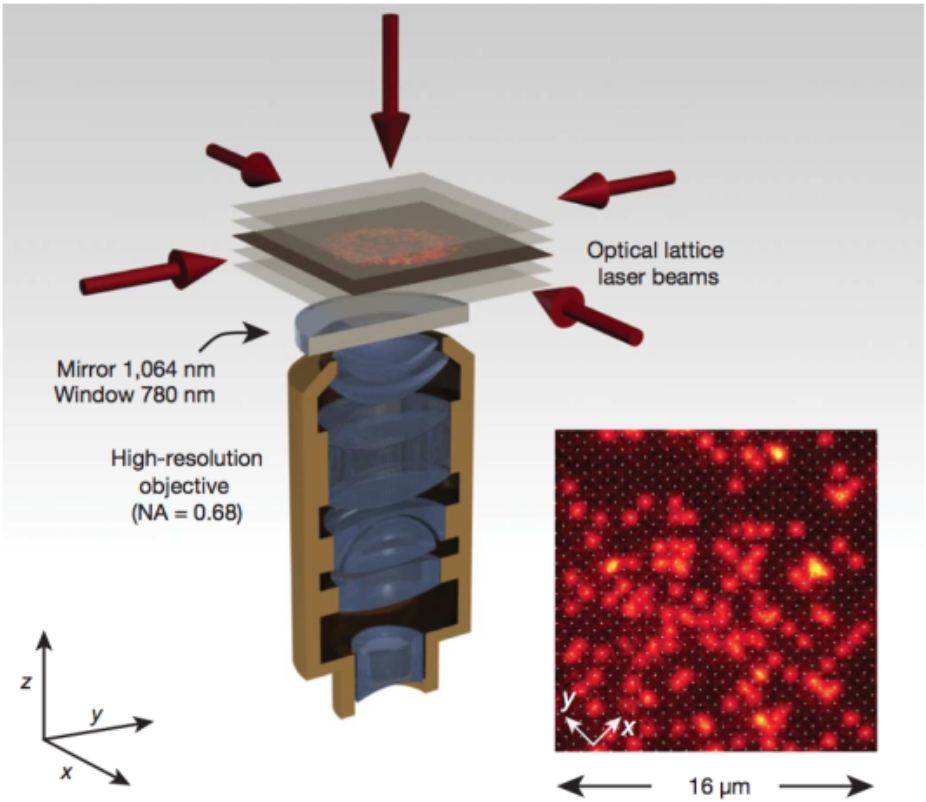
$$\mu(\mathbf{r}) = \mu_0 - \frac{1}{2}m\Omega^2 r^2.$$

Shell structure of a trapped Mott insulator

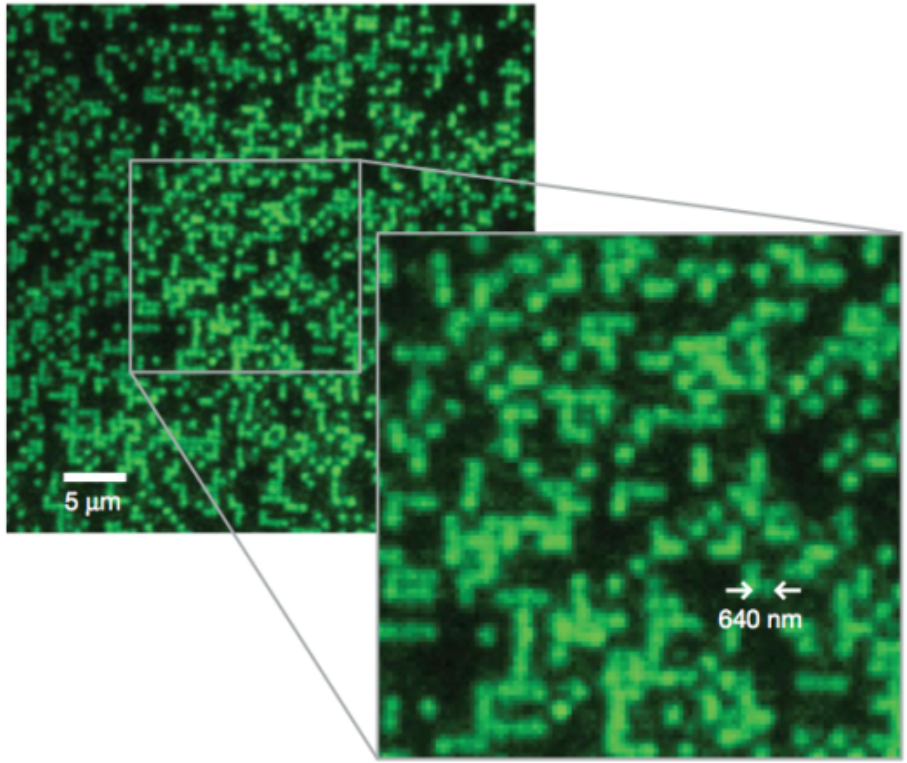




Single-atom imaging



Sherson et al, Nature 2010,



Bakr et al, Nature 2009

Single-atom imaging: protocol

- Atoms in a deep optical lattice (depth $\sim 1\,\mathrm{mK}$)
- Laser cooling with optical molasses/Raman sideband cooling ($T \sim 1\,\mu\mathrm{K} - 20\,\mu\mathrm{K}$)
  $\rightarrow$ no quantum or thermal-assisted tunneling
- fluorescence collected on a microscope objective

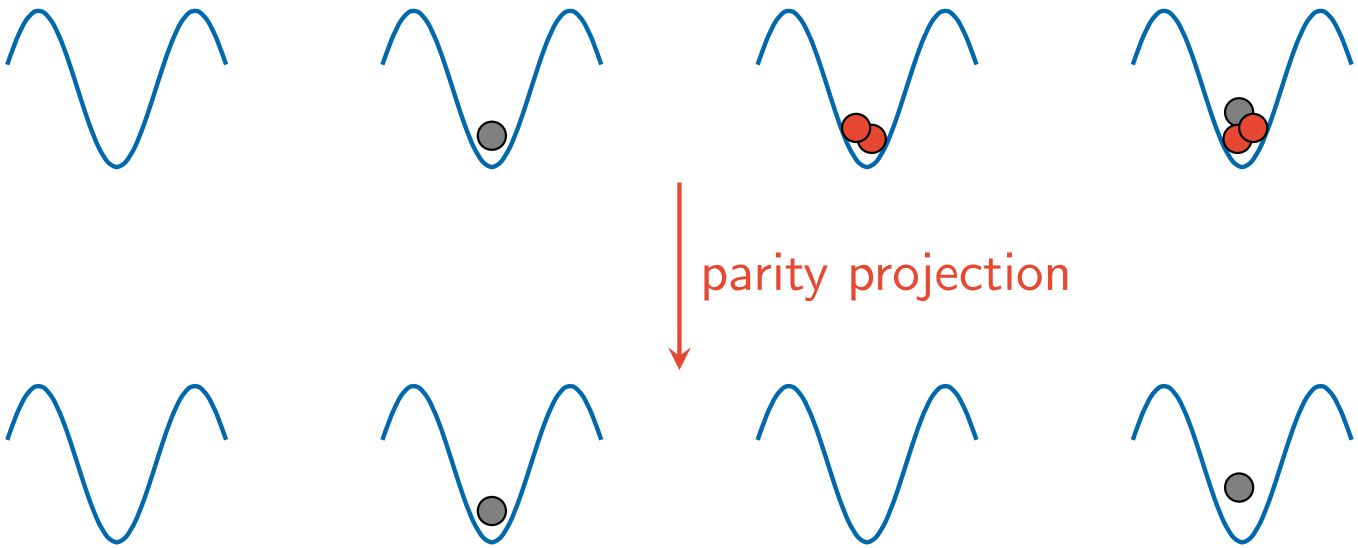
Single-atom imaging: protocol

- Atoms in a deep optical lattice (depth $\sim 1\,\mathrm{mK}$)
- Laser cooling with optical molasses/Raman sideband cooling ($T \sim 1\,\mu\mathrm{K} - 20\,\mu\mathrm{K}$)
  $\rightarrow$ no quantum or thermal-assisted tunneling
- fluorescence collected on a microscope objective
- light-assisted collisions (pairwise) $\rightarrow$ parity occupation measurement

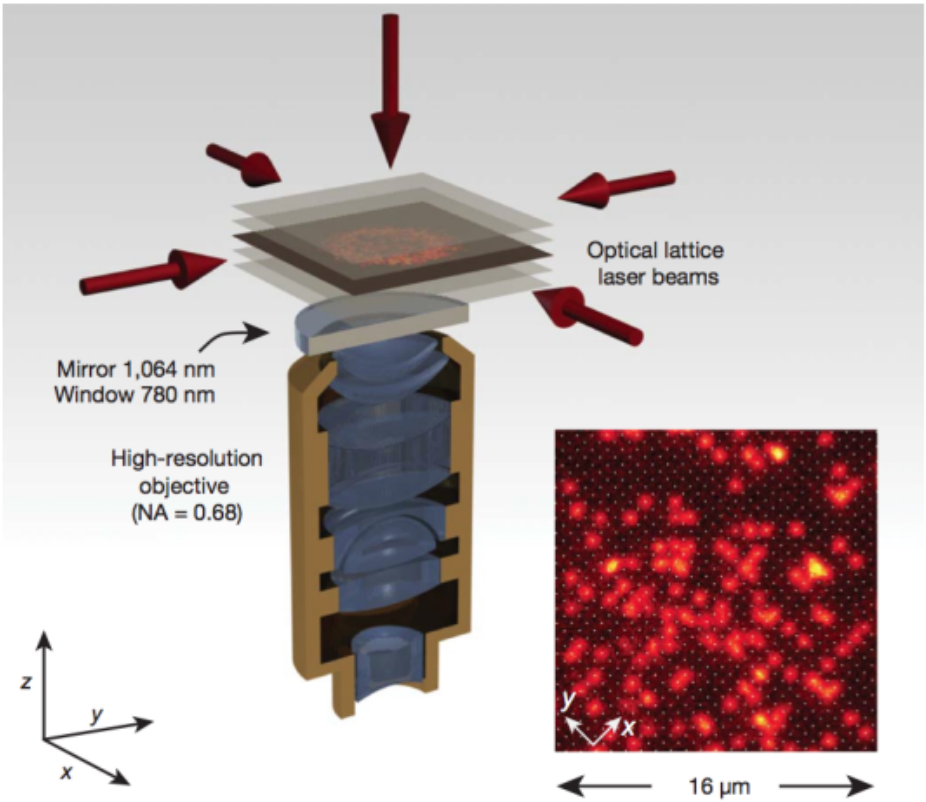


Single-atom imaging: protocol

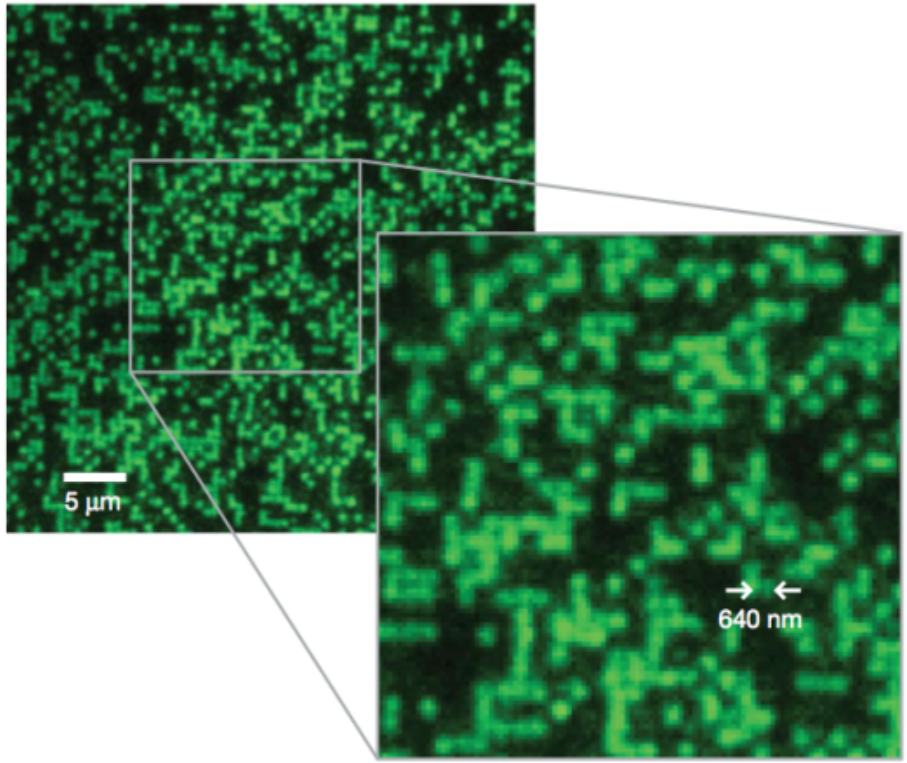
- Atoms in a deep optical lattice (depth $\sim 1\,\mathrm{mK}$)
- Laser cooling with optical molasses/Raman sideband cooling ($T \sim 1\,\mu\mathrm{K} - 20\,\mu\mathrm{K}$)
  $\rightarrow$ no quantum or thermal-assisted tunneling
- fluorescence collected on a microscope objective
- light-assisted collisions (pairwise) $\rightarrow$ parity occupation measurement



Single-atom imaging

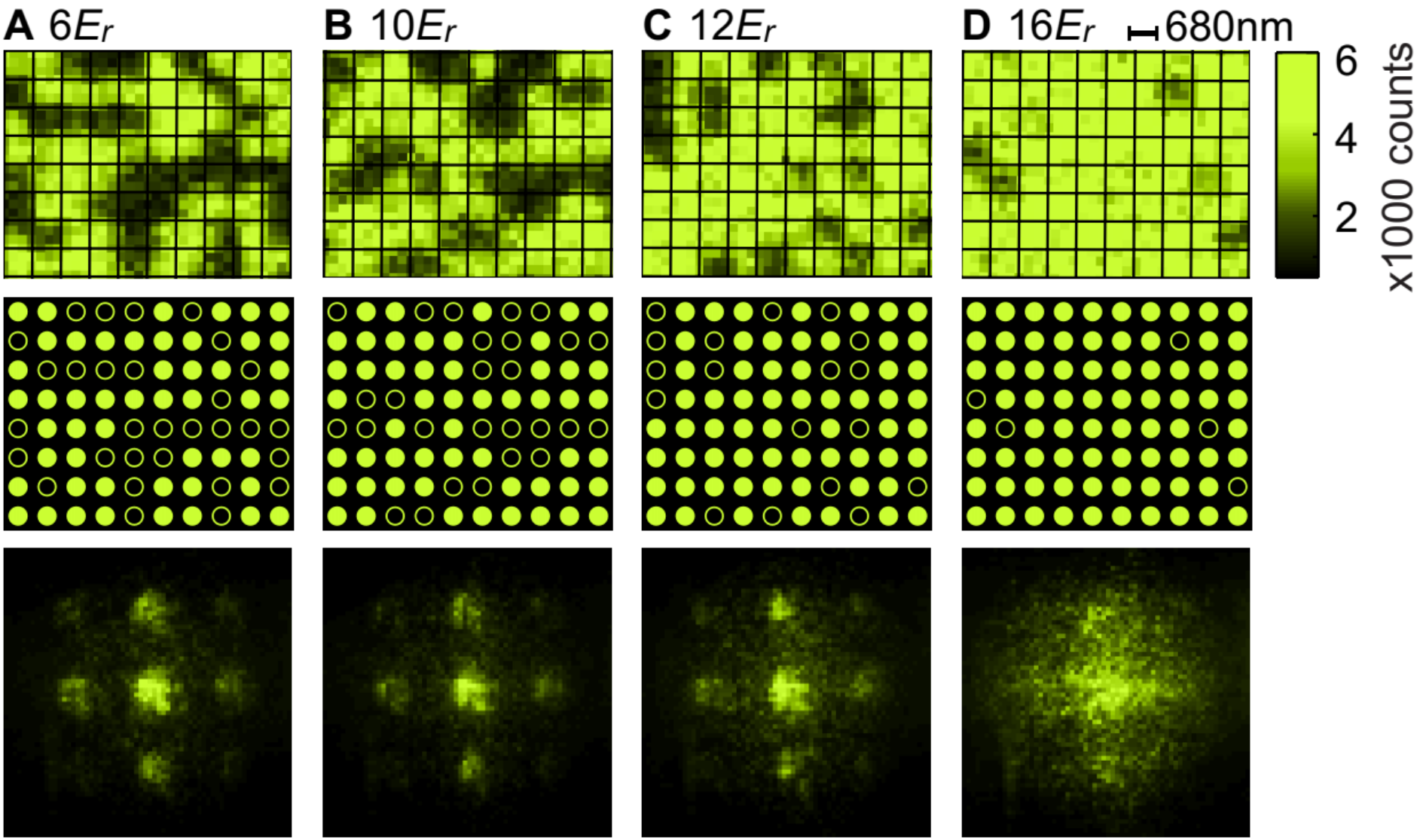


Sherson et al, Nature 2010,



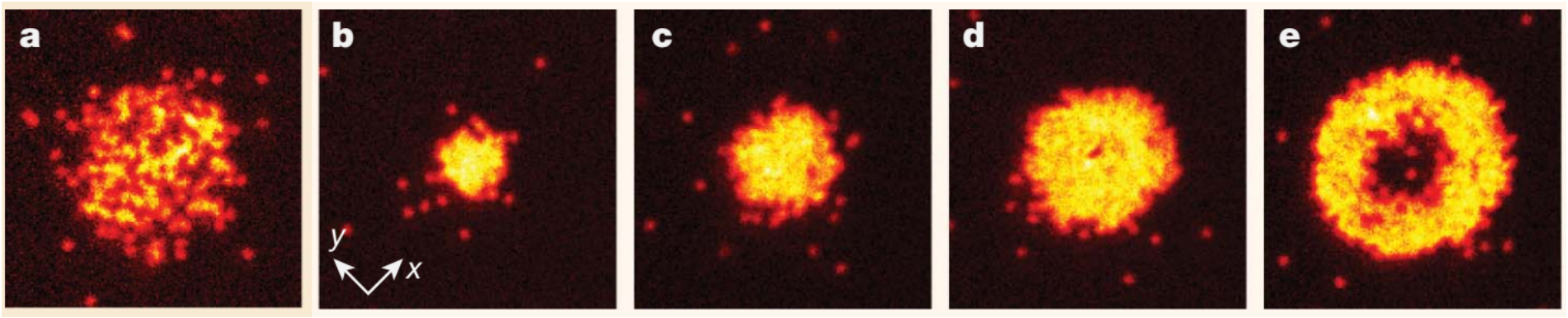
Bakr et al, Nature 2009

In situ imaging of a Mott insulator



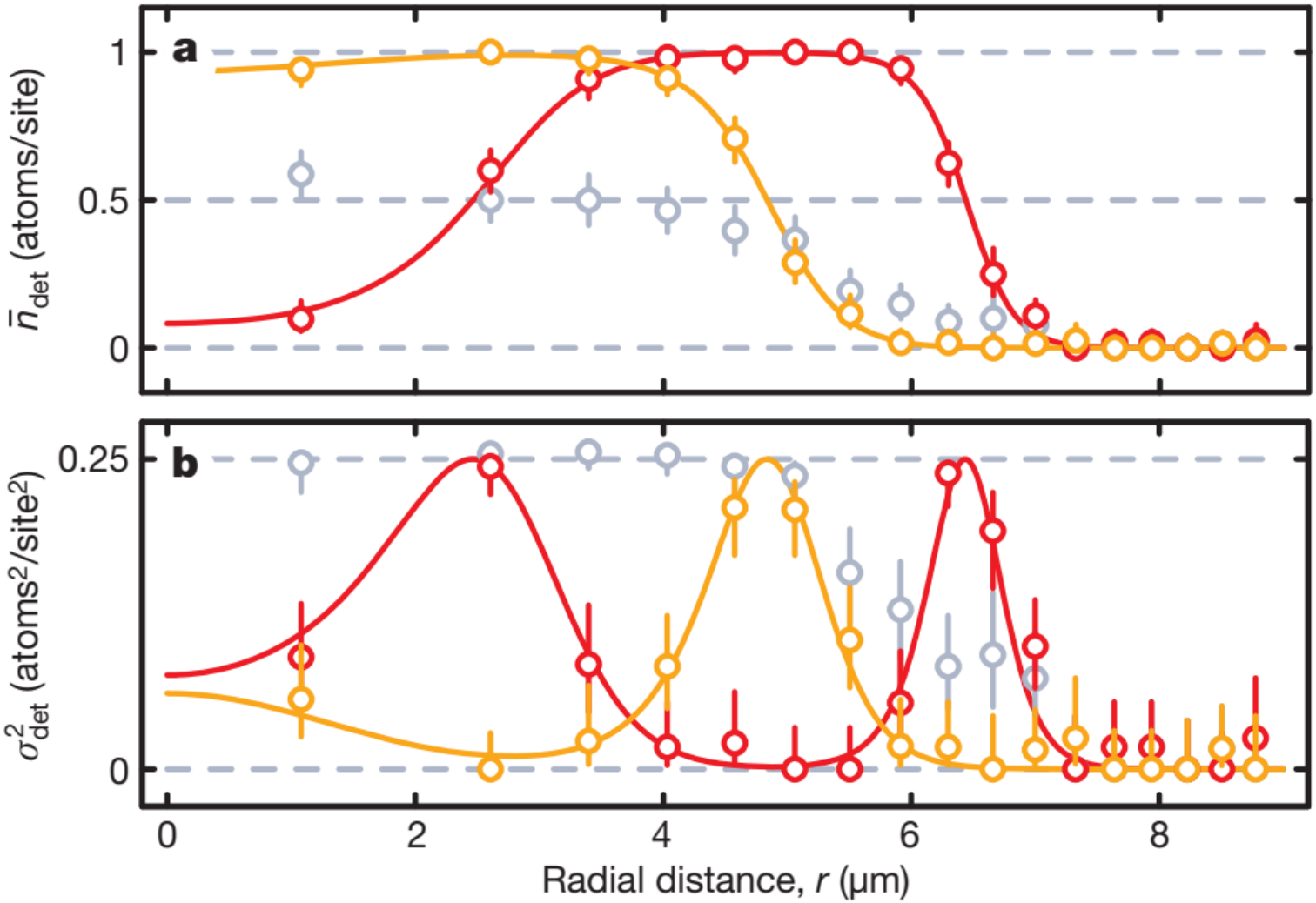
Bakr et al, Science 2010

In situ imaging of a Mott insulator



Sherson et al, Nature 2010

The wedding cake structure



Sherson et al, Nature 2010

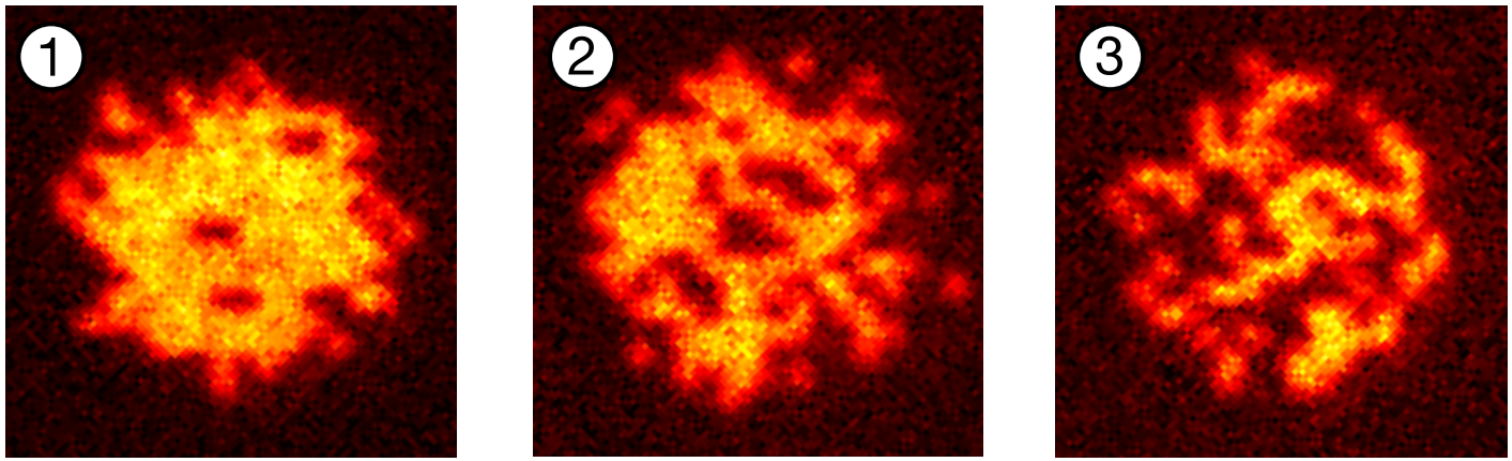
Consistent with a finite temperature $T = 0.09\, U/k_B$.

Outline

1. Band structure and dynamics in optical lattices
   - Band structure in one dimension
   - Dynamics of a particle in an optical lattice
   - Wannier functions and tight-binding limit
   - Complex lattices in 1D: SSH model
   - Complex lattices in 2D: graphene and quantum Hall bands
2. Superfluid/Mott insulator transition
   - Hubbard Hamiltonian
   - Superfluid/Mott insulator: phase diagram
   - Gutzwiller variational approach
   - Interference experiments
   - Transport experiments
   - Mott shell structure
   - Low-energy excitations
3. Fermi-Hubbard model and quantum magnetism
   - Attractive Fermi-Hubbard model
   - Repulsive Fermi-Hubbard model and Mott insulator
   - Quantum magnetism

In situ observation of particle-hole excitations

Mott insulator $\rightarrow$ superfluid



Endres et al, Science 2011

For dynamics in 1D only: non-local string order

Higgs mode

We come back to Gutzwiller description in the particle-hole regime:

$$c(n-1) = \sin\theta\, e^{-i\phi}/\sqrt{2},$$
$$c(n) = \cos\theta,$$
$$c(n+1) = \sin\theta\, e^{i\phi}/\sqrt{2}.$$

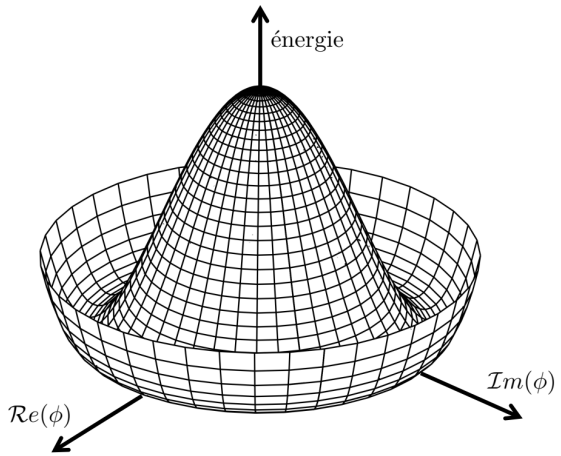
We write

$$\psi = \rho e^{i\phi}, \quad \rho = \frac{1}{2}\sin(2\theta).$$

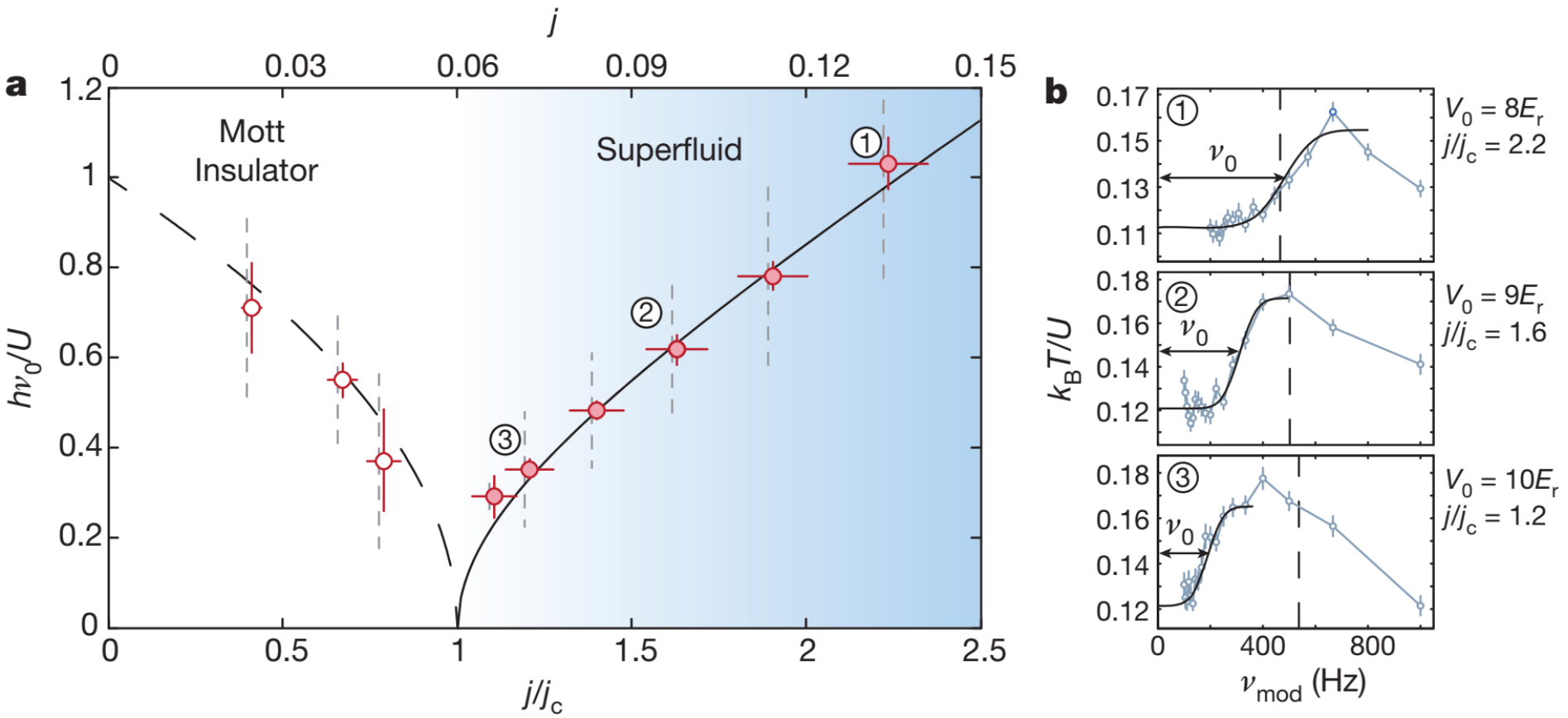
The free energy then reads

$$E[\psi] = \frac{U}{2}|\psi|^4 + \frac{U - U_c}{2}|\psi|^2$$

For $U < U_c$: energy is minimum for $\rho > 0$: superfluid phase.



Softening of the Higgs mode at the critical point



Endres et al, Nature 2012

Outline

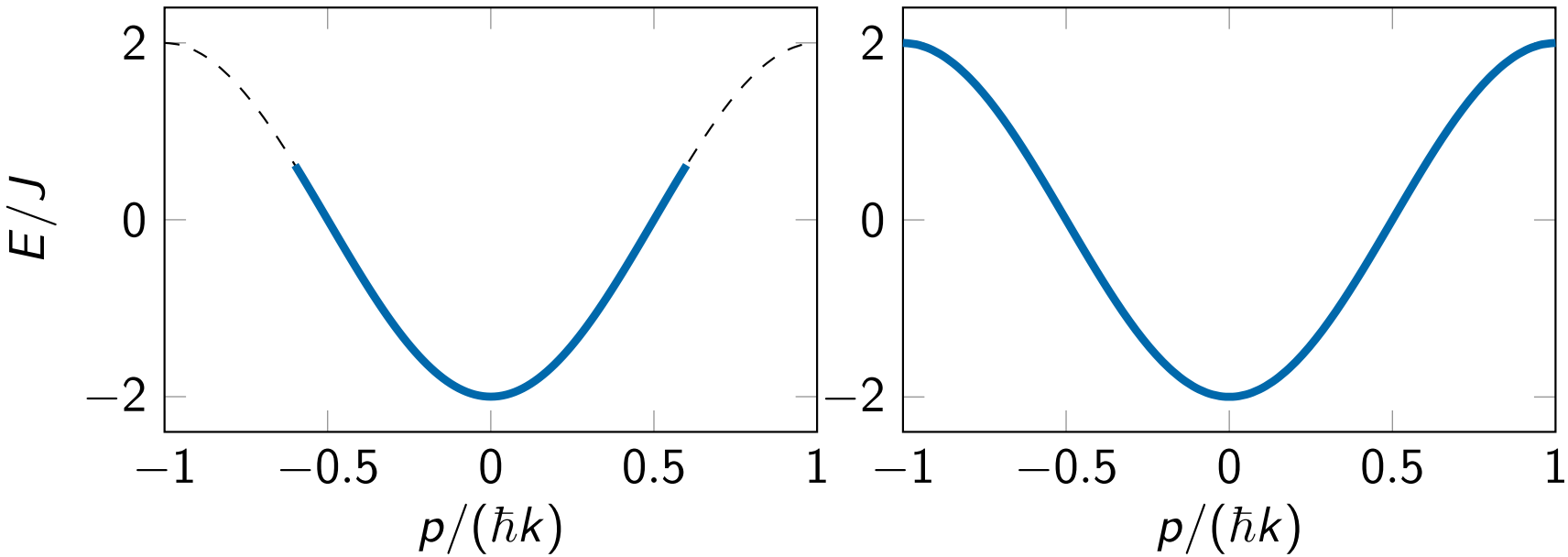
1. Band structure and dynamics in optical lattices
   - Band structure in one dimension
   - Dynamics of a particle in an optical lattice
   - Wannier functions and tight-binding limit
   - Complex lattices in 1D: SSH model
   - Complex lattices in 2D: graphene and quantum Hall bands
2. Superfluid/Mott insulator transition
   - Hubbard Hamiltonian
   - Superfluid/Mott insulator: phase diagram
   - Gutzwiller variational approach
   - Interference experiments
   - Transport experiments
   - Mott shell structure
   - Low-energy excitations
3. Fermi-Hubbard model and quantum magnetism
   - Attractive Fermi-Hubbard model
   - Repulsive Fermi-Hubbard model and Mott insulator
   - Quantum magnetism

Fermi-Hubbard model

We extend the Bose-Hubbard model to fermions in two spin states $\uparrow$ and $\downarrow$:

$$H = -J \sum_{j,\sigma} (a^\dagger_{j,\sigma} a_{j+1,\sigma} + \text{h.c.}) + U \sum_j n_{j,\uparrow} n_{j,\downarrow}.$$

- Non-interacting: metal or band insulator (filling $n = 2$)



- Attractive: $U < 0 \rightarrow$ connected to the BEC-BCS crossover
- Repulsive: $U > 0 \rightarrow$ Mott insulator (half filling) or superfluid phase?

Outline

1. Band structure and dynamics in optical lattices
   - Band structure in one dimension
   - Dynamics of a particle in an optical lattice
   - Wannier functions and tight-binding limit
   - Complex lattices in 1D: SSH model
   - Complex lattices in 2D: graphene and quantum Hall bands
2. Superfluid/Mott insulator transition
   - Hubbard Hamiltonian
   - Superfluid/Mott insulator: phase diagram
   - Gutzwiller variational approach
   - Interference experiments
   - Transport experiments
   - Mott shell structure
   - Low-energy excitations
3. Fermi-Hubbard model and quantum magnetism
   - Attractive Fermi-Hubbard model
   - Repulsive Fermi-Hubbard model and Mott insulator
   - Quantum magnetism

Attractive Fermi-Hubbard model and BEC-BCS crossover

The attractive Fermi Hubbard model shares similar behavior with the BEC-BCS crossover in the continuum.

- Mapping in the dilute limit $\langle n \rangle \ll 1$.

Attractive Fermi-Hubbard model and BEC-BCS crossover

The attractive Fermi Hubbard model shares similar behavior with the BEC-BCS crossover in the continuum.

- Mapping in the dilute limit $\langle n \rangle \ll 1$.
- Two-body bound state of binding energy E_{m} (N_s sites, $U < 0$):

$$\frac{1}{|U|} = \frac{1}{N_s} \sum_{\mathbf{k}} \frac{1}{4J[3 - \cos(k_x a) - \cos(k_y a) - \cos(k_z a)] + E_{\mathrm{m}}},$$

for

$$|U| > |U_c| = 7.9\, J.$$

Attractive Fermi-Hubbard model and BEC-BCS crossover

The attractive Fermi Hubbard model shares similar behavior with the BEC-BCS crossover in the continuum.

- Mapping in the dilute limit $\langle n \rangle \ll 1$.
- Two-body bound state of binding energy E_{m} (N_s sites, $U < 0$):

$$\frac{1}{|U|} = \frac{1}{N_s} \sum_{\mathbf{k}} \frac{1}{4J[3 - \cos(k_x a) - \cos(k_y a) - \cos(k_z a)] + E_{\mathrm{m}}},$$

for

$$|U| > |U_c| = 7.9\, J.$$

U_c corresponds to the unitary limit.

Attractive Fermi-Hubbard model and BEC-BCS crossover

The attractive Fermi Hubbard model shares similar behavior with the BEC-BCS crossover in the continuum.

- Mapping in the dilute limit $\langle n \rangle \ll 1$.
- Two-body bound state of binding energy E_{m} (N_s sites, $U < 0$):

$$\frac{1}{|U|} = \frac{1}{N_s} \sum_{\mathbf{k}} \frac{1}{4J[3 - \cos(k_x a) - \cos(k_y a) - \cos(k_z a)] + E_{\mathrm{m}}},$$

for

$$|U| > |U_c| = 7.9\, J.$$

U_c corresponds to the unitary limit.

New features:

- for large attraction $|U| \gg J$: deep molecules with a small dimer tunnel coupling

$$T_c \sim J^2/|U|.$$

Attractive Fermi-Hubbard model and BEC-BCS crossover

The attractive Fermi Hubbard model shares similar behavior with the BEC-BCS crossover in the continuum.

- Mapping in the dilute limit $\langle n \rangle \ll 1$.
- Two-body bound state of binding energy E_{m} (N_s sites, $U < 0$):

$$\frac{1}{|U|} = \frac{1}{N_s} \sum_{\mathbf{k}} \frac{1}{4J[3 - \cos(k_x a) - \cos(k_y a) - \cos(k_z a)] + E_{\mathrm{m}}},$$

for

$$|U| > |U_c| = 7.9\, J.$$

U_c corresponds to the unitary limit.

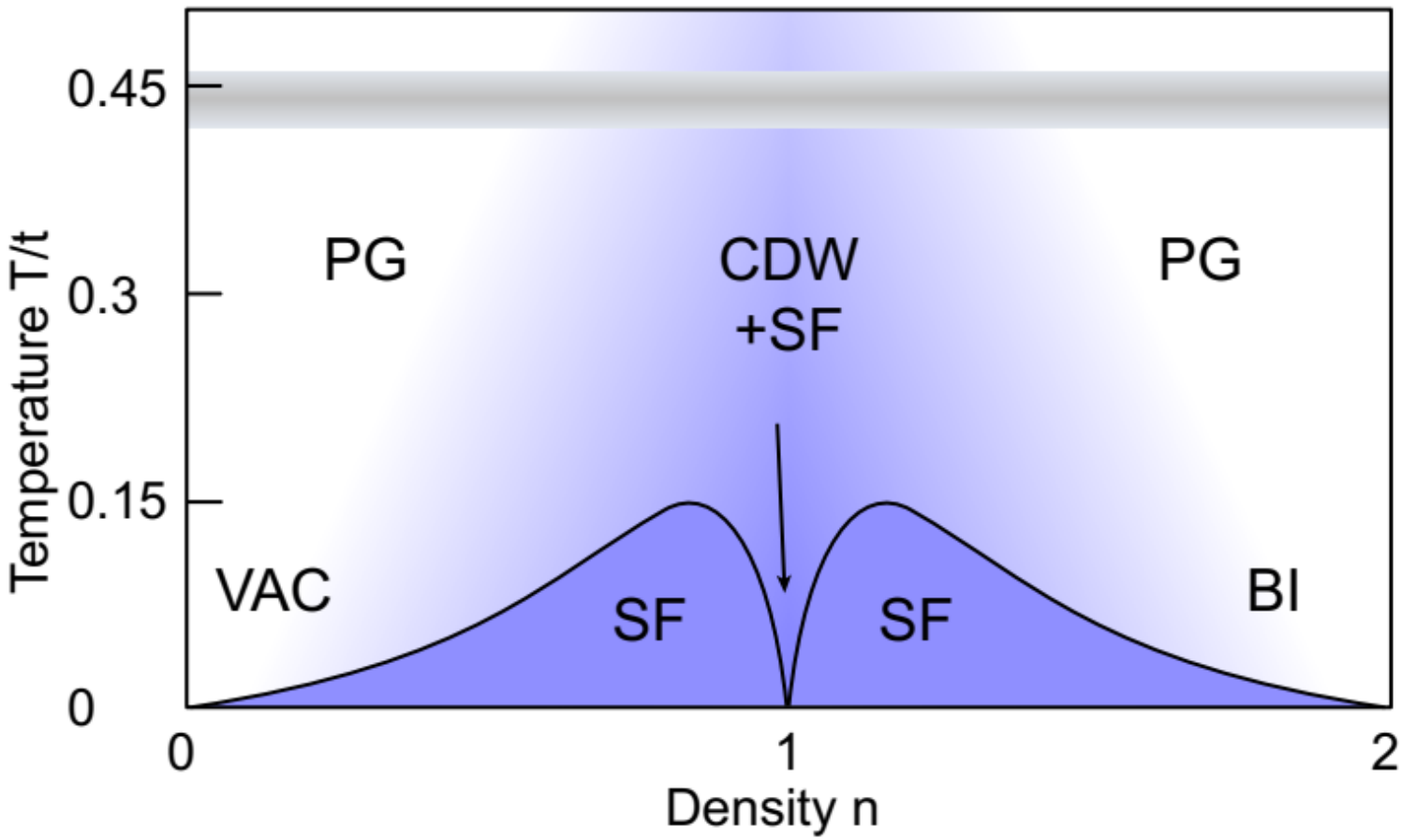
New features:

- for large attraction $|U| \gg J$: deep molecules with a small dimer tunnel coupling

$$T_c \sim J^2/|U|.$$

- particle/hole symmetry at half filling $\langle n_\uparrow \rangle = \langle n_\downarrow \rangle = 1/2$

Attractive Fermi-Hubbard model: phase diagram



from Mitra et al, Nature Phys. 2018

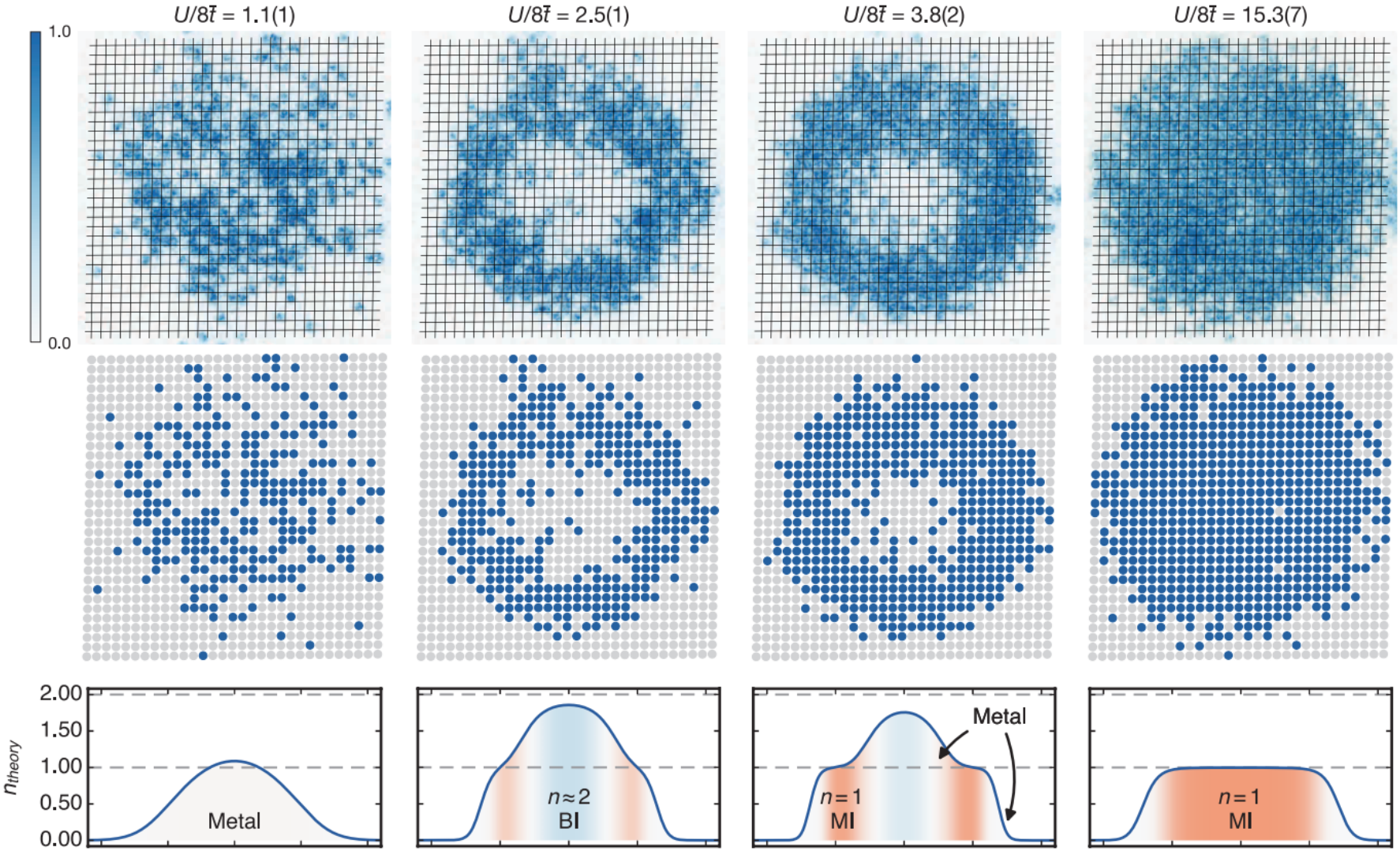
So far the temperature is not low enough to observe superfluidity.

Outline

1. Band structure and dynamics in optical lattices
   - Band structure in one dimension
   - Dynamics of a particle in an optical lattice
   - Wannier functions and tight-binding limit
   - Complex lattices in 1D: SSH model
   - Complex lattices in 2D: graphene and quantum Hall bands
2. Superfluid/Mott insulator transition
   - Hubbard Hamiltonian
   - Superfluid/Mott insulator: phase diagram
   - Gutzwiller variational approach
   - Interference experiments
   - Transport experiments
   - Mott shell structure
   - Low-energy excitations
3. Fermi-Hubbard model and quantum magnetism
   - Attractive Fermi-Hubbard model
   - Repulsive Fermi-Hubbard model and Mott insulator
   - Quantum magnetism

Repulsive Fermi-Hubbard model: Mott insulator

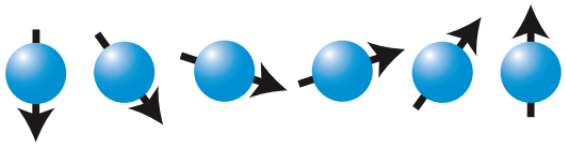
At half filling, we expect each site to be occupied by one atom (energy gap U).



Greif et al, Science 2016

Mott insulator with SU(N) symmetry

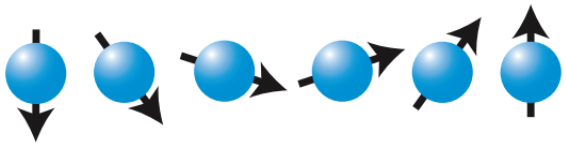
In two-electron atoms: electronic spin $J = 0$, nuclear spin $I \neq 0$.



example of ^{173}Yb

Mott insulator with SU(N) symmetry

In two-electron atoms: electronic spin $J = 0$, nuclear spin $I \neq 0$.

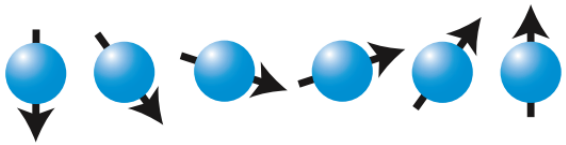


example of ^{173}Yb

Interactions do not depend on the spin state ($N = 2I + 1$).

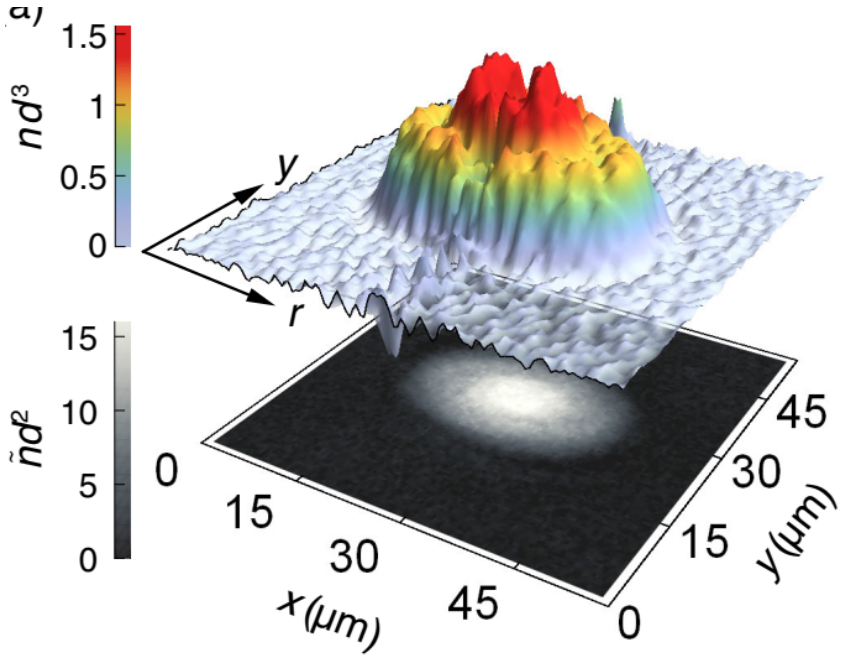
Mott insulator with SU(N) symmetry

In two-electron atoms: electronic spin $J = 0$, nuclear spin $I \neq 0$.



example of ^{173}Yb

Interactions do not depend on the spin state ($N = 2I + 1$).



Hofrichter et al, PRX 2016

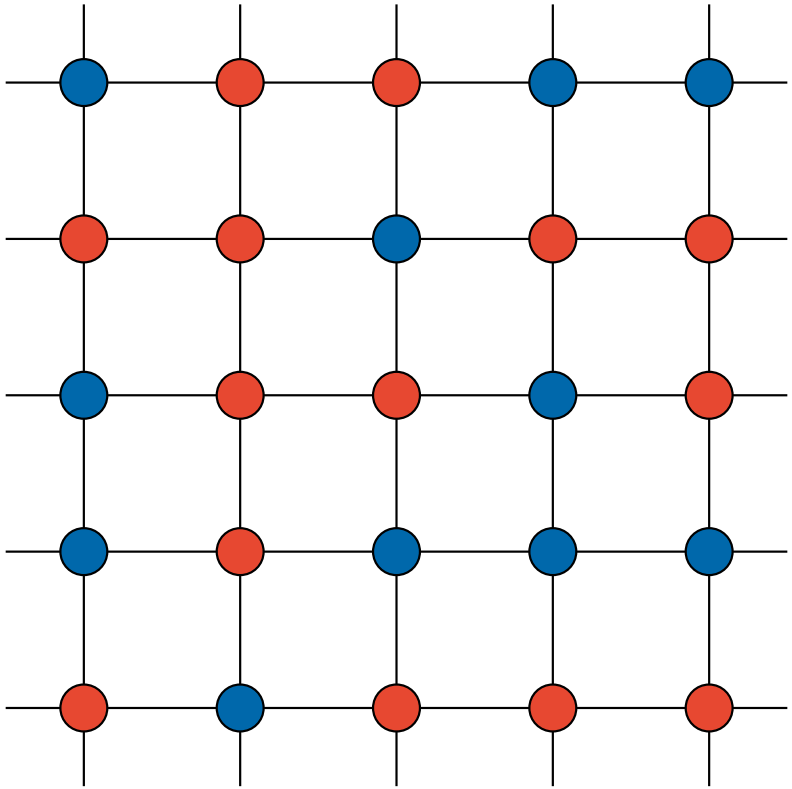
Entropy goes in the spin degree of freedom (Pomeranchuk cooling)

Outline

1. Band structure and dynamics in optical lattices
   - Band structure in one dimension
   - Dynamics of a particle in an optical lattice
   - Wannier functions and tight-binding limit
   - Complex lattices in 1D: SSH model
   - Complex lattices in 2D: graphene and quantum Hall bands
2. Superfluid/Mott insulator transition
   - Hubbard Hamiltonian
   - Superfluid/Mott insulator: phase diagram
   - Gutzwiller variational approach
   - Interference experiments
   - Transport experiments
   - Mott shell structure
   - Low-energy excitations
3. Fermi-Hubbard model and quantum magnetism
   - Attractive Fermi-Hubbard model
   - Repulsive Fermi-Hubbard model and Mott insulator
   - Quantum magnetism

Quantum magnetism in a fermionic Mott insulator

In a Mott insulator, how do the spin order at low temperature?



Toy model: quantum magnetism in a double-well

We consider two atoms of opposite spins located on 2 sites only.

$$H = \begin{array}{c} \\ |\uparrow\downarrow,\emptyset\rangle \\ |\emptyset,\uparrow\downarrow\rangle \\ |\uparrow,\downarrow\rangle \\ |\downarrow,\uparrow\rangle \end{array} \begin{array}{c} \begin{array}{cccc} |\uparrow\downarrow,\emptyset\rangle & |\emptyset,\uparrow\downarrow\rangle & |\uparrow,\downarrow\rangle & |\downarrow,\uparrow\rangle \end{array} \\ \begin{pmatrix} U & 0 & -J & J \\ 0 & U & -J & J \\ -J & -J & 0 & 0 \\ J & J & 0 & 0 \end{pmatrix} \end{array}.$$

Toy model: quantum magnetism in a double-well

We consider two atoms of opposite spins located on 2 sites only.

$$H = \begin{array}{c} \\ |\uparrow\downarrow,\emptyset\rangle \\ |\emptyset,\uparrow\downarrow\rangle \\ |\uparrow,\downarrow\rangle \\ |\downarrow,\uparrow\rangle \end{array} \begin{array}{c} \begin{array}{cccc} |\uparrow\downarrow,\emptyset\rangle & |\emptyset,\uparrow\downarrow\rangle & |\uparrow,\downarrow\rangle & |\downarrow,\uparrow\rangle \end{array} \\ \begin{pmatrix} U & 0 & -J & J \\ 0 & U & -J & J \\ -J & -J & 0 & 0 \\ J & J & 0 & 0 \end{pmatrix} \end{array}.$$

In the limit $J \ll U$ the low-energy dynamics occurs between $|\uparrow,\downarrow\rangle$ and $|\downarrow,\uparrow\rangle$.

Toy model: quantum magnetism in a double-well

We consider two atoms of opposite spins located on 2 sites only.

$$H = \begin{array}{c} \\ |\uparrow\downarrow,\emptyset\rangle \\ |\emptyset,\uparrow\downarrow\rangle \\ |\uparrow,\downarrow\rangle \\ |\downarrow,\uparrow\rangle \end{array} \begin{array}{c} \begin{array}{cccc} |\uparrow\downarrow,\emptyset\rangle & |\emptyset,\uparrow\downarrow\rangle & |\uparrow,\downarrow\rangle & |\downarrow,\uparrow\rangle \end{array} \\ \begin{pmatrix} U & 0 & -J & J \\ 0 & U & -J & J \\ -J & -J & 0 & 0 \\ J & J & 0 & 0 \end{pmatrix} \end{array}.$$

In the limit $J \ll U$ the low-energy dynamics occurs between $|\uparrow,\downarrow\rangle$ and $|\downarrow,\uparrow\rangle$.
Degenerate perturbation theory at second order:

$$H_{\text{mag}} = \begin{array}{c} \\ |\uparrow,\downarrow\rangle \\ |\downarrow,\uparrow\rangle \end{array} \begin{array}{c} \begin{array}{cc} |\uparrow,\downarrow\rangle & |\downarrow,\uparrow\rangle \end{array} \\ \begin{pmatrix} -2J^2/U & 2J^2/U \\ 2J^2/U & -2J^2/U \end{pmatrix} \end{array}.$$

Toy model: quantum magnetism in a double-well

We consider two atoms of opposite spins located on 2 sites only.

$$H = \begin{array}{c} \\ |\uparrow\downarrow,\emptyset\rangle \\ |\emptyset,\uparrow\downarrow\rangle \\ |\uparrow,\downarrow\rangle \\ |\downarrow,\uparrow\rangle \end{array} \begin{array}{c} \begin{array}{cccc} |\uparrow\downarrow,\emptyset\rangle & |\emptyset,\uparrow\downarrow\rangle & |\uparrow,\downarrow\rangle & |\downarrow,\uparrow\rangle \end{array} \\ \begin{pmatrix} U & 0 & -J & J \\ 0 & U & -J & J \\ -J & -J & 0 & 0 \\ J & J & 0 & 0 \end{pmatrix} \end{array}.$$

In the limit $J \ll U$ the low-energy dynamics occurs between $|\uparrow,\downarrow\rangle$ and $|\downarrow,\uparrow\rangle$.
Degenerate perturbation theory at second order:

$$H_{\text{mag}} = \begin{array}{c} \\ |\uparrow,\downarrow\rangle \\ |\downarrow,\uparrow\rangle \end{array} \begin{array}{c} \begin{array}{cc} |\uparrow,\downarrow\rangle & |\downarrow,\uparrow\rangle \end{array} \\ \begin{pmatrix} -2J^2/U & 2J^2/U \\ 2J^2/U & -2J^2/U \end{pmatrix} \end{array}.$$

Ground state is the singlet state $|s\rangle = (|\uparrow,\downarrow\rangle - |\downarrow,\uparrow\rangle)/\sqrt{2}$.
First excited state $|t\rangle = (|\uparrow,\downarrow\rangle + |\downarrow,\uparrow\rangle)/\sqrt{2}$ (energy $J_{\text{ex}} \equiv 4J^2/U$).

Toy model: quantum magnetism in a double-well

We consider two atoms of opposite spins located on 2 sites only.

$$H = \begin{array}{c} \\ |\uparrow\downarrow,\emptyset\rangle \\ |\emptyset,\uparrow\downarrow\rangle \\ |\uparrow,\downarrow\rangle \\ |\downarrow,\uparrow\rangle \end{array} \begin{array}{c} \begin{array}{cccc} |\uparrow\downarrow,\emptyset\rangle & |\emptyset,\uparrow\downarrow\rangle & |\uparrow,\downarrow\rangle & |\downarrow,\uparrow\rangle \end{array} \\ \begin{pmatrix} U & 0 & -J & J \\ 0 & U & -J & J \\ -J & -J & 0 & 0 \\ J & J & 0 & 0 \end{pmatrix} \end{array}.$$

In the limit $J \ll U$ the low-energy dynamics occurs between $|\uparrow,\downarrow\rangle$ and $|\downarrow,\uparrow\rangle$.
Degenerate perturbation theory at second order:

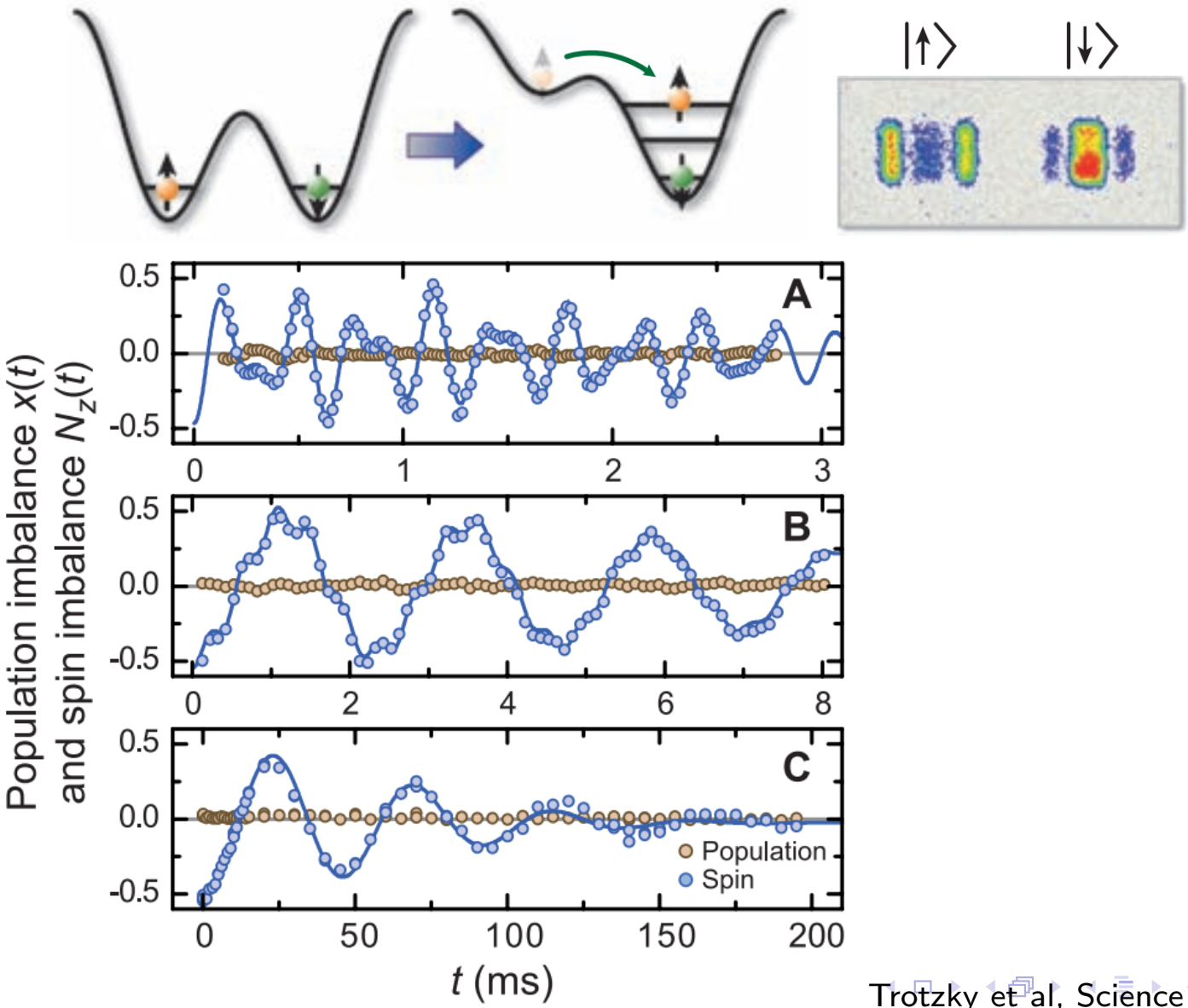
$$H_{\text{mag}} = \begin{array}{c} \\ |\uparrow,\downarrow\rangle \\ |\downarrow,\uparrow\rangle \end{array} \begin{array}{c} \begin{array}{cc} |\uparrow,\downarrow\rangle & |\downarrow,\uparrow\rangle \end{array} \\ \begin{pmatrix} -2J^2/U & 2J^2/U \\ 2J^2/U & -2J^2/U \end{pmatrix} \end{array}.$$

Ground state is the singlet state $|s\rangle = (|\uparrow,\downarrow\rangle - |\downarrow,\uparrow\rangle)/\sqrt{2}$.
First excited state $|t\rangle = (|\uparrow,\downarrow\rangle + |\downarrow,\uparrow\rangle)/\sqrt{2}$ (energy $J_{\text{ex}} \equiv 4J^2/U$).
Effective spin model (antiferromagnetic Heisenberg)

$$H_{\text{mag}} = J_{\text{ex}} \mathbf{S}_1 \cdot \mathbf{S}_2.$$

Probing superexchange interactions

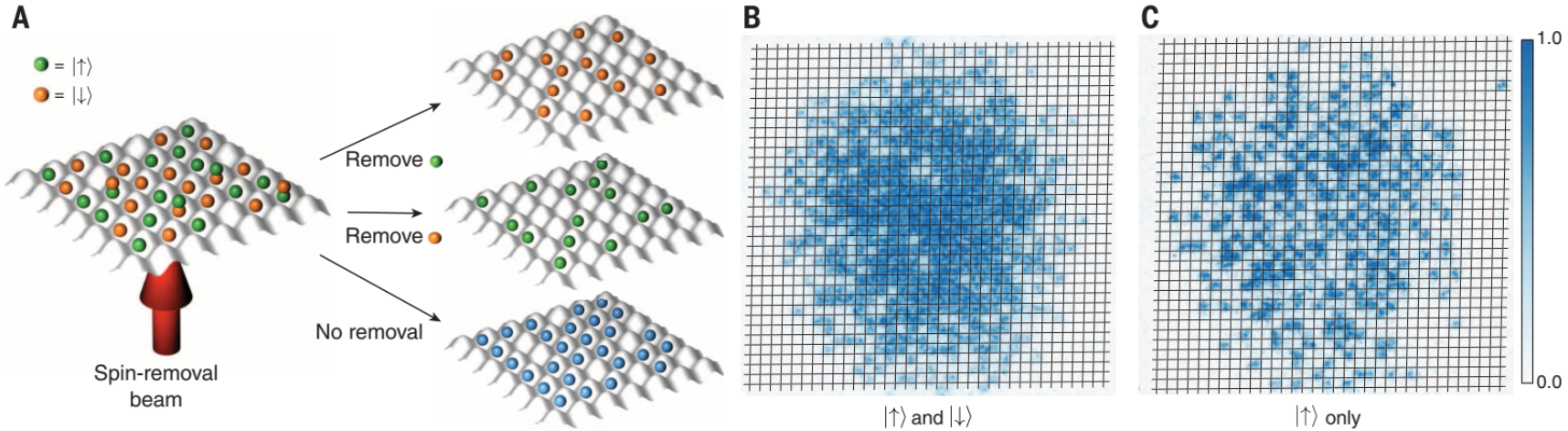
Deforming a lattice of double-wells brings left wells to higher Bloch bands.



Trotzky et al, Science 2008

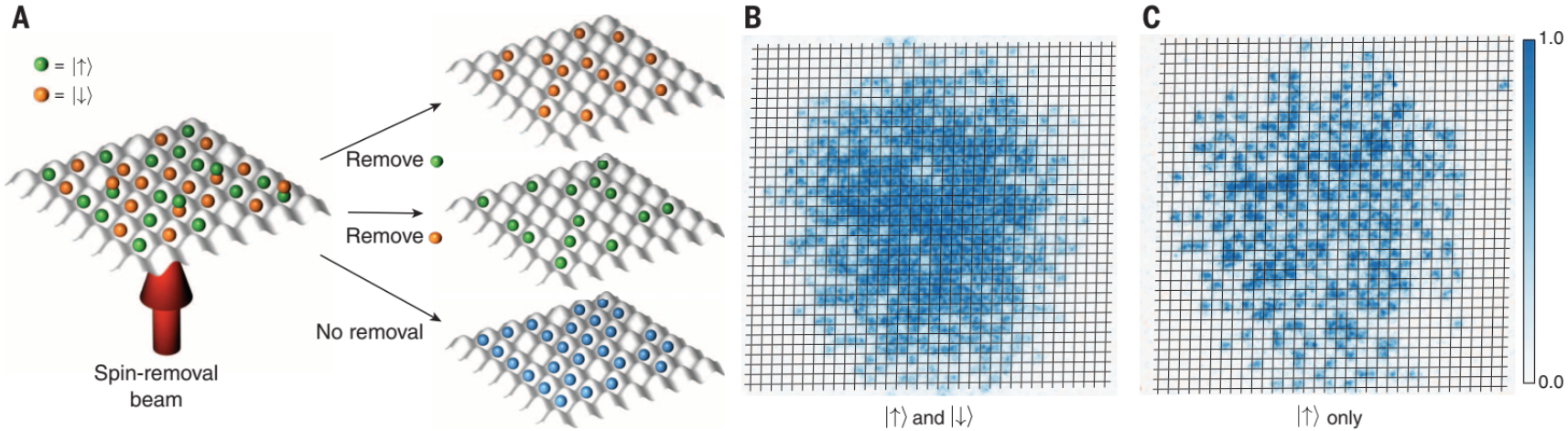
Short-range antiferromagnetic spin ordering

Single-atom imaging usually does not distinguish the spin levels.

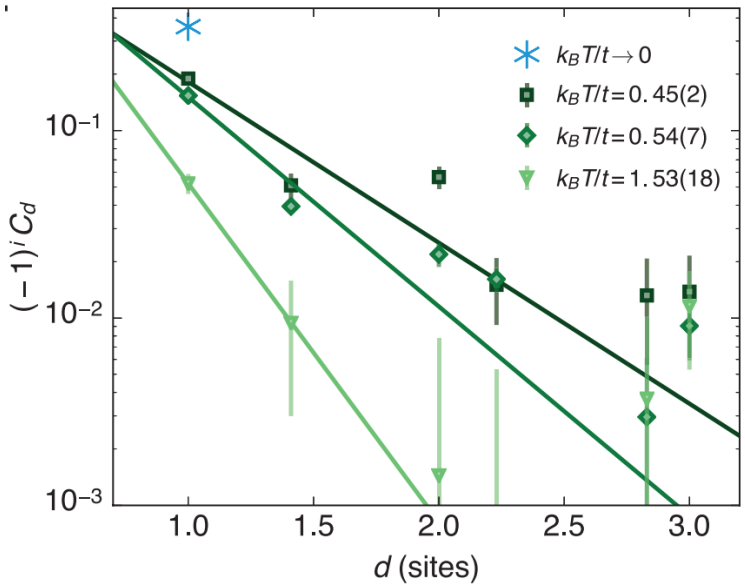


Short-range antiferromagnetic spin ordering

Single-atom imaging usually does not distinguish the spin levels.

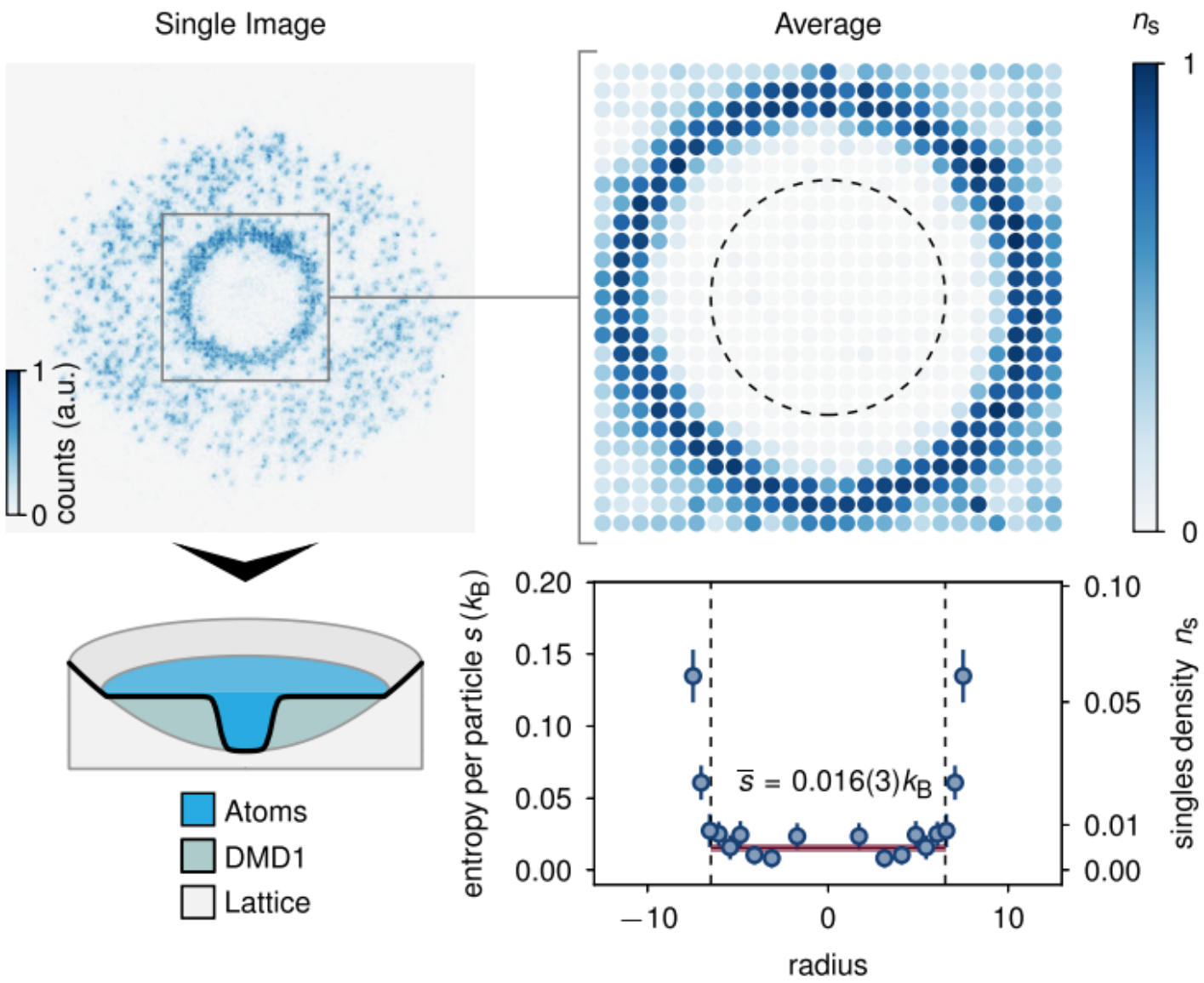


Study of the correlator $C_{\mathbf{d}} = 4(\langle S_z(\mathbf{r}+\mathbf{d})S_z(\mathbf{r})\rangle - \langle S_z(\mathbf{r}+\mathbf{d})\rangle\langle S_z(\mathbf{r})\rangle)$



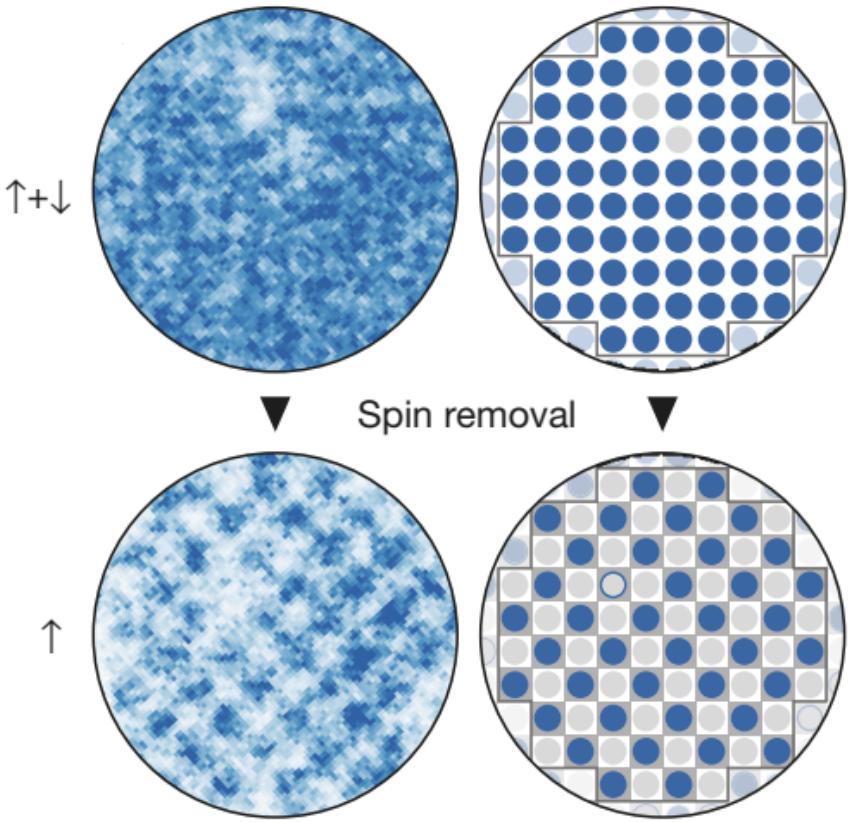
Parsons et al, Science 2016

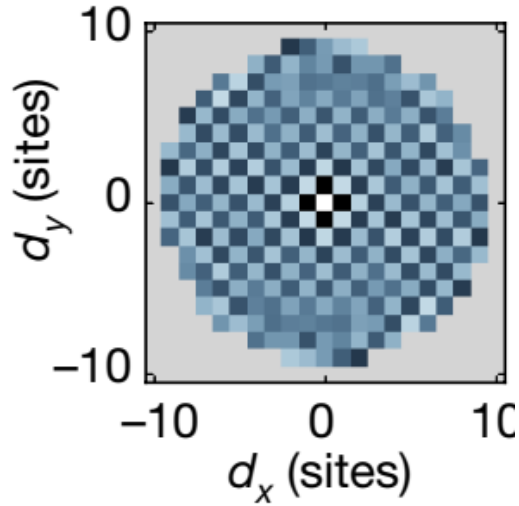
Potential shaping to ‘remove’ entropy

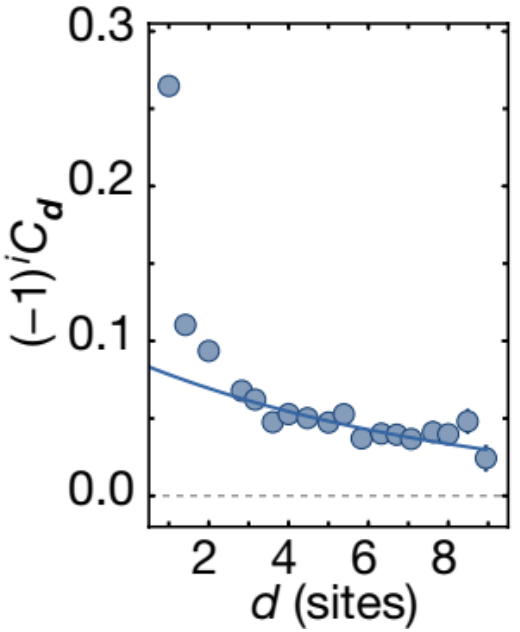


Chiu et al, PRL 2018

Observation of a long-range antiferromagnet

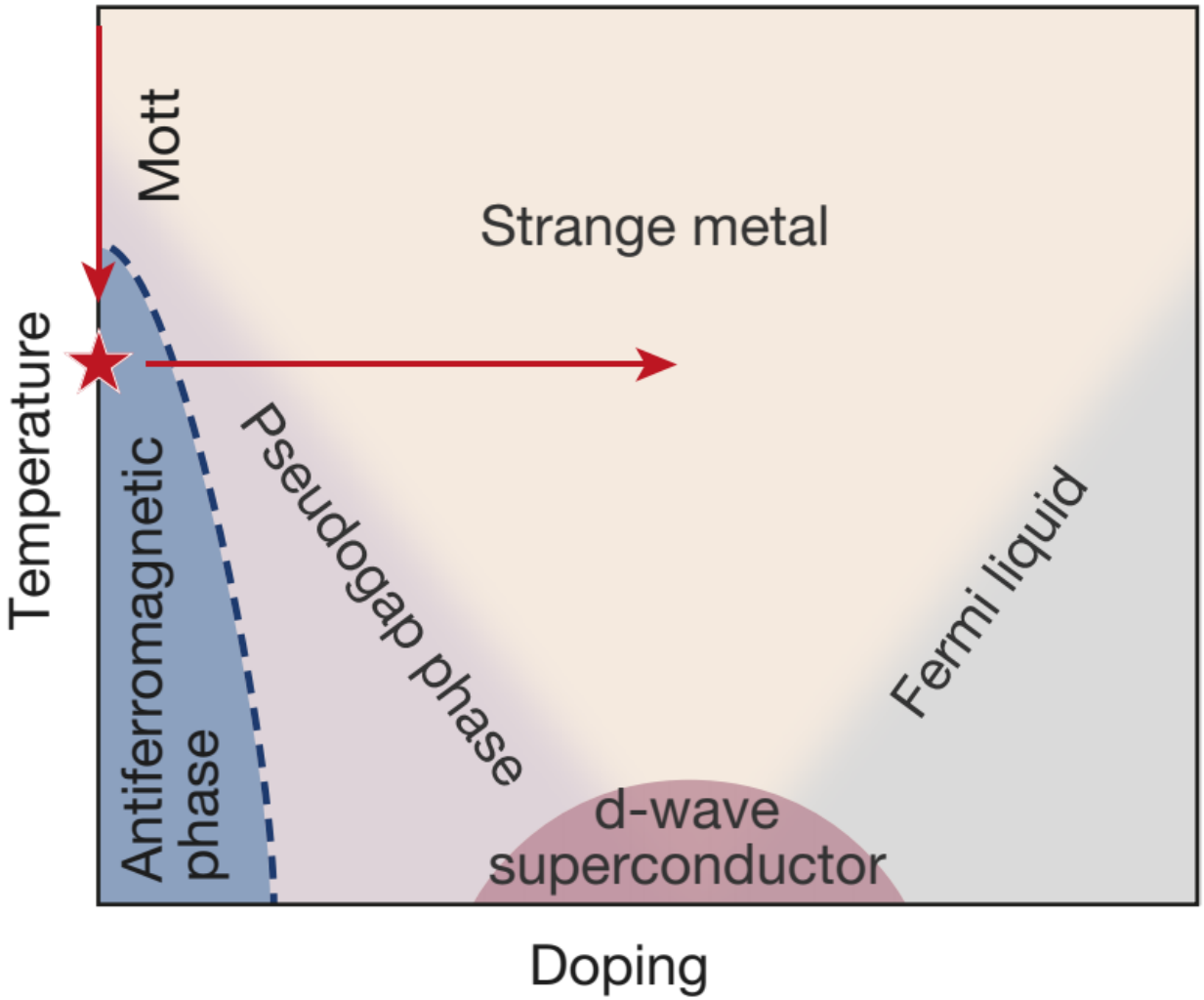






Mazurenko et al, Nature 2017

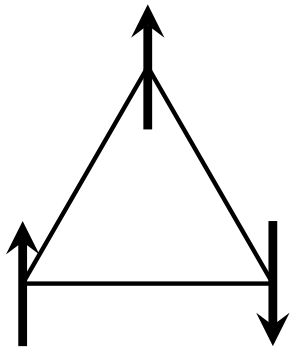
Expected phase diagram



The existence of a d-wave superfluid is a major open question, related to the understanding of high-T_c superconductivity.

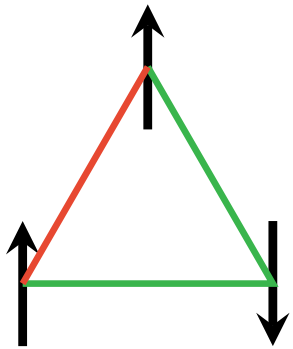
Quantum magnetism with frustration

Some geometries do not allow antiferromagnetic correlations for all links.



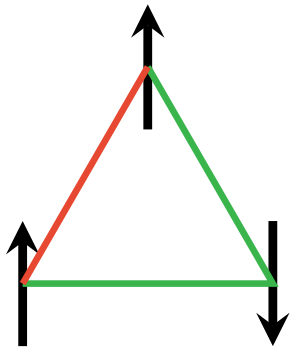
Quantum magnetism with frustration

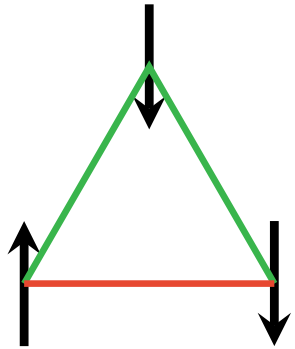
Some geometries do not allow antiferromagnetic correlations for all links.



Quantum magnetism with frustration

Some geometries do not allow antiferromagnetic correlations for all links.





Quantum magnetism with frustration

Some geometries do not allow antiferromagnetic correlations for all links.



In a frustrated lattice one expects a massive degeneracy at low energy
$\rightarrow$ complex ground state (quantum spin liquid)

